A FINITE ELEMENT TECHNIQUE FOR PREDICTING THE SOUND ABSORPTION AND TRANSMISSION COEFFICIENTS OF MATERIALS

by

Scott Higginson
B.Eng (Aerospace Engineering),
Ryerson University (Canada), 2004.

A thesis
Presented to Ryerson University
In partial fulfillment of the
Requirements for the degree of
Master of Applied Science
In the program of
Mechanical Engineering

Toronto, Ontario, Canada, 2006

Authors Declaration

I hereby declare that I am the sole author of this thesis.

I authorize Ryerson University to lend this thesis or dissertation to other institutions or individuals for the purpose of scholarly research.

Scott Higginson

I further authorize Ryerson University to reproduce this thesis by photocopying or by other means, in total or in part, at the request of other institutions or individuals for the purpose of scholarly research.

Scott Higginson

Borrower's Page

Ryerson University requires the signatures of all persons using or photocopying this thesis. Please sign below, and give the address and date.

Name	Address	Date

Abstract

A FINITE ELEMENT TECHNIQUE FOR PREDICTING THE SOUND ABSORPTION AND TRANSMISSION COEFFICIENTS OF MATERIALS

© Scott Higginson, 2006

Master of Applied Science

in the program of

Mechanical Engineering

Ryerson University

An efficient displacement-based finite element procedure is developed to investigate sound propagation in one-dimensional acoustic systems. The systems considered involve components made up of air and acoustic porous and solid materials, with the air boundary subjected to a sinusoidal sound source. Each component is modeled using higher order three node finite elements. Continuity of acoustic velocity and force equilibrium are satisfied at the interface between the air and the porous/solid media. The global equations of motion for the acoustic systems are assembled using the Lagrange multipliers method. The finite element procedure is implemented by means of MATLAB. The code is used to calculate various acoustic parameters including the sound absorption coefficient for a representative porous material and the sound transmission loss for several materials. The predicted results presented are in excellent agreement with available analytical solutions, which have been validated by published experimental data.

Acknowledgements

I would like to express my sincere thanks and appreciation to Dr. Greg Kawall and Dr. Shudong Yu for their attention, guidance, insight, and support during my studies. I have surely grown as a researcher and engineer in my time studying with them.

In addition, I would like to thank my family for their unfailing encouragement, patience, understanding and support. I may not always make it obvious, but it is always appreciated.

Table of Contents

List of Figures

List of Tables

Nomenclature

Character	Definition	Units
A	Cross sectional area	m^2
A_c	Complex pressure amplitude for an incident or transmitted wave	Pa
A_k	Cross sectional area of the k-th component	
A_0	A constant	
B_c	Complex pressure amplitude for a reflected wave	Pa
B_0	A constant	
c	Speed of sound	m/s
c_k	Speed of sound in the k-th component	m/s
C	Damping coefficient per unit cross sectional area	rayls/m or kg/m^3s
C_k	Damping coefficient per unit cross sectional area of the k-th component	rayls/m or kg/m^3s
$[C_e]_k$	Element damping matrix for the k-th component	
$[C]_k$	Damping matrix for the k-th component	
$[C]_g$	Global damping matrix	
d_a	Viscous damping coefficient	rayls/m or kg/m^3s
$[D_e]_k$	Element geometric matrix for the k-th component	
$[D]_k$	Geometric matrix for the k-th component	
$[D]_g$	Global geometric matrix	
E_k	Modulus of elasticity for solids or compressibility for fluids	N/m^2
f	Frequency	Hz
$\{f\}$	constraint force at interface	N
$\{g\}$	constraint force at interface	N
Im	Imaginary component of a complex quantity	
k	Wave number	

k_a	Linear spring constant	N/m
K_s	Structure factor	
$[K_e]_k$	Element stiffness matrix for the k-th component	
$[K]_k$	Stiffness matrix for the k-th component	
$[K]_g$	Global stiffness matrix	
l_k	Length of k-th component (applies to both air, and solid for finite element formulation)	m
$l_{e,k}$	Element length in the k-th component (applies to both air, and solid for finite element formulation)	m
L	Length of component	m
L_k	Lagrangian of the k-th component	
$[M_e]_k$	Element mass matrix for the k-th component	
$[M]_k$	Mass matrix for the k-th component	
$[M]_g$	Global mass matrix	
n	Number of elements	
N_p	Number of positions	
n_{req}	Required number of elements	
N_w	Number of waves	
$[N(\xi)]$	Shape function matrix	
O	Denotes the origin	
p	Pressure	Pa
p_C	Complex acoustic pressure as a function of x and t	Pa
$\hat{p}$	Complex acoustic pressure as a function of x	Pa
P	Acoustic Power	W
P_{ANAL}	Pressure predicted by an analytical solution procedure	Pa
P_{FEM}	Pressure predicted by a finite element solution procedure	Pa
$\{Q\}_{kc}$	Cosine force vector associated with the k-th component	N
$\{Q\}_{ks}$	Sine force vector associated with the k-th component	N

R	Flow resistivity	rayls/m or kg/m^3s
R_c	Complex pressure amplitude ratio for reflected and incident waves	Pa
Re	Real component of a complex quantity	
t	Time	s
T_k	Kinetic energy in the k-th component	Nm
u	Acoustic displacement	m
u_o	Initial (prescribed) acoustic displacement	m
u_k	Acoustic displacement in the k-th element	m
U	Displacement amplitude	m
U_o	Initial (prescribed) displacement amplitude	m
U_{oc}	Cosine component of initial displacement amplitude	m
U_{os}	Sine component of initial displacement amplitude	m
u_C	Complex acoustic displacement as a function of x and t	m
$\hat{u}$	Complex acoustic displacement as a function of x	m
U_k	Raleigh damping function for k-th component	
$\{\overline{u}_e\}_k$	Element nodal displacement vector for k-th component	m
$\{\overline{u}\}_k$	Nodal displacement vector for k-th component	m
$\{u\}_k$	Global nodal displacement vector	m
v	Velocity	m/s
v'	Volume flow rate per unit cross-sectional area	m/s
V	Velocity amplitude	m/s
v_o	Initial (prescribed) velocity	m/s
V_o	Initial (prescribed) velocity amplitude	m/s
V_{oc}	Cosine component of initial velocity amplitude	m/s
V_{os}	Sine component of initial velocity amplitude	m/s
v_C	Complex acoustic velocity as a function of x and t	m
$\hat{v}$	Complex acoustic velocity as a function of x	m
V_k	Potential energy of k-th component	Nm

W	Characteristic acoustic impedance	rayls or kg/m^2s
$\delta\overline{W}_{nc,k}$	Virtual work done by non-conservative forces for the k-th component	Nm
x	Location along the axis	m
z	Normalized acoustic impedance as a function of x	
z_{Re}	Normalized acoustic resistance (real part of z)	
z_{Im}	Normalized acoustic reactance (imaginary part of z)	
Z	Acoustic impedance as a function of x	rayls
Z_{Re}	Acoustic resistance (real part of Z)	rayls
Z_{Im}	Acoustic reactance (imaginary part of Z)	rayls
Z*	Specific acoustic impedance at a given x	rayls
α	Attenuation constant	
α_a	Absorption coefficient	
α_t	Transmission coefficient	
β	Phase constant	
ε	Strain	
E	RMS error between analytical and finite element predictions	
γ	Propagation constant	
κ	Bulk modulus	Pa
λ	Wavelength	m
ρ	Density	kg/m^3
ρ_k	Density of k-th component	kg/m^3
σ	Area density	kg/m^2
ω	Frequency	rad/sec
Ω	Porosity	
ξ	Location along x-axis in an element	m

Subscript	Definition
c	Denotes cosine component
i	Denotes incident wave
I	Denotes first interfacial degree of freedom
Im or *I*	Denotes imaginary component of a complex quantity
j	Represents the j-th node
J	Denotes second interfacial degree of freedom
k	Represents the k-th component
n	Represents the n-th element
nn	Represents the total number of nodes in a component
O	Denotes interior interfacial degree of freedom
Re or *R*	Denotes real component of a complex quantity
r	Denotes reflected wave
s	Denotes sine component
t	Denotes transmitted wave

Acronym	Definition
FE	Finite Element
FEM	Finite Element Method
HUD	The department of Housing and Urban Development
OSHA	Occupational Safety and Health Administration
RMS	Root Mean Square
TL	Transmission Loss

CHAPTER ONE – INTRODUCTION

Noise is an ever present industrial pollutant whose impact on society is a considerable and increasing concern. In recent years, much legislation has evolved in an attempt to recognize and combat the problem of noise pollution. Various studies have recognized noise as a threat to human well being. As such, an increased demand for sound insulation and noise control solutions has developed making noise and vibration major factors in the design and marketability of a wide range of products and infrastructure [1].

1.1 The Noise Problem

In general, a noise control problem can be divided into three elements: source, path, and receiver. The source may be a machine or appliance, a highway, or any number of mechanical noisemakers that are common in society. The path may be a direct airborne path, a structural path through walls, or a complex path made up of a combination of air and solid materials. The receiver is a person, or group of persons receiving the unwanted sound [2].

The most effective means of controlling noise is at its source. However, it is not always possible to attain acceptable noise levels in the engineering phase, or by modifying current products and infrastructure. The next best way to control sound is by attenuating as much sound energy as possible along its path from the source to the receiver. The three mechanisms of noise control important to this thesis are:

- Reflection of sound energy back toward the source
- Transmission of sound energy
- Absorption of sound energy

However, other mechanisms such as material damping, vibration isolation, and the elimination of alternate paths for sound propagation are also of importance. When efforts to reduce noise at its source or along the path of transmission are insufficient, measures such as using ear plugs and limiting exposure time can be used to protect the receiver [2].

1.2 Noise Regulations

Noise regulation is an important aspect of governments' responsibility around the globe. General noise standards are set where they will affect the health and hearing of workers. Regulations are set to limit the noise of everything from motor vehicles, airports, and machines to stereo levels in apartment buildings. In the United States, the Occupational Safety and Health Administration (OSHA) sets regulations designed to protect workers engaged in interstate commerce. The Department of Housing and Urban Development (HUD) has developed regulations for sound insulating characteristics of walls and floors, and sets guidelines for permissible noise levels in residential areas [2].

In combating the problem of noise pollution, it is necessary to use a means of measuring noise levels and a system of classification. The decibel (dB) is used for this. It is a number based on sound intensity or sound pressure. The lowest audible sound that the human ear can detect is used as the reference point for determining the decibel level of a noise. At 140 dB or more, acute pain is experienced; however, any noise rating above 80 dB produces physiological effects, and long term exposure to noise above 90 decibels will cause permanent damage to a person's hearing. Some common noise values are given in Table 1-1. Many governments have enacted noise control ordinances that dictate a maximum decibel level for various noise sources.

Table 1-1 - Common noise sources and levels [2]

Source	dB level
Calm breathing	10 dB
Normal talking, 1 m distance	40 – 60 dB
Major road, 10 m distance	80 – 90 dB
Jack hammer, 1 m distance	approx. 100 dB
Rock Concert	100 – 130 dB
Jet plane, 30 m distance	150 dB

Noise generally consists of many tones with varying rates of vibration or frequencies. Frequencies expressed in cycles per second or Hertz (Hz) usually are in the range of 20 Hz to 20,000 Hz. This range is often referred to as the audible range as it is bounded by the threshold of human hearing. Acoustic waves whose frequencies are below the audible range are referred to as infrasonic, whereas those with frequencies above the audible range are called ultrasonic waves. Industrial noise, generally, will be made up of sound waves which encompass the spectrum of 100 Hz to 8,000 Hz [2].

1.3 Numerical Analysis of Acoustics Problems

The issues associated with the experimental study of noise control, such as cost, complexity, and time constraints have led to growing interest in the development of numerical techniques to accurately and efficiently predict acoustic properties of various materials and systems. In many acoustic problems, the interaction between air and structures has a significant effect on the response of the structure and the attenuation of sound energy, and so this interaction needs to be properly taken into account. The finite element method has found growing use in the acoustic field for predicting the acoustic properties of both solid and porous materials that are used in fluid/structure systems. The goal of this research is to produce a novel numerical technique for predicting sound transmission phenomena in one-dimensional coupled air/solid systems. A displacement based finite element method is developed and employed to investigate the one-dimensional sound propagation through fluid, solid and porous media.

Early work in one-dimensional acoustics problems was done by Gladwell [3,4], who determined that a fluid/structure problem could be formulated variationally either entirely in terms of displacement or forces. Craggs [5,6,7,8] published a series of papers on applications of the finite element to acoustics using Gladwell's variational approach. Craggs [5] used a mixed formulation to describe the behavior of a window-room system. This mixed formulation showed good agreement with analytical predictions; however, a large number of degrees of freedom was required for an accurate solution. This suggests that a consistent field variable across the system is desired for computational efficiency.

Craggs [6,7] went on to develop finite element models to describe both a damped acoustic system and a porous absorbing material. The formulations allow for a number of input and output nodes, and use pressure as the field variable. The absorption model was based on the Raleigh model for an absorbing material given by Morse and Ingard [9], which will be discussed in later chapters. Results from his finite element models showed good agreement with exact analytical solutions for various test cases. Craggs [8] then presented a procedure to link the acoustic and porous models. The goal was to investigate and successfully satisfy the continuity of pressure conditions at the interface of the two components. The procedure was illustrated and tested using a one-dimensional coupled acoustic absorption model to calculate the specific acoustic impedance and absorption coefficient for a porous material. The results compare favourably with the exact solution.

The finite element analysis of acoustic fluid/structure interaction problems has been carried on by other researchers; however, there appears to be a gap in the published research regarding the one-dimensional prediction of various acoustic parameters. In a paper by Everstine [10], several finite element formulations which can be used to solve structural acoustic and fluid/structure interaction problems are presented. Formulations based on fluid pressure, displacement, velocity potential, and displacement potential are examined and shown to be valid field variables for formulating acoustic problems. The formulations presented in further papers deal with two- and three-dimensional systems. However, a great deal of practical information can be obtained from one-dimensional acoustic systems, and there appears to be a lack of research regarding the prediction of acoustic parameters for these systems.

The objective of this thesis is to present a novel finite element procedure for sound propagation in different media using acoustic displacement as the field variable. The wave equation considered herein is one-dimensional, although the procedure may be extended to handle two- or three-dimensional problems.

The one-dimensional formulation presented in this thesis is implemented using MATLAB to take advantage of the built-in functions and algorithms. The MATLAB code developed in this thesis can be used to accurately and efficiently predict the sound absorption coefficient and the sound transmission loss through different media for plane waves. The reason for developing a procedure rather than attempting to use commercially

available finite element packages is that they cannot be used with confidence to deal with the air/solid interaction. The acoustic systems considered in this thesis involve components consisting of air and a porous or solid material. Boundary and interface conditions are identified and satisfied at the interface between the two components. Various test cases are explored and the results are compared to other independent solutions available in the literature.

CHAPTER TWO – ACOUSTIC FUNDAMENTALS

2.1 Acoustic Waves

Acoustic waves are pressure disturbances which can propagate through compressible solids, liquids, and gasses. They are longitudinal waves, meaning that the particles transmitting the wave oscillate in the direction of propagation of the wave. This produces alternate regions of compression and rarefaction in the medium. The total sound energy may be considered as the sum of the kinetic and potential energies. The kinetic energy is the result of the motion of the particles in the medium, and the potential energy is due to the elastic displacement of those particles. Sound waves can be reflected, refracted, scattered, transmitted, and absorbed [11].

This thesis deals with plane acoustic waves which can be defined as disturbances with no variations in acoustic pressure, density, particle displacement and velocity in any direction other than the direction of propagation. The wave fronts are planes perpendicular to the direction of propagation and parallel to one another at all times. It is also assumed that (1) there are no viscous effects for non-porous materials, (2) the fluid medium is homogenous and continuous, (3) the process is adiabatic, and (4) the fluid medium is isotropic and perfectly elastic. The development of the plane wave equation and its solution can be found in [11].

2.2 Acoustic Impedance

The specific acoustic impedance of a material is an important property which is needed to determine the reflection and transmission of acoustic waves at the boundary of two dissimilar media and to assess the absorption of sound in a medium.

The acoustic impedance for progressive plane waves in a coupled system is a complex quantity given by:

$$Z = \frac{p_C}{v_C} = Z_{\mathrm{Re}} + iZ_{\mathrm{Im}} \qquad [2\text{-}1]$$

where p_C denotes a complex acoustic pressure as a function of x and t, v_C denotes the corresponding complex acoustic velocity as a function of x and t, and $i^2 = -1$. The real component, Z_{Re}, is referred to as the acoustic resistance and the imaginary component, Z_{Im}, as the acoustic reactance of the medium [11]. Further information about the acoustic impedance pertaining to progressive plane waves can be found in Appendices A, B, and C.

2.3 Sound Absorption

When a sound wave propagates through a medium, some of its energy is dissipated by the medium. The source of the energy loss can be attributed to the following mechanisms: viscous losses, heat conduction losses, and losses associated with molecular exchanges of energy [1].

Sound absorbent materials generally find use as enclosures, wall coverings and wrappings where they aid to reduce reverberant build-up of sound and hence increase sound transmission losses. Sound absorption is very useful in applications where it is necessary to keep reflected sound energy to a minimum.

2.3.1 Sound Absorbing Materials

Porous materials lend themselves well to use as absorbing materials. According to Zwikker and Kosten [12], there are three major parameters that significantly influence the acoustic absorption characteristics of a rigid porous material. They are the flow resistivity, the porosity, and the structure factor.

Flow Resistivity (R)

The flow resistivity is a measure of the viscous resistance to a steady flow of fluid (e.g., air) through the pores or interstices of the porous material. The resistance gives rise to a static pressure gradient, $\partial p/\partial x$. The flow resistivity, R, is defined by means of the following relationship:

$$-Rv' = \partial p/\partial x \qquad \text{[2-2]}$$

where v' is the volume flow rate per unit cross sectional area [1].

Porosity (Ω)

The porosity, which is a dimensionless parameter, is the ratio of volume of voids to the total volume of the porous material. Porosity influences the effective compressibility or bulk modulus of the fluid. It normally falls between 0.90 and 0.95 for effective absorption materials. [1]

Structure Factor (K_s)

The structure factor, which is also a dimensionless parameter, expresses the influence of the geometric form of the pores on the effective density of the fluid. The vibrating fluid undergoes accelerations in various directions as a result of the irregular pore shapes found in a porous material. This increases the effective fluid density and so decreases the effective speed of sound. The structure factor generally lies in the range of 1.2-2.0.

The conceptual Raleigh porous model proposed by Morse and Ingard [9] has been modified by Craggs [6] through introduction of the structure factor, porosity, and resistivity for application of the generalized Rayleigh model to a sound absorbing material. The material's sound absorption behavior in a coupled air/porous body system can be modeled by using an effective speed of sound, an effective density, and damping (or resistivity), which are given by:

$$c_2 = c_1/\sqrt{K_s\Omega}$$

$$\rho_2 = (K_s/\Omega)\rho_1 + R/i\omega$$

$$C_2 = R \qquad \text{[2-3]}$$

where c_2 is the effective speed of sound, c_1 is the speed of sound in air, ρ_2 is the effective density, ρ_1 is the density of air, and C_2 is the damping coefficient associated with the porous material. Note that ρ_2 is a complex quantity involving $i = \sqrt{-1}$. The development of the wave equation for a porous material is given in Appendix B.

2.3.2 Absorption Coefficient

The absorption coefficient represents the fraction of incident sound energy that is absorbed by a material on a scale of 0 (0%) to 1 (100%), assuming that the acoustic energy penetrating the material is absorbed, and that the solid does not vibrate (no particle motion). For a coupled air/porous body system, the absorption coefficient, is given by (see Appendix B):

$$\alpha_a = \frac{4\,\mathrm{Re}(Z_1^*)}{(\mathrm{Re}(Z_1^*)+1)^2 + (\mathrm{Im}(Z_1^*))^2} \qquad [2\text{-}4]$$

In this expression $\mathrm{Re}(Z_1^*)$ and $\mathrm{Im}(Z_1^*)$ are, respectively, the real and imaginary components of the so-called *input* impedance of the air/porous body system and $\rho_1 c_1$ is the characteristic impedance of the air. Also, it can be shown from equation [A-22] of Appendix A that:

$$\mathrm{Re}\left(\frac{Z_1^*}{\rho_1 c_1}\right) = \frac{z_{2R}^*}{(\cos k_1 L_1 + z_{2I}^* \sin k_1 L_1)^2 + z_{2R}^{*2} \sin^2 k_1 L_1} \qquad [2\text{-}5]$$

and,

$$\mathrm{Im}\left(\frac{Z_1^*}{\rho_1 c_1}\right) = \frac{(\sin k_1 L_1 - z_{2I}^* \cos k_1 L_1)(\cos k_1 L_1 + z_{2I}^* \sin k_1 L_1) - z_{2R}^{*2} \cos k_1 L_1 \sin k_1 L_1}{(\cos k_1 L_1 + z_{2I}^* \sin k_1 L_1)^2 + z_{2R}^{*2} \sin^2 k_1 L_1} \qquad [2\text{-}6]$$

Here, $k_1 = 2\pi f / c_1$ is the wave number of the air, L_1 is the air column length, and z_{2R}^* and z_{2I}^* are the real and imaginary parts of the acoustic impedance of the porous material given by:

$$z_{2R}^* = \mathrm{Re}\{W_2 \coth \gamma_2 L_2\}/\rho_1 c_1$$

and

$$z_{2I}^* = \mathrm{Im}\{W_2 \coth \gamma_2 L_2\}/\rho_1 c_1$$

where $W_2 = \sqrt{\kappa_2 \rho_2}$, $\kappa_2 = \rho_1 c_1^2 / \Omega$, $\rho_2 = K_s \rho_1 / \Omega + R / i\omega$, $\gamma = i\omega\sqrt{\rho_2 / \kappa_2}$, and L_2 is the porous body length. (See Appendix B.)

2.4 Sound Transmission

The phenomenon of sound transmission is used extensively in the design of partitions and barriers to control noise. When a sound wave impinges on the boundary of a solid medium, the vibrational response of the solid radiates sound energy into the surrounding air [1]. The transmission of sound energy through a solid medium depends on the amount of sound energy radiated to the air on the opposite side of the solid from that which the sound is incident upon.

2.4.1 Transmission Loss

Transmission loss in a solid is the accumulated decrease in acoustic intensity as an acoustic pressure wave propagates through the solid. For steady state conditions, there exists an exact analytical solution for the sound transmission behavior of single thick solids. The derivation of this solution is detailed in Appendix C.

The transmission coefficient represents the fraction of incident sound energy that is transmitted into a material on a scale of 0 (0%) to 1 (100%), assuming that none of the acoustic energy penetrating the material is absorbed. The transmission coefficient is the ratio of the acoustic power of the transmitted wave to that of the incident wave and is given by:

$$\alpha_t = \frac{4}{4\cos^2 k_2 L_2 + \left(\frac{\rho_2 c_2}{\rho_1 c_1} + \frac{\rho_1 c_1}{\rho_2 c_2} \right)^2 \sin^2 k_2 L_2} \qquad \text{[2-7]}$$

where $k_2 = 2\pi f / c_2$, L_2 refers to the length of the solid, and $\rho_1 c_1$ is the characteristic impedance of the air. From this, the transmission loss for the system can be calculated as:

$$TL(dB) = 10 \log\left(\frac{1}{\alpha_t} \right) \qquad \text{[2-8]}$$

2.4.2 Mass Law

The mass law is a practical rule that applies to most materials in certain frequency ranges [11]. (It has been verified by experimental data [11].) It involves the assumption that the solid medium in the system is perfectly rigid. This results in a specific acoustic impedance which is entirely reactive (imaginary). The procedure for obtaining the mass law can be found in Appendix C. Equation [C-50] of this Appendix gives the transmission loss of a solid obeying the mass law as:

$$TL(dB) = 20\log_{10}\left(\frac{\pi\sigma_2}{\rho_1 c_1}\right) + 20\log_{10} f \qquad \text{[2-9]}$$

CHAPTER THREE – FINITE ELEMENT FORMULATION

A displacement-based finite element formulation of one-dimensional sound propagation through solid and porous media is developed. A displacement based formulation is chosen over the pressure based formulations used by Gladwell [3] and Craggs [5] for a number of reasons. In a displacement based formulation, Hamilton's variational principle can be used to derive the system's equations of motion and boundary conditions, and the interface conditions between two media can be defined without the need to define the direction of wave propagation.

One of the advantages of this formulation is that it offers a high level of computational efficiency. As such, three-node higher order, non-isoparametric finite elements are used to model the wave propagation in the one-dimensional acoustic systems under consideration. Each of the three nodes has two degrees of freedom, the acoustic displacement and its derivative with respect to position (i.e., the gradient). These two degrees of freedom are exactly what are needed to correctly formulate the interface conditions. This three-node finite element allows quintic polynomials to be used as the shape function for acoustic displacement. The benefits of this are realized when dealing with systems having large wave numbers, i.e., high frequency sound propagating in a thick solid.

When sound propagation across different media is studied, it is often necessary to formulate and implement interface conditions. According to Craggs [5], when two media are linked together, it may be assumed that there exists an incompressible fluid boundary layer whose dimensions are small compared with the acoustic wavelength. This ensures that the two media have continuous acoustic displacements and acoustic pressures across the interface. For the one-dimensional situation, the pressure on either side of the

boundary layer can be related to the displacement gradient through compressibility or bulk modulus, for fluids, and modulus of elasticity, for solids.

The equations of motion for the one-dimensional acoustic system shown in Figure 3-1 are presented and the finite element model of the system is developed. The system is excited by the harmonic motion of a rigid piston at the left end of the tube. To study the sound absorption and sound transmission loss through the solid, it is assumed that the sound waves either terminate or are transmitted to the ambient air at the right end of the tube. However, other boundary conditions can be implemented.

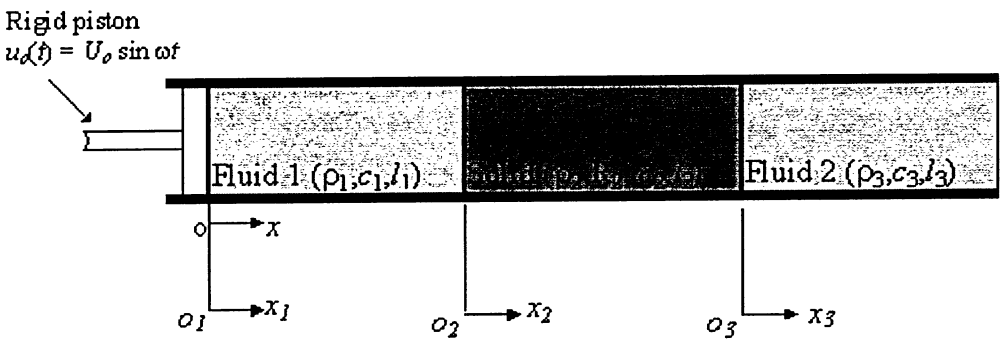

Figure 3-1 – Three component sound system

3.1 Variational Principle

In dealing with linear waves in the multi-component system depicted in Figure 3-1, the following assumptions are made:

(1) No ambient fluid flow;

(2) Heat transfer associated with acoustic waves is negligible;

(3) The fluids are inviscid;

(4) Walls of the tube are smooth, rigid and adiabatic;

(5) The cross section of each media is much smaller than its length.

The longitudinal displacement or acoustic displacement is used as the field variable for a column of solid or porous material. With this displacement field, the velocities and stresses inside the material can be easily obtained. For a column of fluid with no flow, one of the following three field variables can be chosen: acoustic pressure, acoustic displacement, and acoustic velocity. For consistency, in the case of the solid, the

fluid's acoustic displacement is chosen as the field variable. From this, the acoustic velocity and acoustic pressure in the fluid can be calculated. This choice also makes it easier to derive the ordinary differential equations for transient and steady state responses of an acoustic system to excitations through Hamilton's principle [14].

When deriving the equations of motion for a system with multiple media, it is prudent to begin by studying a single one-dimensional, unconstrained medium, as shown in Figure 3-2.

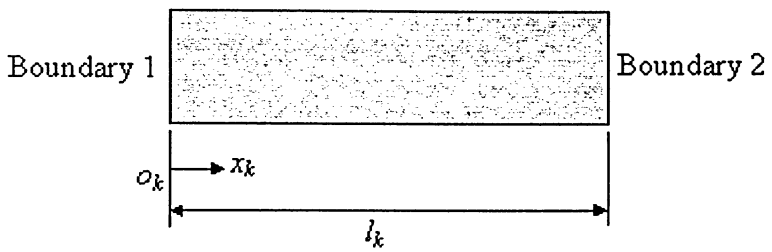

Figure 3-2 – single unconstrained component

For generality, k refers to the k-th medium or system component. The associated acoustic material and geometric properties are:

ρ_k - density

c_k - speed of wave propagation

E_k - modulus of elasticity for solids, or compressibility for fluids

C_k - damping coefficient per unit cross-sectional area

l_k - length of component

A_k - cross-sectional area

By the extended Hamilton's principle [14], the equations of motion of a single medium can be determined by

$$\int_{t_1}^{t_2} (\delta L_k + \delta \overline{W}_{nc,k}) dt = 0 \qquad [3\text{-}1]$$

Here, L_k is known as the Lagrangian and is defined by $T_k - V_k$, where T_k represents kinetic energy in the system and V_k represents potential energy; $\delta \overline{W}_{nc,k}$ represents the virtual work done by distributed non-conservative forces and the damping force; and t is time.

In terms of acoustic displacement, the acoustic wave equation under the above assumptions is given by [11]:

$$\frac{1}{c^2}\frac{\partial^2 u}{\partial t^2}-\frac{\partial^2 u}{\partial x^2}=0 \qquad [3\text{-}2]$$

where c represents the speed of sound, u is the acoustic displacement, t is time, and x is direction of propagation.

3.2 Finite Element Formulation for a System Component

The component equations of motion may be obtained from the wave equation and Galerkin's weak form of the variational principle [13], or using the Lagrange multipliers method. Here, it shall be developed using the Lagrange multipliers method.

Suppose that the *k*-th system component is modeled using $N_{e,k}$ one-dimensional, three node finite elements, as shown in Figure 3-3.

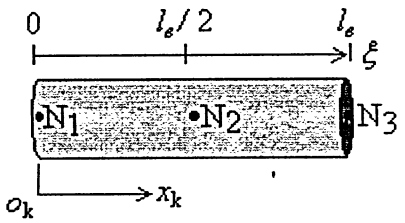

Figure 3-3 – three node higher order element

The acoustic displacement, u_k, varies with the local axial co-ordinate, ξ, as

$$u_k=[N(\xi)][D_e]_k\{\overline{u}_e\}_k,(0\le\xi\le l_{e,k}) \qquad [3\text{-}3]$$

where $[N(\xi)]$ is the shape function matrix; $[D_e]_k$ is the element geometric matrix; and $\{\overline{u}_e\}_k$ is the element nodal displacement vector. These quantities are defined as follows:

$$[N(\xi)]^T=\begin{Bmatrix}1\\ \xi\\ \xi^2\\ \xi^3\\ \xi^4\\ \xi^5\end{Bmatrix} \qquad [3\text{-}4]$$

$$[D_e]_k = \begin{bmatrix} 1 & 0 & 0 & 0 & 0 & 0 \\ 0 & 1 & 0 & 0 & 0 & 0 \\ \frac{-23}{l_{e.k}^2} & \frac{-6}{l_{e.k}} & \frac{16}{l_{e.k}^2} & \frac{-8}{l_{e.k}} & \frac{7}{l_{e.k}^2} & \frac{-1}{l_{e.k}} \\ \frac{66}{l_{e.k}^3} & \frac{13}{l_{e.k}^2} & \frac{-32}{l_{e.k}^3} & \frac{32}{l_{e.k}^2} & \frac{-34}{l_{e.k}^3} & \frac{5}{l_{e.k}^2} \\ \frac{-68}{l_{e.k}^4} & \frac{-12}{l_{e.k}^3} & \frac{16}{l_{e.k}^4} & \frac{-40}{l_{e.k}^3} & \frac{52}{l_{e.k}^4} & \frac{-8}{l_{e.k}^3} \\ \frac{24}{l_{e.k}^5} & \frac{4}{l_{e.k}^4} & 0 & \frac{16}{l_{e.k}^4} & \frac{-24}{l_{e.k}^5} & \frac{4}{l_{e.k}^4} \end{bmatrix} \quad \text{[3-5]}$$

$$\{\bar{u}_e\}_k = \begin{Bmatrix} u_1 \\ \varepsilon_1 \\ u_2 \\ \varepsilon_2 \\ u_3 \\ \varepsilon_3 \end{Bmatrix}_k \quad \text{[3-6]}$$

The kinetic and potential energies can be written as:

$$T_k = \frac{1}{2}\int_0^{l_k} \rho_k A_k (\dot{u}_k)^2 dx_k = \frac{1}{2}\sum_{e=1}^{N_{e.k}} \{\dot{\bar{u}}_e\}_k^T [M_e] \{\dot{\bar{u}}_e\}_k \quad \text{[3-7]}$$

$$V_k = \frac{1}{2}\int_0^{l_k} \rho_k c_k^2 \left(\frac{\partial u_k}{\partial x_k}\right)^2 dx_k = \frac{1}{2}\sum_{e=1}^{N_{e.k}} \{\bar{u}_e\}_k^T [K_e] \{\bar{u}_e\}_k \quad \text{[3-8]}$$

where $[M_e]_k$ is the element mass matrix, and $[K_e]_k$ is the element stiffness matrix, defined by

$$[M_e]_k = [D_e]_k^T \left[\int_0^{l_{e.k}} \rho_k A_k [N(\xi)]^T [N(\xi)] d\xi\right] [D_e]_k \quad \text{[3-9]}$$

$$[K_e]_k = [D_e]_k^T \left[\int_0^{l_{e.k}} \rho_k c_k^2 A_k \left[\frac{dN(\xi)}{d\xi}\right]^T \left[\frac{dN(\xi)}{d\xi}\right] d\xi\right] [D_e]_k \quad \text{[3-10]}$$

And the component nodal displacement, $\{\bar{u}\}_k$, is given by:

$$\{\bar{u}\}_k = \begin{Bmatrix} \begin{Bmatrix} u \\ \varepsilon \end{Bmatrix}_{\text{node 1}} \\ \begin{Bmatrix} u \\ \varepsilon \end{Bmatrix}_{\text{node 2}} \\ \vdots \\ \begin{Bmatrix} u \\ \varepsilon \end{Bmatrix}_{\text{node } nn} \end{Bmatrix}_k = \begin{Bmatrix} u_1 \\ \varepsilon_1 \\ u_2 \\ \varepsilon_2 \\ \vdots \\ u_{nn} \\ \varepsilon_{nn} \end{Bmatrix}_k \quad [3\text{-}11]$$

where subscript *nn* represents the number of nodes in the *k*-th component.

The element displacement vector can be related to the component displacement vector through a transformation matrix as follows:

$$\{\bar{u}_e\}_k = [T_{e\to g}]_k \{\bar{u}\}_k \quad [3\text{-}12]$$

The kinetic and potential energies can be re-written in component form as:

$$T_k = \frac{1}{2}\{\dot{\bar{u}}\}_k^T [M]_k \{\dot{\bar{u}}\}_k \quad [3\text{-}13]$$

$$V_k = \frac{1}{2}\{\bar{u}\}_k^T [K]_k \{\bar{u}\}_k \quad [3\text{-}14]$$

where $\dot{\bar{u}}$ represents the nodal velocity, and the component mass and stiffness matrices are given by:

$$[M]_k = \sum_{e=1}^{N_{e,k}} [T_{e\to g}]_k^T [M_e]_k [T_{e\to g}]_k \quad [3\text{-}15]$$

$$[K]_k = \sum_{e=1}^{N_{e,k}} [T_{e\to g}]_k^T [K_e]_k [T_{e\to g}]_k \quad [3\text{-}16]$$

If damping is present in the component, the non-conservative distributed damping force will do work. For viscous damping, the effect can be considered through a Raleigh dissipation function, U_k, which is given by:

$$U_k = \frac{1}{2}\int_0^{l_k} C_k A_k (\dot{u}_k)^2 dx_k = \frac{1}{2}\{\dot{\bar{u}}\}_k^T [C]_k \{\dot{\bar{u}}\}_k \quad [3\text{-}17]$$

Here, C_k is the damping coefficient; $[C]_k$ is the damping matrix, which is written in element and component form as follows:

$$[C_e]_k = [D_e]_k^T \left[\int_0^{l_{e,k}} C_k A_k [N(\xi)]^T [N(\xi)] d\xi \right] [D_e]_k \quad [3\text{-}18]$$

$$[C]_k = \sum_{e=1}^{N_{e,k}} [T_{e\to g}]_k^T [C_e]_k [T_{e\to g}]_k \quad [3\text{-}19]$$

For a Rayleigh material, the generalized damping force vector may be obtained from the following relation:

$$\{Q_{nc}\}_k = -\frac{\partial U_k}{\partial \{\dot{\bar{u}}\}_k^T} = -[C]_k \{\dot{\bar{u}}\}_k \quad [3\text{-}20]$$

The work done by the generalized force vector for a virtual displacement of $\delta\{\bar{u}\}_k^T$ is given by:

$$\delta W_{nc,k} = \delta\{\bar{u}\}_k^T \{Q_{nc}\}_k \quad [3\text{-}21]$$

When the component nodal displacement vector is chosen as the generalized co-ordinate, it can be shown that Hamilton's principle yields the following from [3-1]:

$$\frac{d}{dt}\frac{\partial L_k}{\partial \{\dot{\bar{u}}\}_k^T} + \frac{\partial U_k}{\partial \{\dot{\bar{u}}\}_k^T} - \frac{\partial L_k}{\partial \{\bar{u}\}_k^T} = \mathbf{0} \quad [3\text{-}22]$$

If one substitutes [3-13] and [3-14] and [3-17] into[3-22], the equations of motion for a single unconstrained component in terms of the nodal displacement vector are given as:

$$[M]_k \{\ddot{\bar{u}}\}_k + [C]_k \{\dot{\bar{u}}\}_k + [K]_k \{\bar{u}\}_k = \mathbf{0} \quad [3\text{-}23]$$

where $\ddot{\bar{u}}$ represents nodal acceleration. For a system made up of multiple components, the above equation describes each component individually. Interaction between components is done by coupling the individual equations of motion through displacements at the interfacial nodes.

3.3 Boundary Conditions

According to Hamilton's principle [14], the *natural* boundary conditions at each end of a component are either:

(1) the acoustic displacement is prescribed, or

(2) the acoustic pressure is zero.

The first case includes situations where the boundary moves with a rigid piston and where sound propagation terminates. The second case is generally not encountered in practice for components of finite size. Besides these two natural boundary conditions, there may be non-natural, or *forced*, boundary conditions imposed on the system. These boundary conditions may include inertial, stiffness and damping elements.

Referring to Figure 3-1, where the left end of Fluid 1 is coupled to the movement of the rigid vibrating piston, the acoustic velocity at the first node must be equal to that of the piston. For a harmonic excitation at a single frequency, this acoustic velocity may be written as:

$$\dot{u}_1(x_1,t)\big|_{x_1=0} = \dot{u}_0(t) = V_{0c}\cos\omega t + V_{0s}\sin\omega t \qquad \text{[3-24]}$$

where $\dot{u}$ denotes velocity, V_{0s} and V_{0c} are the sine and cosine components of the acoustic velocity and $\omega = 2\pi f$ is the frequency of excitation of the system. [3-24] can be written in terms of the acoustic displacement as follows:

$$u_1(x_1,t)\big|_{x_1=0} = u_0(t) = U_{0c}\cos\omega t + U_{0s}\sin\omega t \qquad \text{[3-25]}$$

Here, $U_{0s} = V_{0c}/\omega$ and $U_{0c} = -V_{0s}/\omega$.

3.4 Interface Conditions

It is assumed [7] that, at the interface between two components,

(1) the acoustic displacements or velocities of the components on the two sides of a thin and incompressible boundary layer are identical in the direction normal to the interface, and

(2) the acoustic pressures on the two sides of the boundary layer are also identical.

These conditions ensure that there is continuity and force balance across a thin boundary layer separating the two components. For the acoustic system in Figure 3-1, there are

three components, two interfaces and four interface conditions. Using the co-ordinates shown in Figure 3-1, these interface conditions are given by:

$$u_1(x_1,t)\big|_{x_1=l_1} = u_2(x_2,t)\big|_{x_2=0},\ p_1(x_1,t)\big|_{x_1=l_1} = p_2(x_2,t)\big|_{x_2=0}$$
$$u_2(x_2,t)\big|_{x_2=l_2} = u_3(x_3,t)\big|_{x_1=0},\ p_2(x_2,t)\big|_{x_2=l_2} = p_3(x_3,t)\big|_{x_3=0} \qquad [3\text{-}26]$$

Use of higher order finite elements introduces the displacement gradient or acoustic strain, $\varepsilon = \partial u/\partial x$, into the element nodal displacement vector. For any component, the acoustic pressures and displacements are related through

$$p_k = -\left(\rho c^2 \frac{\partial u}{\partial x}\right)_k = -\rho_k c_k^2 \varepsilon_k,\ \mathrm{k} = 1,2,3 \qquad [3\text{-}27]$$

The negative sign in this equation is due to the fact that compression of a medium corresponds to a positive acoustic pressure and negative acoustic strain, and rarefaction of a medium corresponds to a negative acoustic pressure and positive acoustic strain. By substituting [3-26] into [3-27], the interface conditions can be written in terms of acoustic displacement and acoustic strain as

$$u_1(x_1,t)\big|_{x_1=l_1} = u_2(x_2,t)\big|_{x_2=0}, \rho_1 c_1^2 \varepsilon_1(x_1,t)\big\|_{x_1=l_1} = \rho_2 c_2^2 \varepsilon_2(x_2,t)\big|_{x_2=0} \qquad [3\text{-}28]$$

$$u_2(x_2,t)\big|_{x_2=l_2} = u_3(x_3,t)\big|_{x_1=0}, \rho_2 c_2^2 \varepsilon_2(x_2,t)\big|_{x_2=l_2} = \rho_3 c_3^2 \varepsilon_3(x_3,t)\big\|_{x_3=0} \qquad [3\text{-}29]$$

These interface conditions are valid for waves propagating in either direction, that is, for transmitted and reflected waves. If one made use of the acoustic velocity or pressure as the field variable in the derivation of the equation of motion, separate expressions for transmitted and reflected waves would be required.

3.5 Assembly of the Equations of Motion

Recalling the assumptions made in Section 3.1, the equations of motion for each of the components in the three component acoustic system may be written as

$$[M]_1\{\ddot{\bar{u}}\}_1 + [K]_1\{\bar{u}\}_1 = \mathbf{0} \quad \text{[3-30]}$$

$$[M]_2\{\ddot{\bar{u}}\}_2 + [C]_2\{\dot{\bar{u}}\}_2 + [K]_2\{\bar{u}\}_2 = \mathbf{0} \quad \text{[3-31]}$$

$$[M]_3\{\ddot{\bar{u}}\}_3 + [K]_3\{\bar{u}\}_3 = \mathbf{0} \quad \text{[3-32]}$$

These component equations must be modified to satisfy the boundary and interface conditions described in Sections 3.3 and 3.4, respectively. The first fluid column is directly adjacent to the harmonically vibrating piston; so, from [3-25], it is known that the acoustic displacement of the first node of the first column of fluid must be equal to the piston displacement, i.e.,

$$(\bar{u}_1)_1 = u_0(t) \quad \text{[3-33]}$$

If sound is assumed to terminate on the right side of the solid component, the last node of the second air component must have zero acoustic displacement, i.e.,

$$(\bar{u}_{nn})_3 = 0 \quad \text{[3-34]}$$

However, if it is assumed that the right end of the second fluid column is exposed to open ambient air, the acoustic pressure must be zero, and so the acoustic strain must be zero, i.e.,

$$(\bar{\varepsilon}_{nn})_3 = 0 \quad \text{[3-35]}$$

These boundary conditions may be implemented by modifying the stiffness and mass matrices, or using the penalty method.

Since the acoustic displacement of the first node of the first column of fluid is prescribed, the equation associated with this particular degree of freedom can be deleted from the equations of motion. The modified equations of motion for the first fluid column can be written as

$$[M]_1\{\ddot{\bar{u}}\}_1 + [\tilde{K}]_1\{\bar{u}\}_1 = \{Q\}_{1c}\cos\omega t + \{Q\}_{1s}\sin\omega t \quad \text{[3-36]}$$

where $[\tilde{K}]_1$ is the matrix resulting from the removal of the column and row relating to the first node in $[K]_1$; $\{Q\}_{1c}$ and $\{Q\}_{1s}$ are the acoustic force vectors given by

$$\{Q\}_{1c} = -\begin{Bmatrix} (K_{2,1} - M_{2,1}\omega^2)U_{0c} \\ (K_{3,1} - M_{3,1}\omega^2)U_{0c} \\ \vdots \\ (K_{6,1} - M_{6,1}\omega^2)U_{0c} \\ \mathbf{0} \end{Bmatrix} \quad \text{[3-37]}$$

$$\{Q\}_{1s} = -\begin{Bmatrix} (K_{2,1} - M_{2,1}\omega^2)U_{0s} \\ (K_{3,1} - M_{3,1}\omega^2)U_{0s} \\ \vdots \\ (K_{6,1} - M_{6,1}\omega^2)U_{0s} \\ \mathbf{0} \end{Bmatrix} \quad \text{[3-38]}$$

The boundary condition on the right end of the second fluid column can be implemented by modifying the mass and stiffness matrices, or through the penalty method, by replacing the second to last or last diagonal element (depending on the condition) in $[K]_3$ with k_∞. The modified equations of motion for the third component can then be written as

$$[M]_3\{\ddot{\bar{u}}\}_3 + [\tilde{K}]_3\{\bar{u}\}_3 = \{0\} \quad \text{[3-39]}$$

where $[\tilde{K}]_3$ is the modified stiffness matrix due to the implementation of the boundary conditions.

The four interface conditions for the acoustic system having three components can be written in matrix form as follows:

$$\begin{Bmatrix} \bar{u}_1 \\ \bar{\varepsilon}_1 \end{Bmatrix}_2 = \begin{bmatrix} 1 & 0 \\ 0 & \alpha_1 \end{bmatrix} \begin{Bmatrix} \bar{u}_{nn1} \\ \bar{\varepsilon}_{nn1} \end{Bmatrix}_1, \begin{Bmatrix} \bar{u}_1 \\ \bar{\varepsilon}_1 \end{Bmatrix}_3 = \begin{bmatrix} 1 & 0 \\ 0 & \alpha_2 \end{bmatrix} \begin{Bmatrix} \bar{u}_{nn2} \\ \bar{\varepsilon}_{nn2} \end{Bmatrix}_2 \quad \text{[3-40]}$$

or,

$$\{\bar{u}_I\}_2 - [R_I]\{\bar{u}_I\}_1 = \{0\}, \{\bar{u}_J\}_3 - [R_J]\{\bar{u}_J\}_2 = \{0\} \quad \text{[3-41]}$$

where,

$$\alpha_1 = \rho_1 c_1^2 A_1 / \rho_2 c_2^2 A_2 \quad \text{[3-42]}$$

$$\alpha_2 = \rho_2 c_2^2 A_2 / \rho_3 c_3^2 A_3$$

Note, in this case, $A_1 = A_2 = A_3$. To implement these interface conditions into the global equations of motion of the acoustic system, it is necessary to add to the Lagrangian the potential associated with the work done by the constraint forces, which is defined as [13]:

$$L^c = \left\{\{\bar{u}_I\}_2 - [R_I]\{\bar{u}_I\}_1\right\}^T \{f\} + \left\{\{\bar{u}_J\}_3 - [R_J]\{\bar{u}_J\}_2\right\}^T \{g\} \qquad [3\text{-}43]$$

where $\{f\}$ and $\{g\}$ represent constraint forces between two media at their interfaces I and J, respectively.

Incorporating this, the modified equations of motion in partitioned form, along with the constraint equations, are written for each component as

$$\begin{bmatrix} M_{OO} & M_{OI} \\ M_{IO} & M_{II} \end{bmatrix}_1 \begin{Bmatrix} \ddot{\bar{u}}_O \\ \ddot{\bar{u}}_I \end{Bmatrix}_1 + \begin{bmatrix} \tilde{K}_{OO} & \tilde{K}_{OI} \\ \tilde{K}_{IO} & \tilde{K}_{II} \end{bmatrix}_1 \begin{Bmatrix} \bar{u}_O \\ \bar{u}_I \end{Bmatrix}_1 = \begin{Bmatrix} Q_O(t) \\ \mathbf{0} \end{Bmatrix}_1 + \begin{Bmatrix} \mathbf{0} \\ [R_I]^T f \end{Bmatrix} \qquad [3\text{-}44]$$

$$\begin{bmatrix} M_{II} & M_{IO} & M_{IJ} \\ M_{OI} & M_{OO} & M_{OJ} \\ M_{JI} & M_{JO} & M_{JJ} \end{bmatrix}_2 \begin{Bmatrix} \ddot{\bar{u}}_I \\ \ddot{\bar{u}}_O \\ \ddot{\bar{u}}_J \end{Bmatrix}_2 + \begin{bmatrix} C_{II} & C_{IO} & C_{IJ} \\ C_{OI} & C_{OO} & C_{OJ} \\ C_{JI} & C_{JO} & C_{JJ} \end{bmatrix}_2 \begin{Bmatrix} \dot{\bar{u}}_I \\ \dot{\bar{u}}_O \\ \dot{\bar{u}}_J \end{Bmatrix}_2 + \qquad [3\text{-}45]$$

$$\begin{bmatrix} \tilde{K}_{II} & \tilde{K}_{IO} & \tilde{K}_{IJ} \\ \tilde{K}_{OI} & \tilde{K}_{OO} & \tilde{K}_{OJ} \\ \tilde{K}_{JI} & \tilde{K}_{JO} & \tilde{K}_{JJ} \end{bmatrix}_2 \begin{Bmatrix} \bar{u}_I \\ \bar{u}_O \\ \bar{u}_J \end{Bmatrix}_2 = \begin{Bmatrix} -f \\ \mathbf{0} \\ \mathbf{0} \end{Bmatrix} + \begin{Bmatrix} \mathbf{0} \\ \mathbf{0} \\ [R_J]^T g \end{Bmatrix}$$

$$\begin{bmatrix} M_{JJ} & M_{JO} \\ M_{OJ} & M_{OO} \end{bmatrix}_1 \begin{Bmatrix} \ddot{\bar{u}}_J \\ \ddot{\bar{u}}_O \end{Bmatrix}_3 + \begin{bmatrix} \tilde{K}_{JJ} & \tilde{K}_{JO} \\ \tilde{K}_{OJ} & \tilde{K}_{OO} \end{bmatrix}_3 \begin{Bmatrix} \bar{u}_J \\ \bar{u}_O \end{Bmatrix}_3 = \begin{Bmatrix} -g \\ \mathbf{0} \end{Bmatrix} \qquad [3\text{-}46]$$

where subscripts O, I, J refer to interior, first interfacial and second interfacial degrees of freedom, respectively. Equations [3-41] through [3-46] represent a complete set of dynamic equations for the acoustic displacements and constraining forces between two adjacent media.

After some simple matrix operations to remove the constraining forces, a set of inhomogeneous governing differential equations written in terms of the modified displacement vector is given as

$$[M]_g \{\ddot{\bar{u}}\}_g + [C]_g \{\dot{\bar{u}}\}_g + [K]_g \{\bar{u}\}_g = \{Q\}_{gc} \cos\omega t + \{Q\}_{gs} \sin\omega t \qquad [3\text{-}47]$$

where,

$$\{u\}_g = \begin{Bmatrix} \{\bar{u}_O\}_1 \\ \{\bar{u}_I\}_1 \\ \{\bar{u}_O\}_2 \\ \{\bar{u}_J\}_2 \\ \{\bar{u}_O\}_3 \end{Bmatrix}, \{Q\}_{gc} = \begin{Bmatrix} \{Q\}_{1c} \\ \mathbf{0} \end{Bmatrix}, \{Q\}_{gs} = \begin{Bmatrix} \{Q\}_{1s} \\ \mathbf{0} \end{Bmatrix}$$

[3-48]

$$[M]_g = \begin{bmatrix} [M_{OO}]_1 & [M_{OI}]_1 & \mathbf{0} & \mathbf{0} & \mathbf{0} \\ [M_{IO}]_1 & [M_{II}]_1 + [R_I]^T [M_{II}]_2 [R_I] & [R_I]^T [M_{IO}]_2 & [R_I]^T [M_{IJ}]_2 & \mathbf{0} \\ \mathbf{0} & [M_{OI}]_2 [R_I] & [M_{OO}]_2 & [M_{OJ}]_2 & \mathbf{0} \\ \mathbf{0} & [M_{JI}]_2 [R_I] & [M_{JO}]_2 & [M_{JJ}]_2 + [R_J]^T [M_{JJ}]_3 [R_J] & [R_J]^T [M_{JO}]_3 \\ \mathbf{0} & \mathbf{0} & \mathbf{0} & [M_{OJ}]_3 [R_J] & [M_{OO}]_3 \end{bmatrix}$$

[3-49]

$$[K]_g = \begin{bmatrix} [\tilde{K}_{OO}]_1 & [\tilde{K}_{OI}]_1 & \mathbf{0} & \mathbf{0} & \mathbf{0} \\ [\tilde{K}_{IO}]_1 & [\tilde{K}_{II}]_1 + [R_I]^T [\tilde{K}_{II}]_2 [R_I] & [R_I]^T [\tilde{K}_{IO}]_2 & [R_I]^T [\tilde{K}_{IJ}]_2 & \mathbf{0} \\ \mathbf{0} & [\tilde{K}_{OI}]_2 [R_I] & [\tilde{K}_{OO}]_2 & [\tilde{K}_{OJ}]_2 & \mathbf{0} \\ \mathbf{0} & [\tilde{K}_{JI}]_2 [R_I] & [\tilde{K}_{JO}]_2 & [\tilde{K}_{JJ}]_2 + [R_J]^T [\tilde{K}_{JJ}]_3 [R_J] & [R_J]^T [\tilde{K}_{JO}]_3 \\ \mathbf{0} & \mathbf{0} & \mathbf{0} & [\tilde{K}_{OJ}]_3 [R_J] & [\tilde{K}_{OO}]_3 \end{bmatrix}$$

[3-50]

$$[C]_g = \begin{bmatrix} \mathbf{0} & \mathbf{0} & \mathbf{0} & \mathbf{0} & \mathbf{0} \\ \mathbf{0} & [R_I]^T [C_{II}]_2 [R_I] & [R_I]^T [C_{IO}]_2 & [R_I]^T [C_{IJ}]_2 & \mathbf{0} \\ \mathbf{0} & [C_{OI}]_2 [R_I] & [C_{OO}]_2 & [C_{OJ}]_2 & \mathbf{0} \\ \mathbf{0} & [C_{JI}]_2 [R_I] & [C_{JO}]_2 & [C_{JJ}]_2 & \mathbf{0} \\ \mathbf{0} & \mathbf{0} & \mathbf{0} & \mathbf{0} & \mathbf{0} \end{bmatrix}$$

[3-51]

3.6 Solution Procedure

To determine the steady-state propagation of a sinusoidal acoustic wave in the one-dimensional acoustic tube, one assumes a solution in the form:

$$\{u\}_g = \{u\}_c \cos \omega t + \{u\}_s \sin \omega t \qquad \text{[3-52]}$$

By substituting [3-52] into [3-47] and comparing the coefficients associated with the sine and cosine harmonics, one obtains the following:

$$\begin{bmatrix} [K]_g - \omega^2[M]_g & -\omega[C]_g \\ \omega[C]_g & [K]_g - \omega^2[M]_g \end{bmatrix} \begin{Bmatrix} \{U\}_s \\ \{U\}_c \end{Bmatrix} = \begin{Bmatrix} \{Q\}_{gc} \\ \{Q\}_{gs} \end{Bmatrix} \quad [3\text{-}53]$$

This equation can be solved for the nodal acoustic displacements and strains for the sine and cosine components. The acoustic pressure and acoustic velocity can then be determined by

$$p_k = -(\rho c^2 \varepsilon)_k = (p_c)_k \cos\omega t + (p_s)_k \sin\omega t \quad [3\text{-}54]$$

$$v_k = \dot{u}_k = (\dot{u}_c)_k \cos\omega t + (\dot{u}_s)_k \sin\omega t \quad [3\text{-}55]$$

where $(p_c)_k = -(\rho c^2 \varepsilon_c)_k$, $(p_s)_k = -(\rho c^2 \varepsilon_s)_k$, $\dot{u}_k = du_k/dt$, and subscripts s and c represent the sine and cosine components, respectively.

It is often helpful to give the acoustic pressure in the complex domain as follows:

$$p_k = \mathrm{Re}\{\hat{p}_k e^{-i\omega t}\} \quad [3\text{-}56]$$

It can be shown that the real and imaginary parts, $(\hat{p}_{\mathrm{Re}})$ and $(\hat{p}_{\mathrm{Im}})$, of the complex acoustic pressure are related to the sine and cosine coefficients in [3-54] by

$$\begin{aligned} (\hat{p}_{\mathrm{Re}})_k &= (p_c)_k \\ (\hat{p}_{\mathrm{Im}})_k &= (p_s)_k \end{aligned} \quad [3\text{-}57]$$

Similar relationships hold for other acoustic quantities such as acoustic displacements and acoustic velocities.

3.7 Finite Element Program

It is necessary to validate the finite element procedure formulated here. To do so, the procedure must be implemented and a series of test cases explored for which exact analytical solutions exist for comparison. It was decided that MATLAB would be used to code the finite element procedure.

MATLAB is an integrated technical computing environment that combines numeric computation, advanced graphics and visualization, and a high-level programming language. It is especially designed for, and contains algorithms to carry out, matrix computations, namely, solving systems of linear equations, computing eigenvalues and eigenvectors, factoring matrices, etc., thus making it ideal for programming the finite element technique.

The technique was coded using various modules to increase the versatility of the program, and ease program debugging. The modules used were: input, element equations, global equations, solution, and post processing. All the pertinent system information was defined in the input module. This information was passed onto the element equations module where the mass, stiffness, and damping matrices describing each component in the acoustic system were developed. The global equations module assembled the various element matrices into a single mass, stiffness, and damping matrix describing the system as a whole. The solution module solved the developed system of equations, outputting the pressure and velocity field of the acoustic system. The post-processing module manipulated these data to calculate acoustic parameters such as impedance, absorption coefficient, and transmission loss. Flow charts detailing the operation of the finite element code can be found in Appendix D.

CHAPTER FOUR – RESULTS AND DISCUSSION

It is necessary to validate the finite element procedure before the methodology can be applied to more general acoustics problems. This is done through a series of test cases for which exact analytical solutions exist. Following validation, the method can be applied to practical sound transmission loss problems.

4.1 Impedance Tube

The first test case deals with the propagation of sound through a column of air within a hollow rigid tube and the interaction of the sound with an acoustic material, characterized by a specific acoustic impedance, Z*, at the end of the tube, as shown in Figure 4-1.

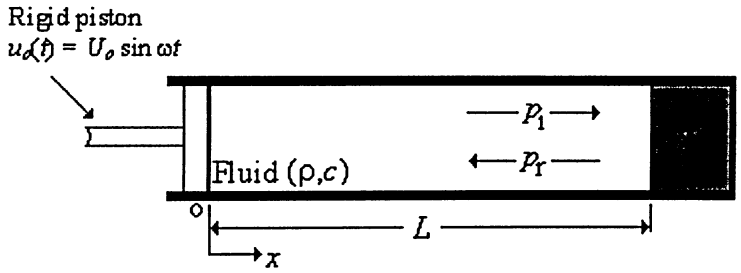

Figure 4-1 – Impedance Tube

The air is excited by an oscillating piston, for which the displacement is defined as:

$$u_o(t) = U_o \sin \omega t$$

where $\omega = 2\pi f$. The piston's velocity is given by:

$$v_o(t) = du_o/dt = U_o \omega \cos \omega t$$
$$= V_o \cos \omega t$$

A portion of the resulting acoustic energy is absorbed by the acoustic material as dictated by its specific acoustic impedance, Z^*, defined as

$$Z^* = Z_R^* + iZ_I^* = \frac{\hat{p}(L)}{\hat{v}(L)}$$

where $\hat{p}(L)$ and $\hat{v}(L)$ are complex values of pressure and velocity, respectively, at the end of the tube.

Under steady state conditions, the combination of incident and reflected waves within the tube creates a standing wave. The exact analytical solution for the complex pressure everywhere is given in Appendix A.

Finite Element Solution

In the displacement-based model, the acoustic material, which has resistive and reacting components, is equivalent to a massless piston subjected to the constraints of a linear spring and viscous damping elements (k_a and d_a), as shown in Figure 4-2.

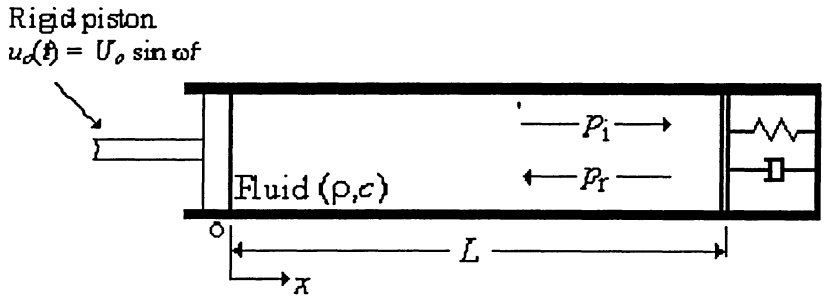

Figure 4-2 - Impedance tube. Equivalent representation for use in the finite element procedure

The equilibrium condition of the massless piston yields the following relationship:

$$p(L) = k_a u(L) + d_a v(L) \qquad \text{[4-1]}$$

where $p(L)$, $u(L)$ and $v(L)$ represent the pressure, displacement and velocity at the air-solid interface. To determine the relationship between the acoustic impedance and the values of k_a and d_a, these values are defined as:

$$p(L) = \mathrm{Re}\left\{\hat{p}(L)e^{-i\omega t}\right\}$$

$$u(L) = \mathrm{Re}\left\{\hat{u}(L)e^{-i\omega t}\right\} \qquad [4\text{-}2]$$

$$v(L) = \mathrm{Re}\left\{\hat{v}(L)e^{-i\omega t}\right\}$$

where $\hat{p}_L$, $\hat{u}_L$ and $\hat{v}_L$ are, respectively, the complex amplitudes of the harmonic acoustic pressure, displacement and velocity at the air-solid interface. [4-1] can be re-written in complex form by substituting [4-2] as follows

$$\hat{p}(L) = k_a\hat{u}(L) + d_a\hat{v}(L) \qquad [4\text{-}3]$$

To obtain the values of the reactance and resistance coefficients from the real and imaginary parts of the specified acoustic impedance, the relationship between complex displacement and complex velocity is used. This relationship is as follows:

$$\hat{u}(L) = \frac{\hat{v}(L)}{-i\omega} \qquad [4\text{-}4]$$

Combination of [4-3] and [4-4] yields:

$$\frac{\hat{p}(L)/\rho c}{\hat{v}(L)} = \frac{k_a}{\rho c\omega}i + \frac{d_a}{\rho c} \qquad [4\text{-}5]$$

Thus, it follows that:

$$\frac{k_a}{\rho c\omega} = Z_I^*, \quad \frac{d_a}{\rho c} = Z_R^* \qquad [4\text{-}6]$$

and,

$$k_a = Z_I^*\rho c\omega, \quad d_a = Z_R^*\rho c \qquad [4\text{-}7]$$

The reactance and resistance coefficients are incorporated into the finite element formulation by adding them to the global stiffness and damping values associated with the node at the air-solid interface.

4.1.1 FEM Validation

Numerical results were obtained using eight three-node finite elements and the analytical solution in [3-54] for two different sets of parameters, which are given in Table 4-1. The real and imaginary parts of the *spatial* component of the acoustic pressure field

along the entire length of the one-dimensional air column are compared in Figure 4-3 through Figure 4-6.

Table 4-1 – FEM Validation test cases

System			
		Case 1	**Case 2**
Density	$\rho\ (kg/m^3)$	1.2	1.2
Speed of Sound	$c\ (m/s)$	341	341
Input Velocity	$U_0\ (m/s)$	0.01	0.01
Frequency	$f\ (Hz)$	1000	1000
Length	$L\ (m)$	1.705	1.6709
Impedance		4+0i	4+3i

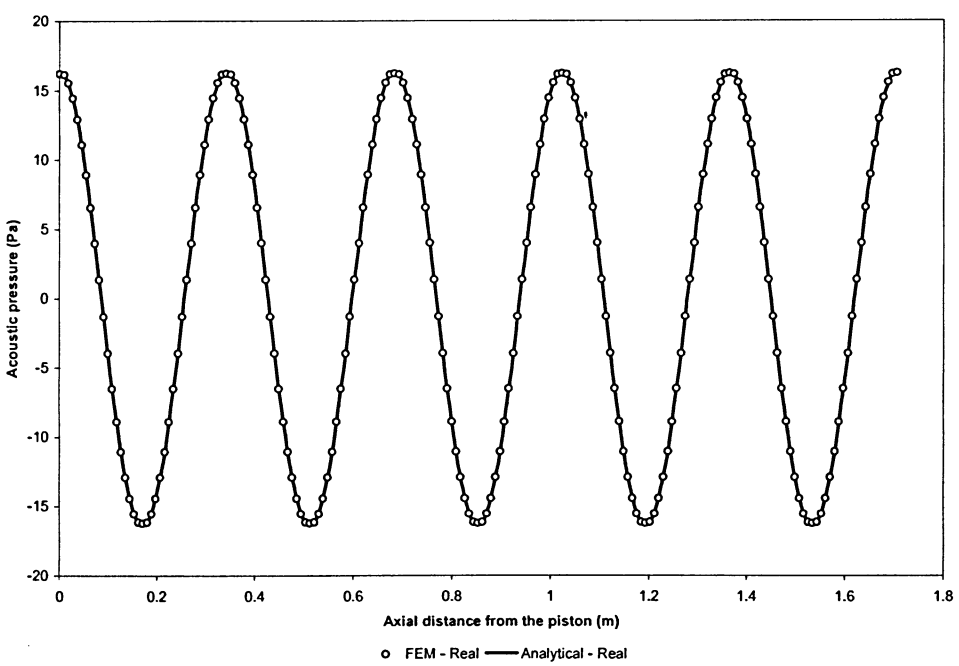

Figure 4-3 Case 1- Real pressure field, (n=8)

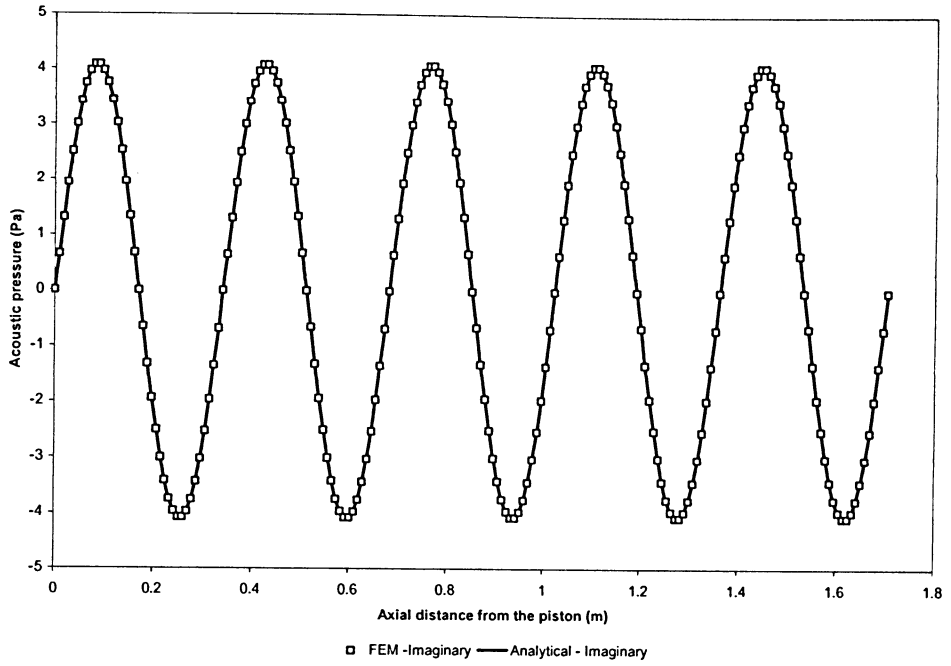

Figure 4-4 Case 1 - Imaginary pressure field, (n=8)

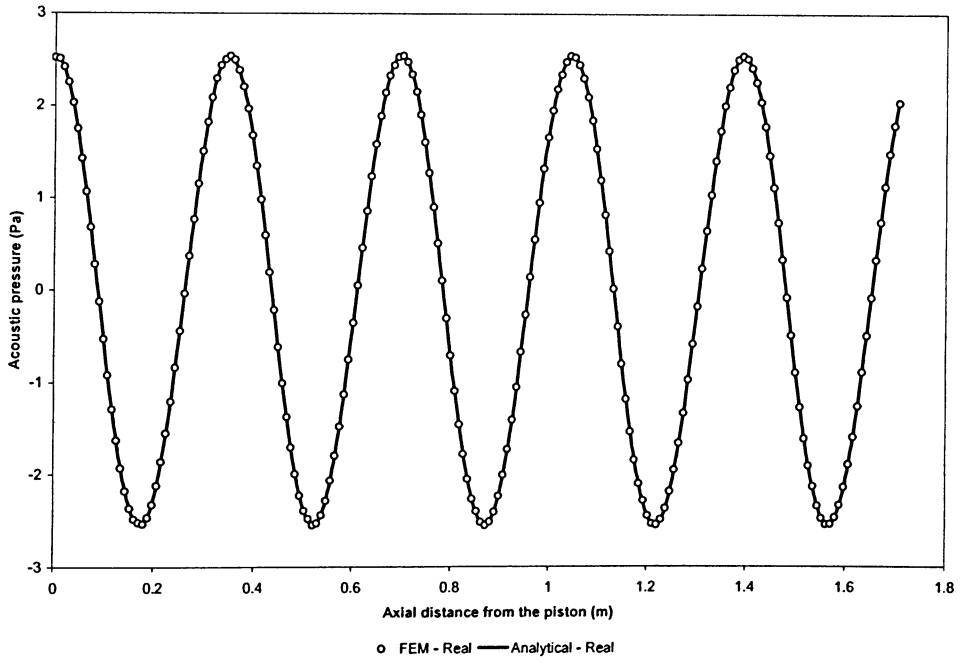

Figure 4-5 Case 2- Real pressure field, (n=8)

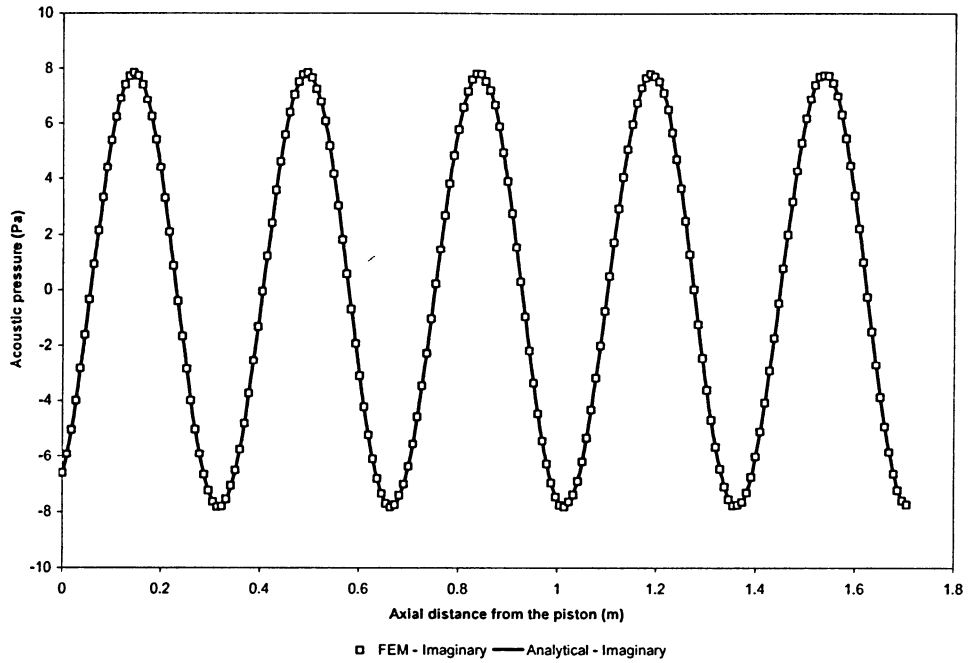

Figure 4-6 Case 2 - Imaginary pressure field, (n=8)

It can be seen that the results from the finite element procedure are in excellent agreement with the analytical solutions. The RMS error, using 8 finite elements, is much less than 1% across the pressure field in each case. This error is defined as:

$$E = 100 \times \sqrt{\sum_{i=1}^{N_p} \left(\frac{P_{FEM} - P_{ANAL}}{P_{ANAL}} \right)_i^2 \Big/ N_p} \qquad [4\text{-}8]$$

where P_{FEM} is the FEM pressure, P_{ANAL} is the analytical pressure, and N_p is the number of axial positions considered.

4.1.2 Sensitivity Analysis

Having confirmed that the finite element procedure is capable of predicting the standing wave pressure field in the impedance tube accurately, it is necessary to perform a sensitivity analysis to optimize the computational efficiency of this technique.

It can be assumed that the number of elements required for an accurate finite element solution is based on the number of waves present in the system. The frequency and length are therefore the determining factors in calculating an appropriate finite element mesh. The sensitivity analysis is carried out using the system parameters given in

Table 4-2. By varying the oscillation frequency of the piston and the number of elements used in the solution, one can determine the number of elements required to accurately describe a single wave.

Table 4-2 – System parameters for sensitivity study

System		
		Sensitivity
Density	$\rho\ (kg/m^3)$	1.2
Speed of Sound	$c\ (m/s)$	341
Input Velocity	$U_0\ (m/s)$	0.01
Length	$L\ (m)$	1.55
Impedance		4+3i
Frequency	$f\ (Hz)$	Variable
Number of Elements	n	Variable

For the given system, the RMS error propagation for both the pressure amplitude and phase angle is shown in Figure 4-7. As expected, increasing the number of elements in the finite element mesh increases the accuracy of the solution.

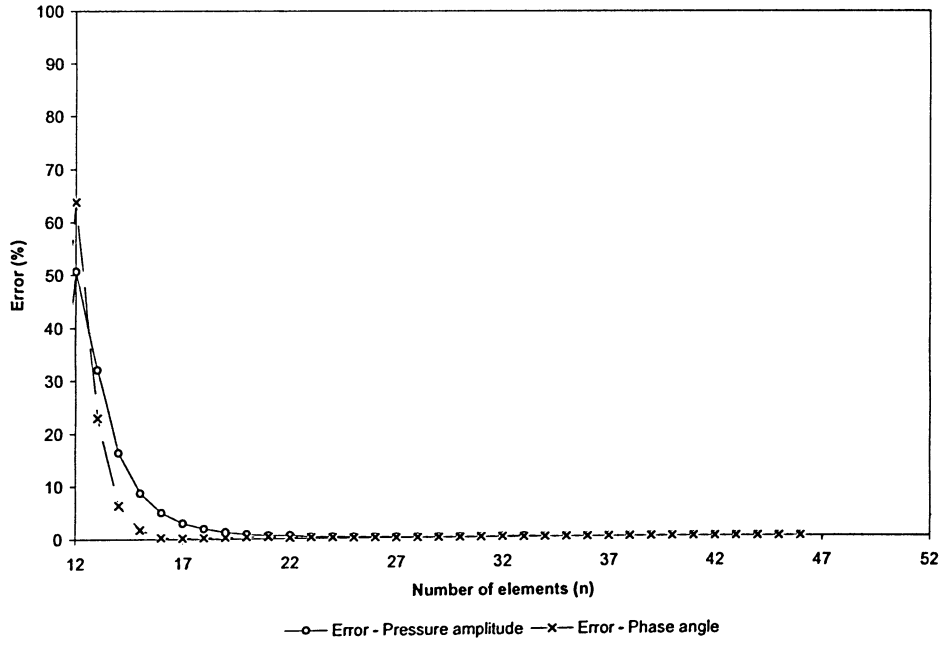

Figure 4-7 Error propagation of finite element scheme

For this system, less than a 20% RMS error required at least 14 elements, less than 10% RMS error required at least 16 elements and less than a 1% RMS error required at least 21 elements. Figure 4-8 and Figure 4-9 depict the various RMS errors associated with the pressure amplitude and phase angle. The element requirements for the system with a varying number of waves can be seen in Figure 4-10. This figure shows that the relationship between the number of waves (N_w) in a column of air of length L, and the number of three-node finite elements (n) required to described the system with a prescribed error (E%) relative to the analytical solution is essentially linear, with:

$$n(1\%)/N_w \approx 2$$

$$n(10\%)/N_w \approx 1.5$$

and,

$$n(20\%)/N_w \approx 1.2$$

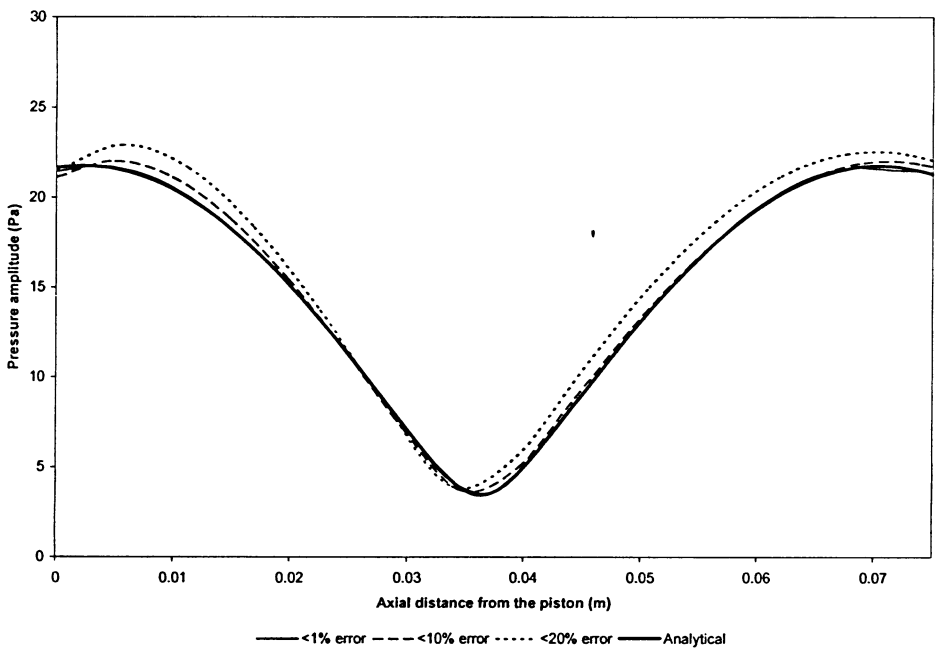

Figure 4-8 Comparison of RMS errors associated with pressure amplitude for a single wave

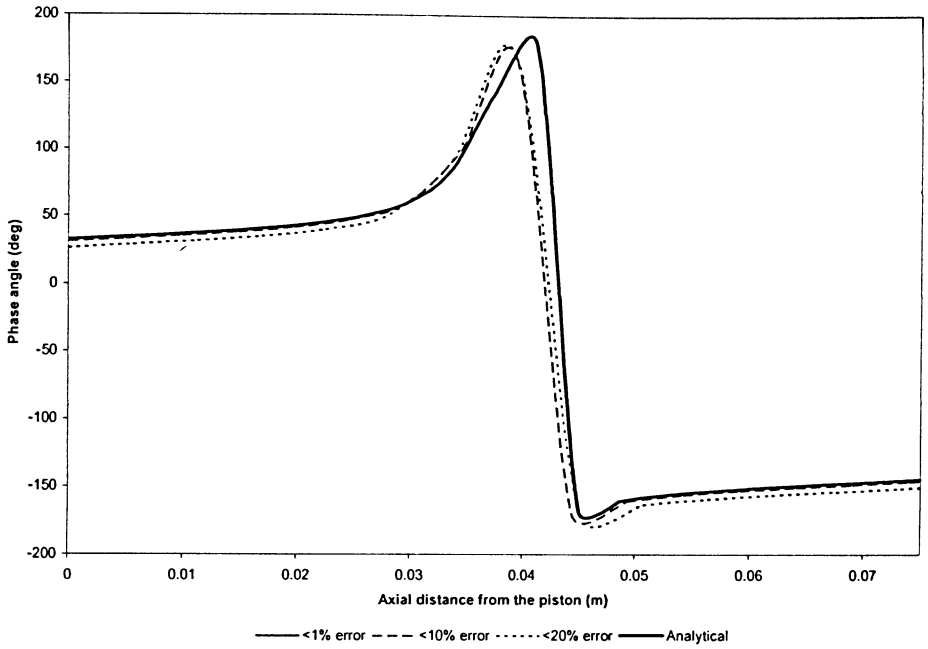

Figure 4-9 Comparison of RMS errors associated with the phase angle for a single wave

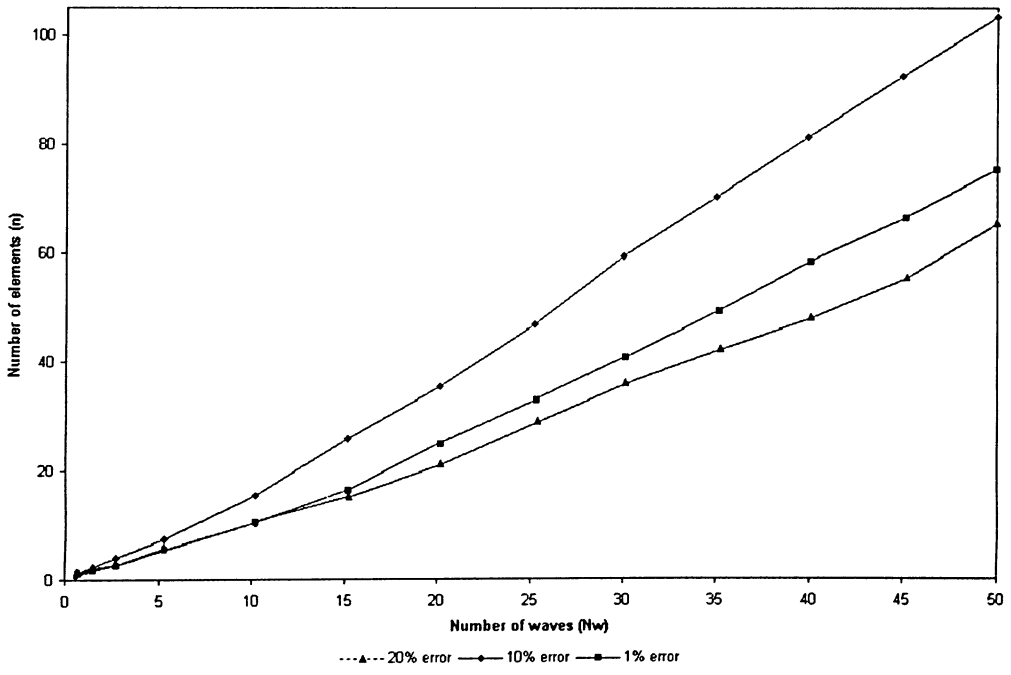

Figure 4-10 – Variation of element requirements with number of waves for a solution accuracy within 1%, 10%, and 20%

The wave length in a system can be calculated from:

$$\lambda = \frac{c}{f} \qquad [4\text{-}9]$$

Knowing the wave length, the number of waves present in the air column can be calculated from:

$$N_w = \frac{L}{\lambda} \qquad [4\text{-}10]$$

Hence, the element requirements are given by:

$$n_{req}(1\%) \approx \frac{2L}{\lambda} \qquad [4\text{-}11]$$

$$n_{req}(10\%) \approx \frac{1.5L}{\lambda} \qquad [4\text{-}12]$$

and,

$$n_{req}(20\%) \approx \frac{1.2L}{\lambda} \qquad [4\text{-}13]$$

The choice of a three-node higher order finite element was driven by the desire for high computational efficiency. For comparison, a two-node element was used to solve the same system and the error propagation can be seen in Figure 4-11. A comparison of Figure 4-7 and Figure 4-11 shows that nearly 25 times the number of elements are required to produce results within 20%, 10% and 1% RMS error when compared with the three-node higher order element used in this thesis. The element requirements for the two-node scheme are not only computationally demanding, but the use of so many elements can cause errors in the stiffness matrix because the system becomes over constrained. The length of each element becomes much smaller than its area, and this can artificially increase the stiffness of each element leading to poor results.

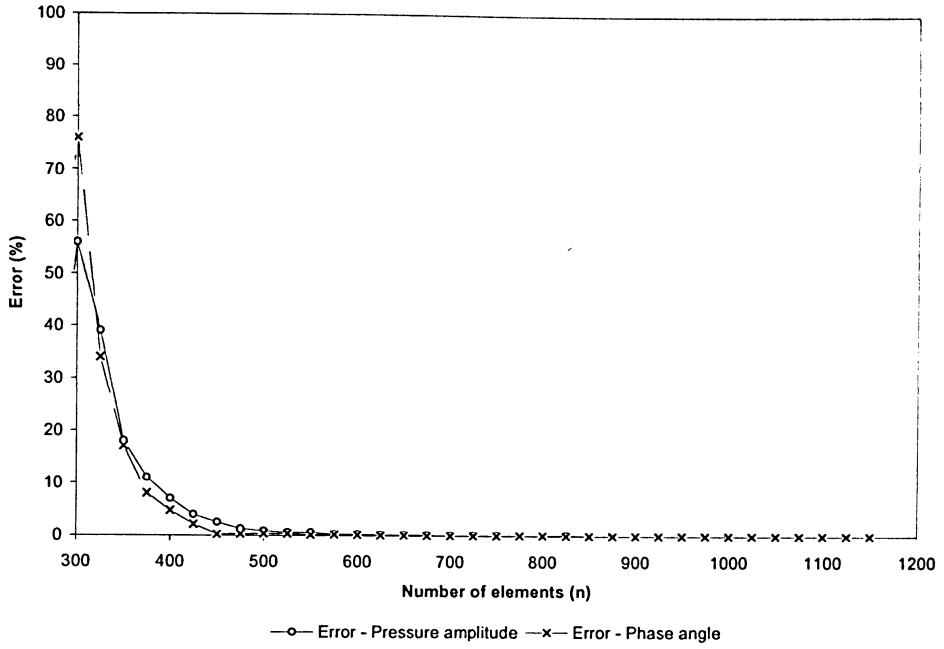

Figure 4-11 - Error propagation of two-node finite element scheme

To further validate the finite element model, it is prudent to investigate the effects of varying parameters such as length, frequency and impedance to ensure the methodology is accurate for a wide range of systems.

4.1.3 Effect of Length

To show the finite element method is valid for systems of varying length, numerical results were obtained using twelve three-node finite elements and the analytical solution derived in Appendix A for two different sets of parameters, which are given in Table 4-3. The pressure amplitude and phase along the entire length of the one-dimensional air column are compared in Figure 4-12 through Figure 4-15.

Table 4-3 – System parameters for studying the effect of length

System			
		Case L1	**Case L2**
Density	$\rho\ (kg/m^3)$	1.2	1.2
Speed of Sound	$c\ (m/s)$	341	341
Input Velocity	$U_0\ (m/s)$	0.01	0.01
Frequency	$f\ (Hz)$	1000	1000
Length	$L\ (m)$	1.5	2.0
Impedance		4+3i	4+3i

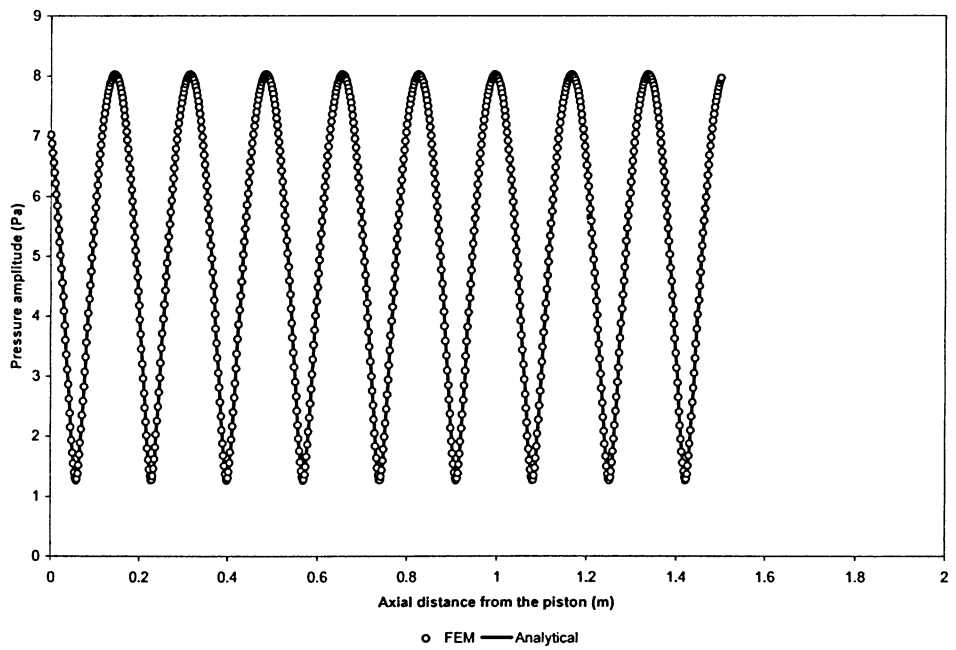

Figure 4-12 Case L1 - Pressure amplitude, (n=12)

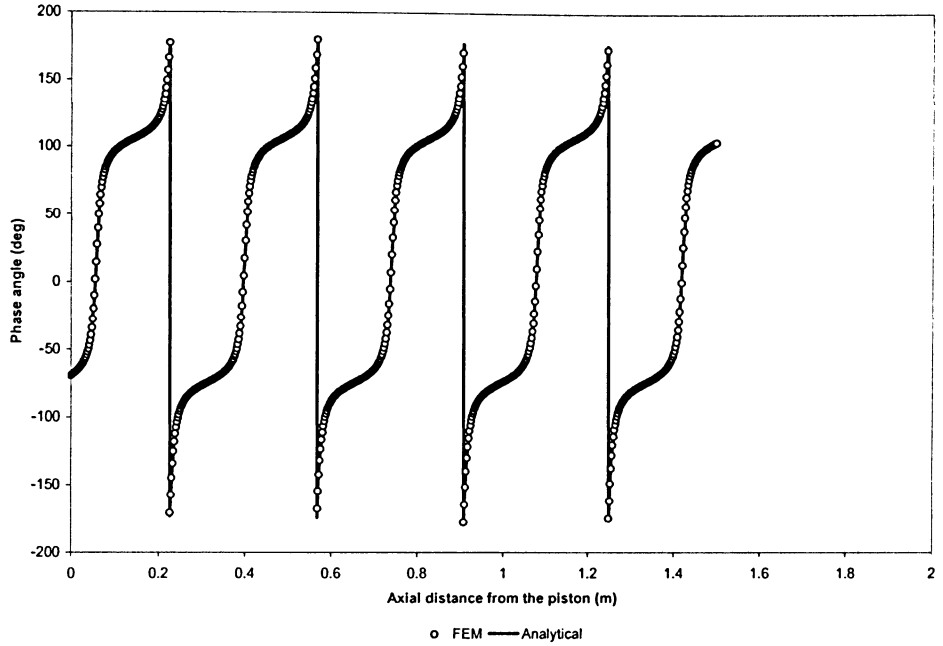

Figure 4-13 Case L1 - Phase angle, (n=12)

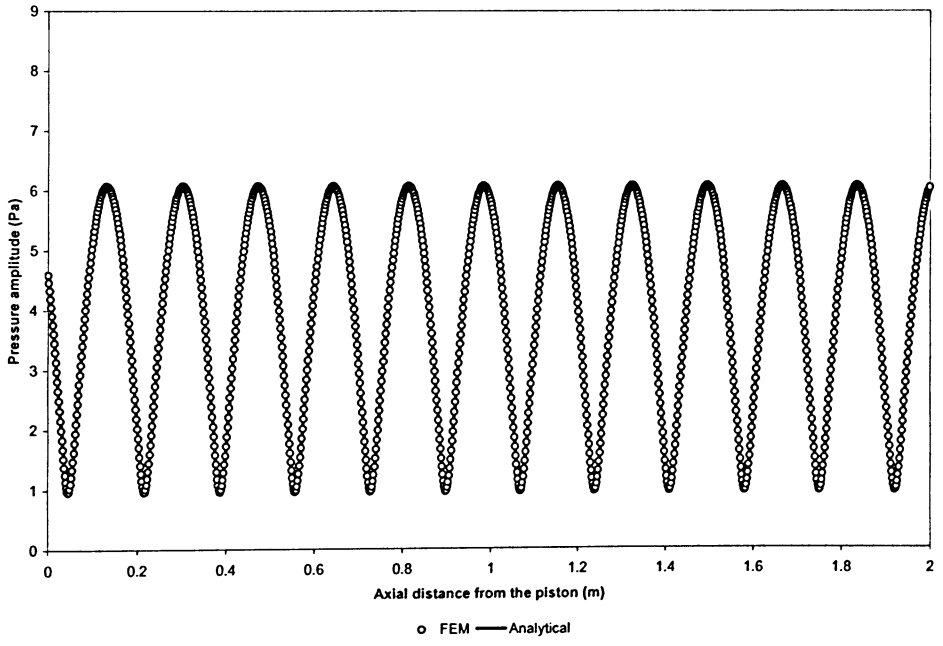

Figure 4-14 Case L2 - Pressure amplitude, (n=12)

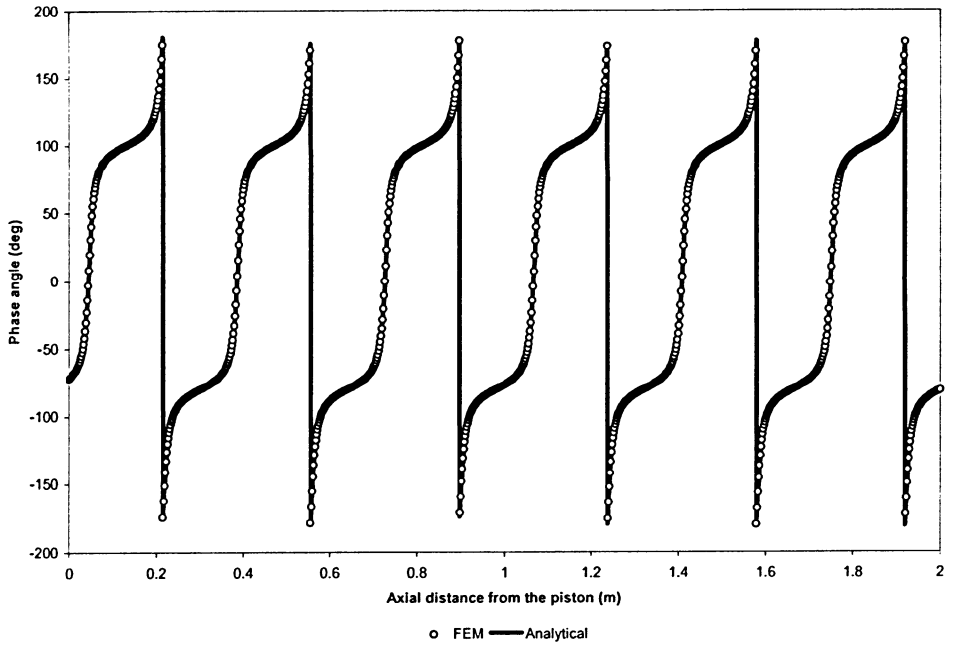

Figure 4-15 Case L2 - Phase angle, (n=12)

Again, it can be seen that the results from the finite element procedure are in good agreement with the analytical solutions. The RMS error, using twelve elements, is less than 1% for both the pressure amplitude and phase angle in each case. To gain further insight into the effect of tube length on the pressure field, and to further validate the finite element model, the peak pressure amplitude is plotted against various tube length for the system described in Table 4-4.

Table 4-4 - System parameters for studying the effect of length on peak pressure

System		
		Case L3
Density	$\rho\ (kg/m^3)$	1.2
Speed of Sound	$c\ (m/s)$	341
Input Velocity	$U_0\ (m/s)$	0.01
Frequency	$f\ (Hz)$	1000
Length	$L\ (m)$	Variable
Impedance		4+3i

A plot of the peak pressure amplitude versus tube length is shown in Figure 4-16 for tubes of length 1.4 m to 1.8 m, where a solution is obtained from the finite element

method at 0.005 m intervals. The results show that the peak pressure amplitude varies with length and oscillates in a repeating manner between a maximum of approximately 25 Pa, and a minimum of approximately 4 Pa. The pattern was shown to repeat for lengths outside of the bounds of this plot, 1 m through 10 m. It can be seen that the finite element solution predicts the peak pressure amplitude pattern and is in good agreement with the analytical solution.

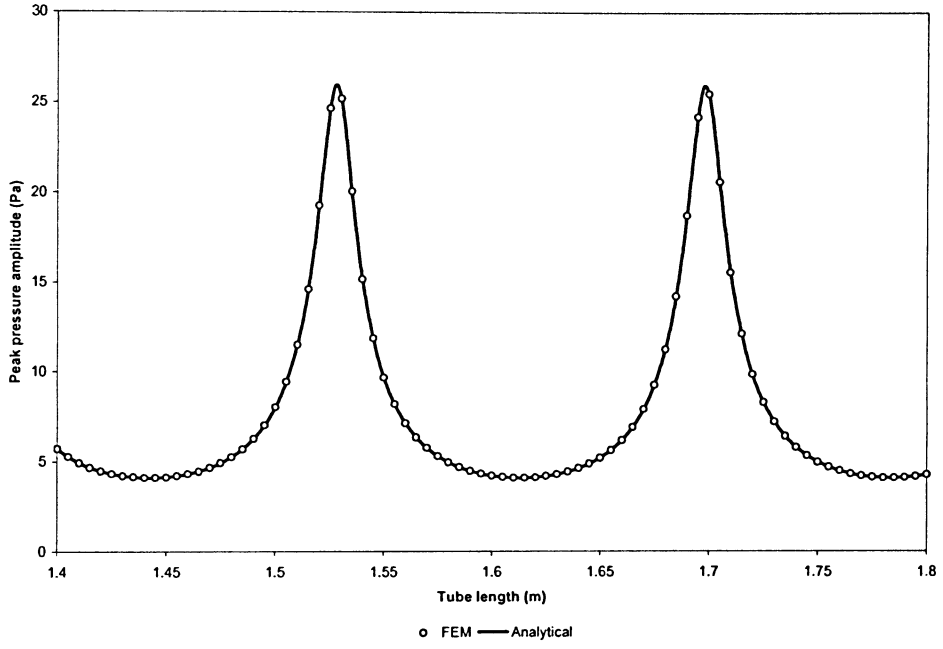

Figure 4-16 Case L3 - Effect of varying tube length on peak pressure amplitude (n=12)

From this, it can be concluded that the accuracy of the finite element method is unaffected by changes in tube length provided an appropriate number of elements are used to model the system.

4.1.4 Effect of Frequency

To show the finite element method is valid for systems of varying frequency, numerical results were obtained using three-node finite elements and the analytical solution for two different sets of parameters, which are given in Table 4-5. The pressure amplitude and phase along the entire length of the one-dimensional air column are compared in Figure 4-17 through Figure 4-20.

Table 4-5 - System parameters for studying the effect of frequency

System			
		Case F1	**Case F2**
Density	$\rho\ (kg/m^3)$	1.2	1.2
Speed of Sound	$c\ (m/s)$	341	341
Input Velocity	$U_0\ (m/s)$	0.01	0.01
Frequency	$f\ (Hz)$	1000	2000
Length	$L\ (m)$	1.55	1.55
Impedance		4+3i	4+3i

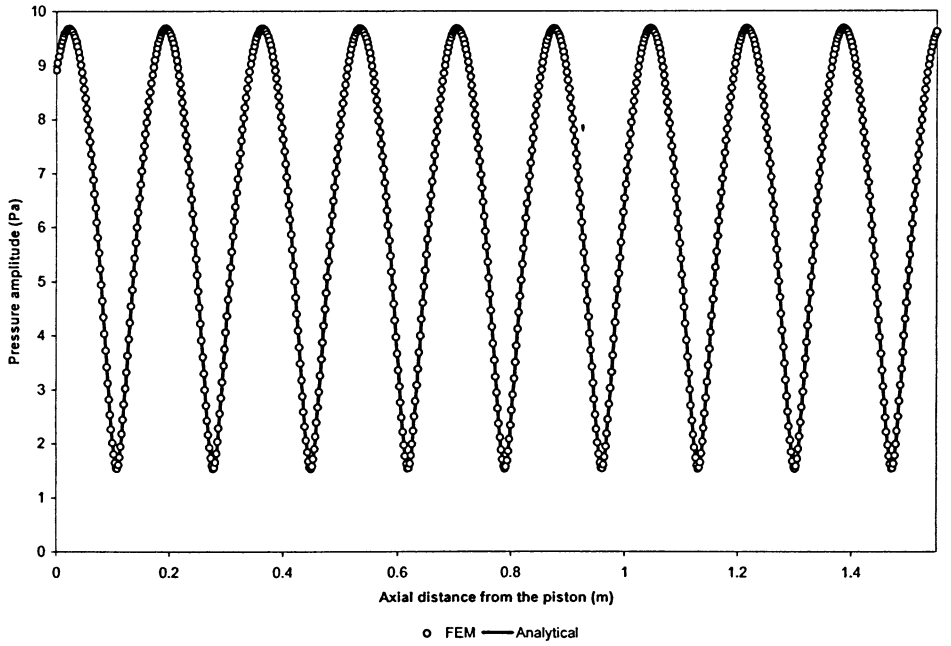

Figure 4-17 Case F1 – Pressure amplitude, (n=10)

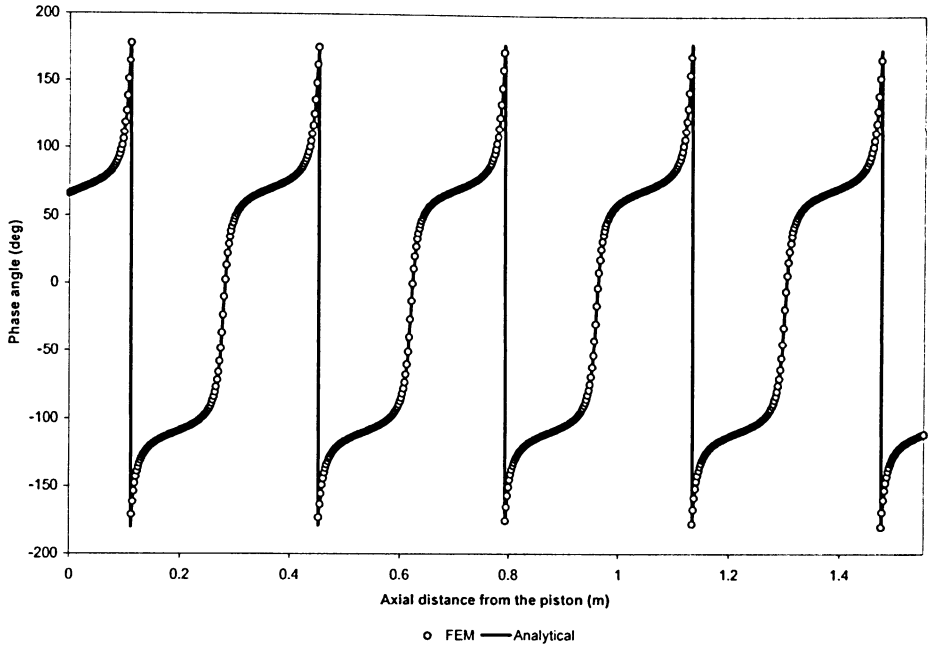

Figure 4-18 Case F1 - Phase angle, (n=10)

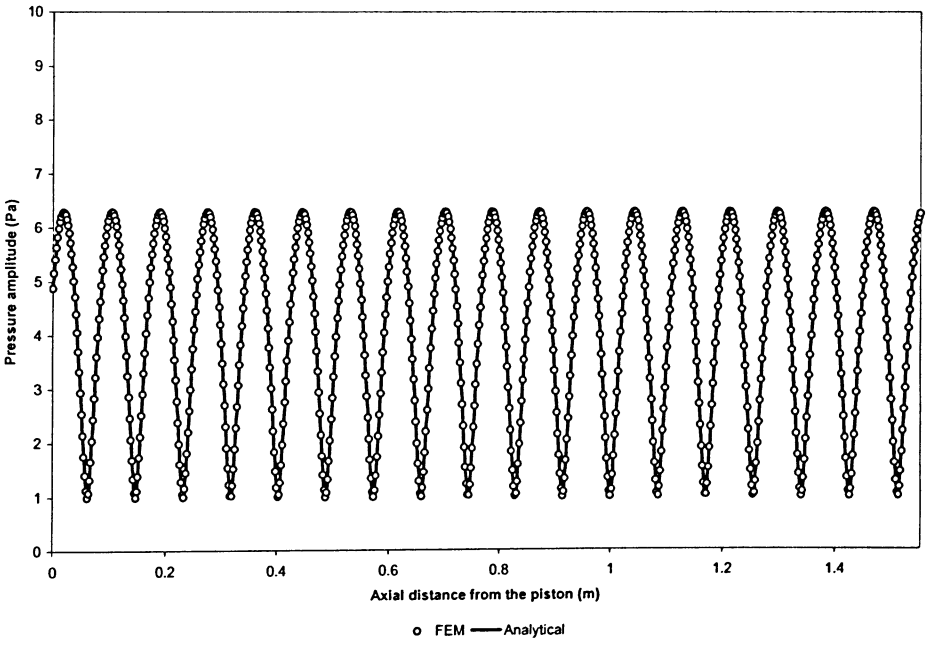

Figure 4-19 Case F2 – Pressure amplitude, (n=20)

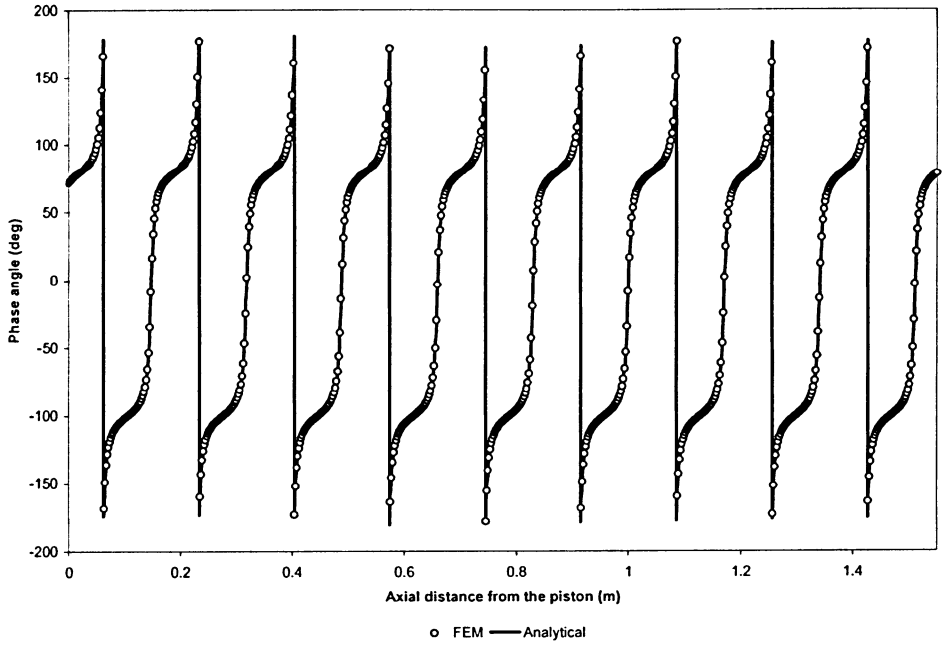

Figure 4-20 Case F1 - Phase angle, (n=20)

Again, it can be seen that the results from the finite element procedure are in good agreement with the analytical solutions. The RMS error is less than 1% for both the pressure amplitude and phase angle in each case. Further validation and insight into the effect of frequency on the accuracy of the finite element solution, peak pressure amplitude and phase angle can be gained by plotting the peak pressure amplitude against frequency for the system described in Table 4-6.

Table 4-6 - System parameters for studying the effect of frequency on peak pressure

System		
		Case F3
Density	$\rho\ (kg/m^3)$	1.2
Speed of Sound	$c\ (m/s)$	341
Input Velocity	$U_0\ (m/s)$	0.01
Frequency	$f\ (Hz)$	Variable
Length	$L\ (m)$	1.55
Impedance		4+3i

A plot of the peak pressure amplitude versus frequency is shown in Figure 4-21 for a frequency range of 1000 Hz to 2000 Hz, where a solution is obtained from the finite element method at 10 Hz intervals. The number of elements used in the finite element

solution was varied between 10 (1000 Hz) and 20 (2000 Hz) depending on the frequency, according to the sensitivity analysis in section 4.1.2. The results show that the peak pressure amplitude varies with frequency and oscillates in a repeating manner between a maximum of approximately 25 Pa, and a minimum of approximately 4 Pa. The pattern was shown to repeat for frequencies outside of the bounds of this plot, 1 Hz through 10,000 Hz. It can be seen that the finite element solution predicts the peak pressure amplitude pattern and is in good agreement with the analytical solution.

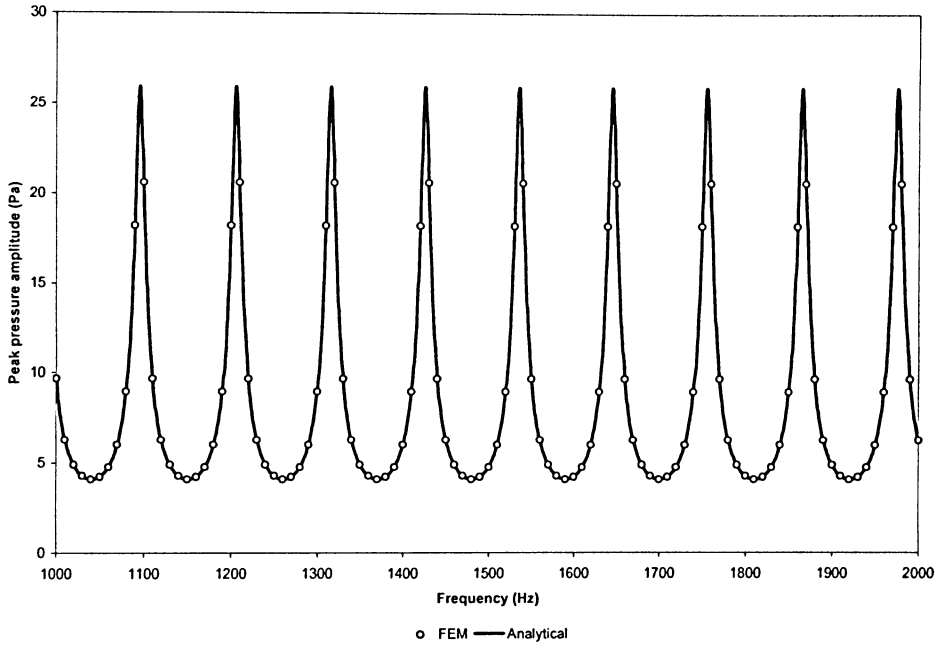

Figure 4-21 Case L3 - Effect of varying frequency on peak pressure amplitude (n varies with frequency from 10 to 20)

It can be concluded that the accuracy of the finite element method is unaffected by changes in frequency, for a range of 0 Hz to 10,000 Hz, provided that an appropriate number of elements are used to model the system

4.1.5 Effect of Impedance

To show the finite element method is valid for systems of varying acoustic impedance, numerical results were obtained using a varying number of three-node finite elements and the analytical solution derived in Appendix A for two different sets of

parameters, which are given in Table 4-7. The pressure amplitude and phase along the entire length of the one-dimensional air column are compared in Figure 4-22 through Figure 4-25.

Table 4-7 - System parameters for studying the effect of impedance

System			
		Case I1	**Case I2**
Density	$\rho\ (kg/m^3)$	1.2	1.2
Speed of Sound	$c\ (m/s)$	341	341
Input Velocity	$U_0\ (m/s)$	0.01	0.01
Frequency	$f\ (Hz)$	1000	1000
Length	$L\ (m)$	1.55	1.55
Impedance		12+1.2i	1.2+12i

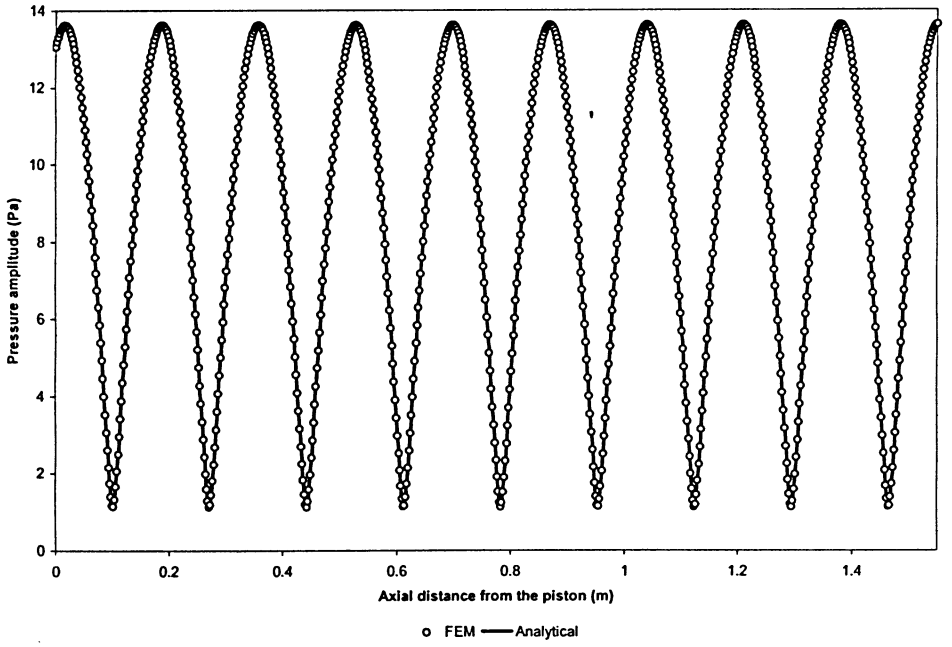

Figure 4-22 Case I1 – Pressure amplitude, (n=10)

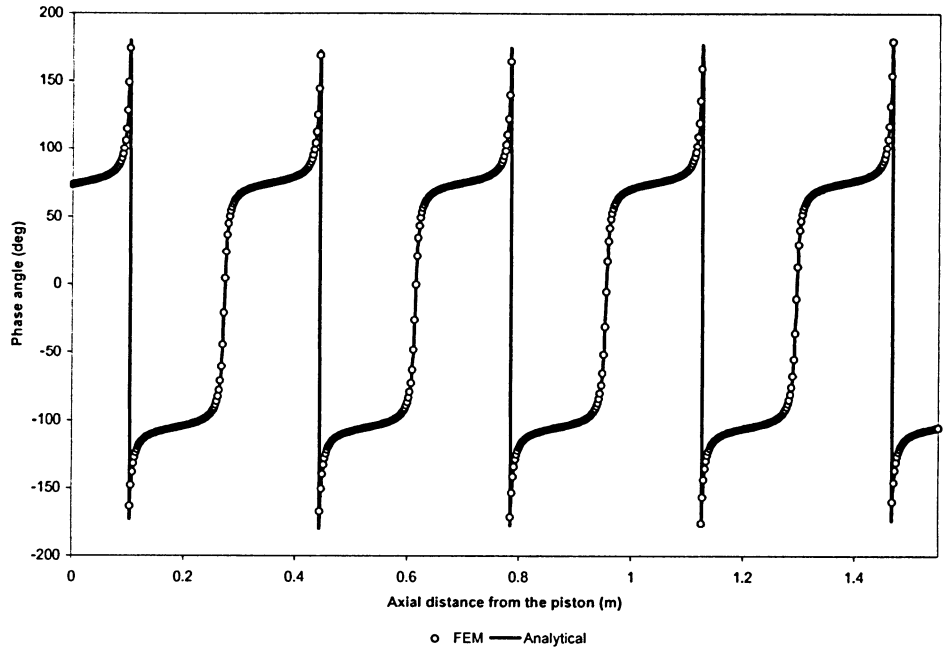

Figure 4-23 Case I1 - Phase angle, (n=10)

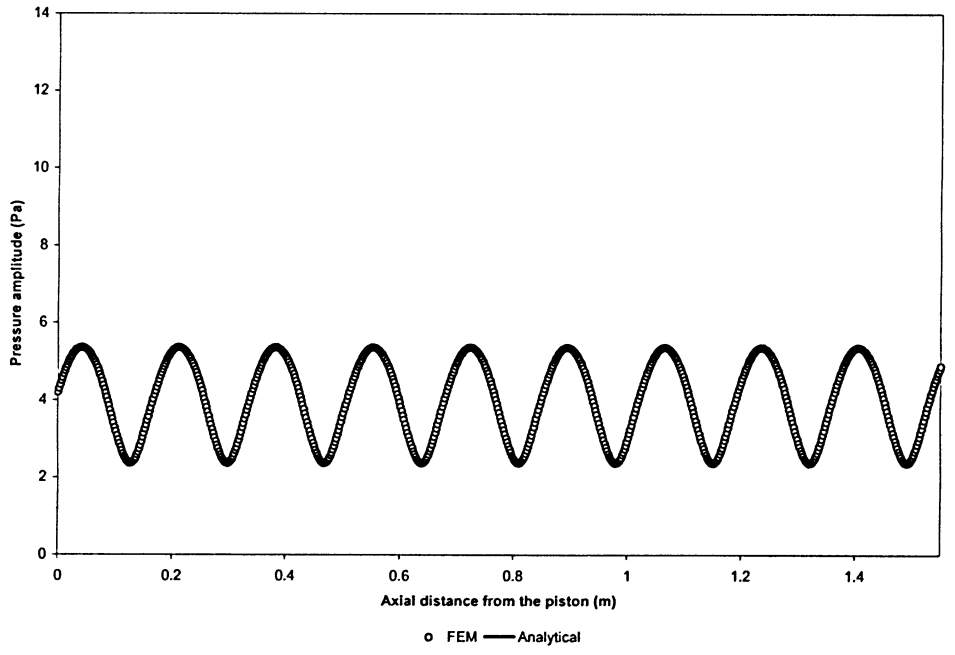

Figure 4-24 Case I2 – Pressure amplitude, (n=10)

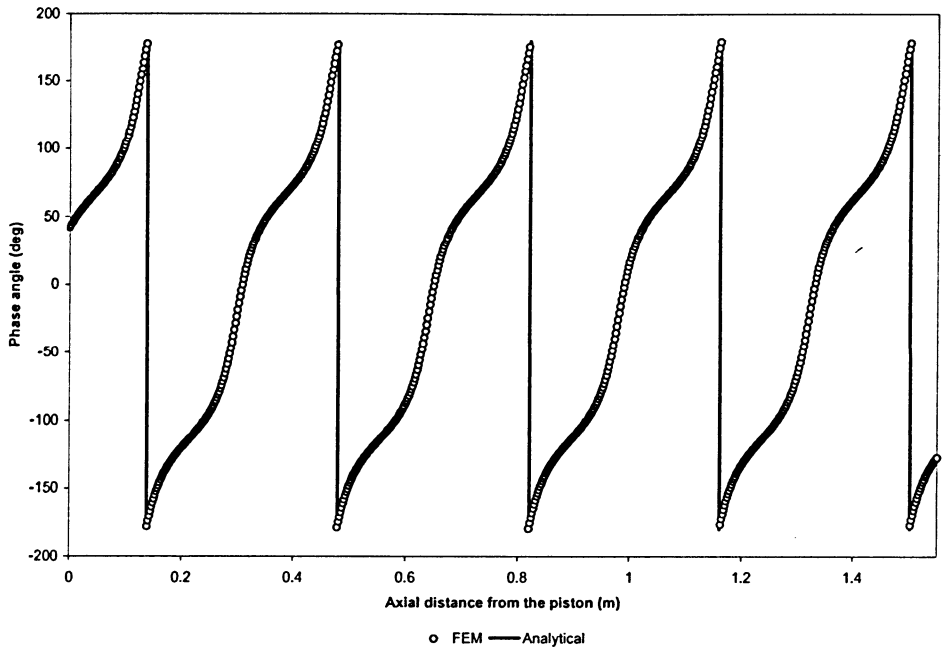

Figure 4-25 Case I1 - Phase angle, (n=10)

It can be seen that the results from the finite element procedure are in good agreement with the analytical solutions. The RMS error is less than 1% for both the pressure amplitude and phase angle in each case. Further validation and insight into the effect of impedance on the accuracy of the finite element solution, peak pressure amplitude and phase angle can be gained by plotting the peak pressure amplitude for various real and imaginary impedances for the system described in Table 4-8.

A plot of the peak pressure amplitude versus the real component of impedance is shown in Figure 4-26 for a real impedance range of 0.01 to 15, where a solution is obtained from the finite element method at intervals of 0.5. The result shows that the peak pressure amplitude increases with increasing real impedance (increasing spring constant) signifying that as the real impedance increases, less energy is absorbed by the material. It can be seen that, again, the finite element solution is in good agreement with the analytical solution.

Table 4-8 - System parameters for studying the effect of impedance on peak pressure

System			
		Case I3	**Case I4**
Density	$\rho\ (kg/m^3)$	1.2	1.2
Speed of Sound	$c\ (m/s)$	341	341
Input Velocity	$U_0\ (m/s)$	0.01	0.01
Frequency	$f\ (Hz)$	1000	1000
Length	$L\ (m)$	1.55	1.55
Impedance		(Variable)+3i	4+(Variable)i

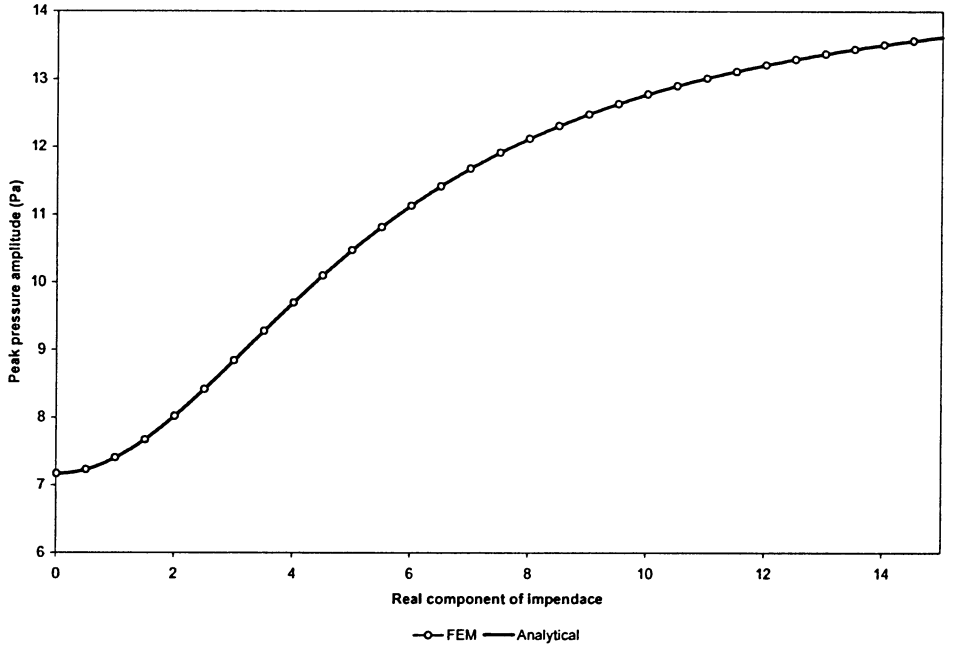

Figure 4-26 Case I3 - Effect of varying the real component of impedance on peak pressure amplitude (n=10)

Figure 4-27 shows a plot of the peak pressure amplitude versus the imaginary component of impedance for an imaginary impedance range of 0.01 to 15, where a solution is obtained from the finite element method at intervals of 0.5. The result shows that the peak pressure amplitude initially decreases, signifying that the imaginary

component of the impedance aids in absorption, as expected. However, as the imaginary impedance increases beyond 3.5, the peak pressure amplitude increases because the system becomes over-damped, effectively increasing the acoustic resistance. The finite element solution is clearly in good agreement with the analytical solution.

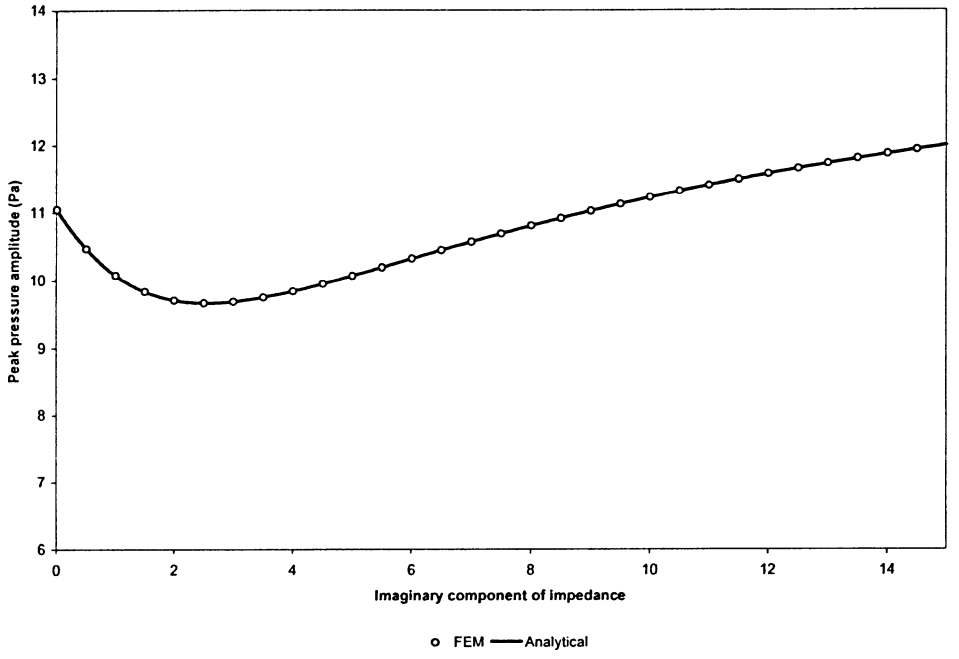

Figure 4-27 Effect of varying the imaginary component of impedance on peak pressure amplitude (n=10)

It can be concluded that the accuracy of the finite element method is unaffected by changes the real and imaginary components impedance of the absorbing material, provided an appropriate number of elements are used to model the system.

4.2 Sound Absorption

Sound absorption is an important aspect of noise control which has applications to a wide range of acoustic problems. To study sound absorption in a porous medium of finite length, which does not bend, an acoustic system having two components, air I and a porous solid II, as depicted in Figure 4-28, is investigated.

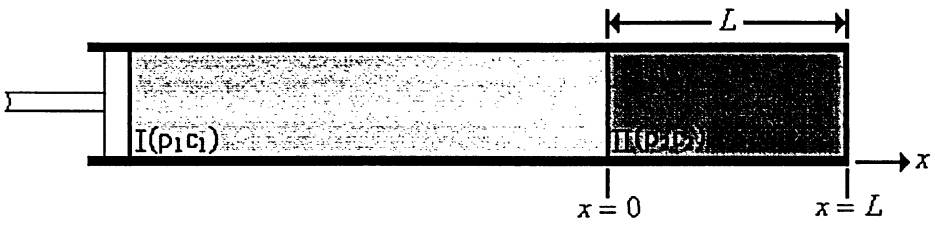

Figure 4-28 – Two component system used for sound absorption analysis

In this system, the air is excited by an oscillating piston with specified velocity amplitude and excitation frequency. The incident wave, initially traveling in the positive x-direction, impinges on the boundary between air I and porous solid II located at $x = 0$. A reflected wave is generated in air I and a transmitted wave is generated in porous solid II. At the right end of the porous material, $x = L$, the sound terminates. So, a portion of the sound energy transmitted to the porous material is absorbed by the material, and the rest is reflected back into air I. The system will reach a steady state when the rate that sound energy is reflected back into air I plus the rate at which it is absorbed by porous solid II equals the rate of arrival of the incident energy. For this steady state condition, the absorption coefficient of the material can be calculated. For the system described above, under steady state conditions, the exact analytical solution is given by equation [B-72], which involves the specific acoustic impedance of the porous material, and equation [B-73], which involves the specific acoustic impedance at the location of the piston. The latter impedance is referred to as the *input* specific acoustic impedance of the system. Both equations give the same results because, physically, there is no absorption of acoustic energy in the air, i.e., the air does not affect the absorption process in the porous material.

Finite Element Solution

To calculate the absorption coefficient of the porous material using the finite element method, a unit velocity amplitude is prescribed at the piston, for convenience. The acoustic impedance is defined as:

$$Z = \frac{p_C}{v_C} = Z_R + iZ_I \qquad \text{[4-14]}$$

where p_C denotes a complex acoustic pressure as a function of x and t, and v_C denotes the corresponding acoustic velocity as a function of x and t. Both are evaluated by the FE procedure using equation [4-14]. The absorption coefficient is then calculated by substituting the real and imaginary components of the calculated acoustic impedance (Z_R and Z_I) into the expression for the absorption coefficient:

$$\alpha_a = \frac{4Z_R(\rho_1 c_1)}{[Z_R + (\rho_1 c_1)]^2 + Z_I^2} \qquad [4\text{-}15]$$

The calculation of the acoustic impedance can be done in two ways: method (1) using conditions at the piston location and method (2) using conditions at the interface ($x = 0$). A comparison of the results for each method is presented later. At the right end of the system, $x = L$, the displacement is zero $(u = 0)$. This ensures that no sound emerges from the porous material, as required physically.

4.2.1 Absorption Coefficient

The absorption coefficient is calculated for the same case as that examined by Craggs [7] for both methods. The porous material is given a structure factor of unity and a porosity factor of unity ($K_s = 1$, $\Omega = 1$), and the resistivity (R) is allowed to vary. The results are presented for five values of resistivity and for excitation frequencies varying between 0 and 16 kHz at 500 Hz intervals. The system parameters are given in Table 4-9. Equation [4-11] suggests that the use of seven finite elements for the porous material, and fourteen finite elements for the air column would achieve results within 1% RMS error. However, Craggs [7] modeled his system using ten finite elements for the air column and five finite elements for the porous material. For consistency, Craggs' element scheme was used. As will be shown, it produces sufficiently accurate results.

Table 4-9 – System properties used for absorption coefficient calculation

System		
		Sensitivity
Density	$\rho\ (kg/m^3)$	1.2
Speed of Sound	$c\ (m/s)$	341
Input Velocity	$U_0\ (m/s)$	1
Length air	$L\ (m)$	0.05
Length air	$L\ (m)$	0.025
Frequency	$f\ (Hz)$	0-16kHz
Porosity	Ω	1
Structure factor	K_s	1
Resistivity	R *rayls/m*	2000 5000 10,000 20,000 50,000

Finite element predictions of the absorption coefficient are shown in Figure 4-29 for the system using conditions at the face of the piston (method 2). Excellent agreement is seen between the analytical and finite element predictions. The RMS error is no more than 1.6% for any value of resistivity tested. The results using conditions at the face of the porous material (method 1) are shown in Figure 4-30. Agreement between the finite element and analytical predictions is good at low frequencies; however, above 4 kHz the results deteriorate. The RMS percentage error is a maximum of 5.2% for a resistivity of 10,000 rayls.

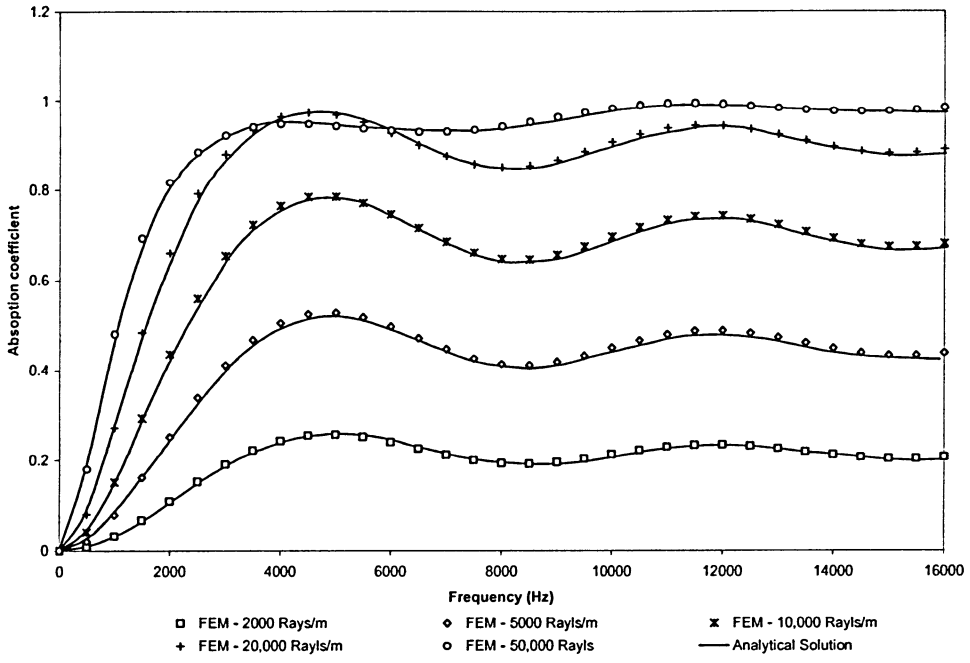

Figure 4-29 Variation of absorption coefficient with frequency. Comparison of exact solution and finite element prediction for various resistivities. Method 1: conditions at the face of the piston. 10 elements for the air, 5 finite elements for the porous material.

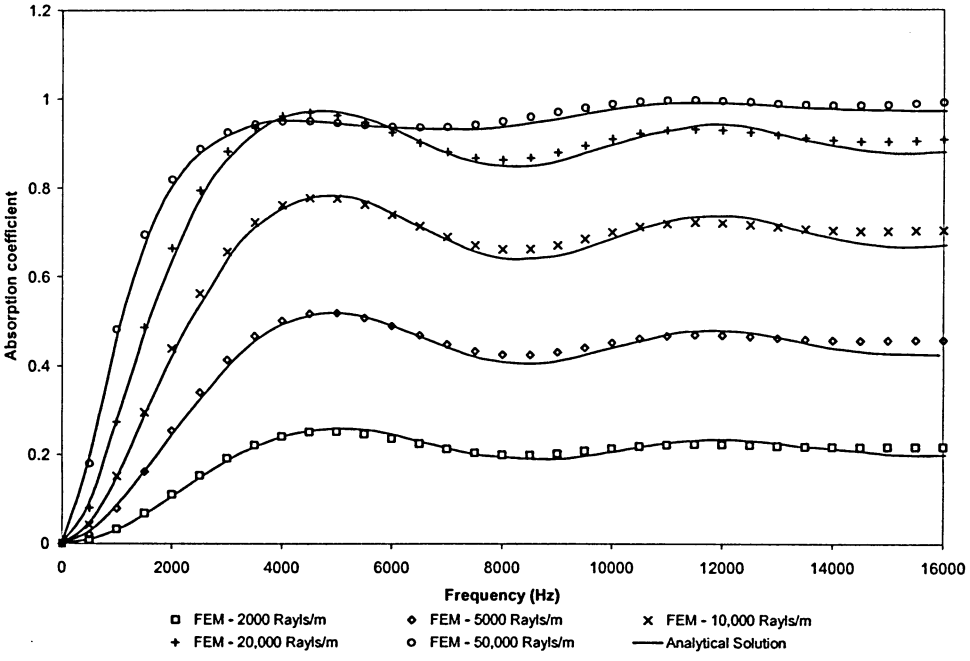

Figure 4-30 - Variation of absorption coefficient with frequency. Comparison of exact solution and finite element prediction for various resistivities. Method 2: conditions at the face of the porous material. 10 finite elements for the air, 5 finite elements for the porous material.

It was found that the 5 element mesh that Craggs [7] used for the porous material, and which was adopted here, was too crude to produce good agreement between the numerical and analytical results for method 2. When the mesh was refined, the results shown in Figure 4-31 were obtained. It can be seen that there is excellent agreement with the analytical solution and the finite element predictions. The RMS percentage error is a maximum of 1.6%.

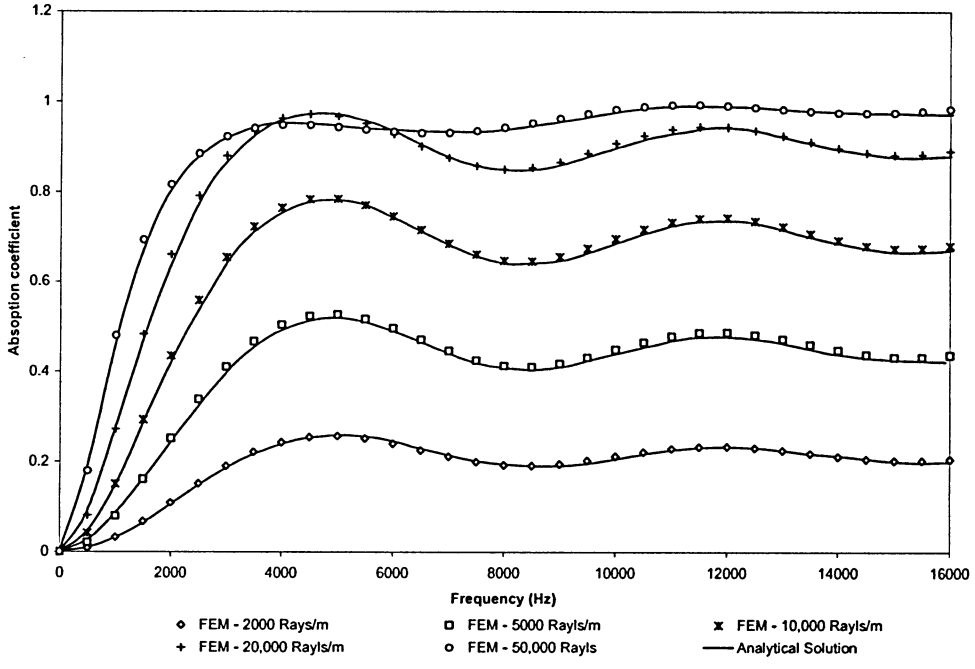

Figure 4-31 - Variation of absorption coefficient with frequency. Comparison of exact solution and finite element prediction for various resistivities. Method 2: conditions at the porous interface. 14 finite elements for the air, 7 finite elements for the porous material.

The excellent agreement shown between the finite element and analytical predictions of the porous material's absorption coefficient serves to validate the finite element formulation. As well, these results demonstrate that the displacement based finite element formulation produces more accurate results than the pressure based formulation used by Craggs [7] for the same computational effort.

It should be noted that, at the time of Craggs publication [7], it was thought that the dominant mode of wave propagation in a porous material was longitudinal. It has since been shown by Kang and Bolton [15] that the model used for the porous material

(Zwikker and Kosten [12]) is not always valid and that longitudinal waves may not dominate in a porous material in practice.

4.3 Transmission Loss

The transmission of sound from one fluid medium to another through a solid partition is an important aspect of noise control which has applications to a wide range of practical acoustic problems. The following section explores the transmission of sound through a thick solid of finite length, which does not bend. To study the sound transmission loss through a thick solid medium, an acoustic system having three components air I, solid II, and air III, as depicted in Figure 4-32 , is investigated. The characteristic impedances of the media are given by $(\rho_1 c_1)$, $(\rho_2 c_2)$, $(\rho_3 c_3)$.

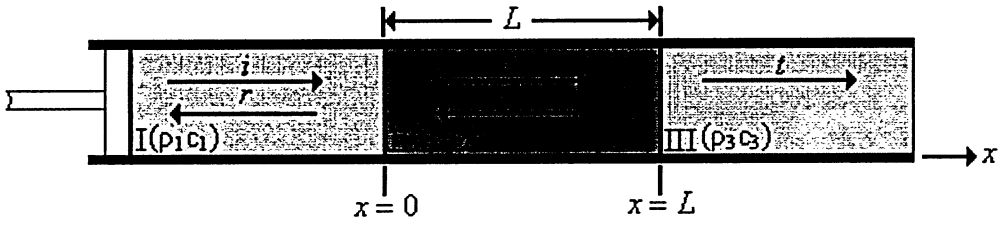

Figure 4-32 – three component system used in TL analysis

In this system, an incident plane acoustic wave, denoted i, originates from a sinusoidally vibrating piston with prescribed velocity amplitude and excitation frequency. The incident wave, initially traveling in the positive x-direction, impinges on the boundary between air I and solid II located at $x = 0$. A reflected wave, r, is generated in air I, and a transmitted wave, t, is generated in solid II. The transmitted wave travels through the solid until it impinges on the boundary between solid II and air II located at $x = L$. At this point, a reflected wave is generated in solid II, and a transmitted wave is generated in air III. Since only the sound transmission loss as the sound propagates through the solid is of interest, the sound is assumed to be completely absorbed at some distance downstream from the solid material on the right edge of the of air III. This assumption ensures that the sound transmission loss calculations are not affected by sound reflected at the downstream boundary of the system under consideration. The system will reach a steady state when the rate that sound energy is reflected back into air

I, plus the rate at which it is transmitted into air III equals the rate of arrival of the incident energy. For this steady state condition, the transmission loss across the system can be calculated using [2-7] and [2-8], and the mass law can be checked using [2-9].

Finite Element Solution

It is not necessary to model the third medium, i.e., air III, in the finite element approach. Instead, the third medium can be replaced by an equivalent system of a massless piston subjected to the constraints of a linear spring element (k_a) at the second boundary, $x = L$, as shown in Figure 4-33. This procedure is similar to that used to model the acoustic material in section 4.1.

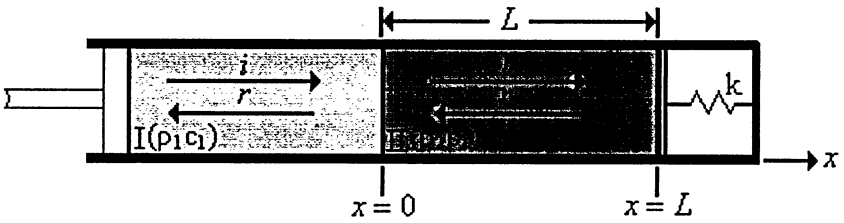

Figure 4-33 – Equivalent finite element model for TL analysis

Since the third component is air, the normalized specific acoustic impedance at $x = L$ is given by $Z^*_{III} = \rho_1 c_1$. This can be incorporated into the finite element formulation by adding its real and imaginary components to the values of the systems global stiffness and damping matrices associated with the node at $x = L$.

The detailed development of the working equations for sound transmission used in the finite element approach can be found in Appendix C. Under steady-state sound propagation conditions, the acoustic impedance can be defined as:

$$Z = \frac{p_c}{v_c} \qquad \text{[4-16]}$$

where p_C denotes a complex acoustic pressure as a function of x and t, and v_c denotes the corresponding acoustic velocity as a function of x and t. Both are evaluated by the FE procedure at $x = 0$ using Equation [4-16]. With the acoustic impedance known, the sound transmission coefficient may be calculated using:

$$\alpha_t = 1 - \frac{|Z - (\rho_1 c_1)|}{|Z + (\rho_1 c_1)|} \quad [4\text{-}17]$$

where $\rho_1 c_1$ is the characteristic impedance of air. The transmission loss is given by:

$$TL(dB) = 10\log\left(\frac{1}{\alpha_t}\right) \quad [4\text{-}18]$$

Numerical results, obtained using the finite element method for a wide range of engineering materials and system geometries are presented in the next section.

4.3.1 Applications

The transmission loss for five engineering materials commonly used in acoustics applications, shown in Table 4-10, are calculated using the finite element procedure for a wide range of frequencies (up to 10,000 Hz), and material lengths (0.1m, 0.25m, 0.5m). These materials represent a wide range of densities and speeds of sound. The results are plotted and compared to the analytical and mass law predictions of transmission loss. The results are presented below in Figure 4-34 through Figure 4-48.

Table 4-10 – Materials and their properties used in TL investigation

MATERIAL	DENSITY	SPEED OF SOUND
	$\rho\,(kg/m^3)$	$c\,(m/s)$
Drywall	700	1100
Pine Wood	400	3500
Concrete	2600	3100
Lead	11300	1200
Aluminium	2700	5150

The number of elements required to accurately calculate the transmission loss in each case is given in the legend of each plot. The required number of elements was based on the sensitivity analysis of Section 4.1.2 and adjusted for different frequencies. Some plots may show a range of elements, for example, n = 2-5. This represents the number of elements required at the lower and upper frequency boundaries of the plot. The number of elements required over the frequency range always fall within those bounds.

Drywall

The first test case involves drywall (Figure 4-34 to Figure 4-36), which has both a low density and a low speed of sound. It is a commonly found material in construction projects, most often used in the construction of walls in residential buildings. As such, the transmission characteristics are of great interest.

Excellent agreement is found between the predicted analytical and finite element transmission loss, with the RMS percentage error for each length being well below 1%. The element requirements for an accurate solution increase with increasing length. A solid of length 0.1m requires 2 elements to accurately predict transmission loss, while a length of 0.25m requires a maximum of 5 elements at high frequencies, and a length of 0.5m requires a maximum of 9 elements at high frequencies.

In each of the plots, there exist various system resonances at which the transmission loss approaches zero. For each solid length, the peak transmission loss is approximately 60 dB. However, as the solid length increases, the location of the frequency associated with the peak transmission loss becomes lower since the solid's natural frequency decreases as the length increases. This is why there is only one resonant frequency in the plot associated with a length of 0.1m and nine resonant frequencies in the plot associated with a length of 0.5m. For frequencies lower than the first resonant frequency, the transmission loss is in good agreement with the mass law.

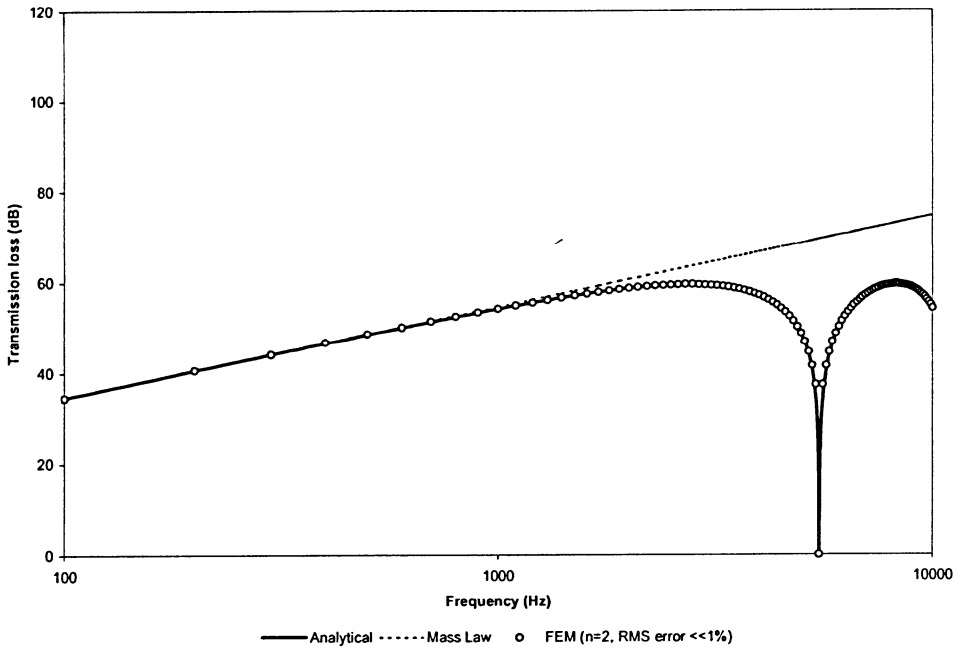

Figure 4-34 - Comparison of analytical and FE transmission loss predictions for drywall (L=0.1m)

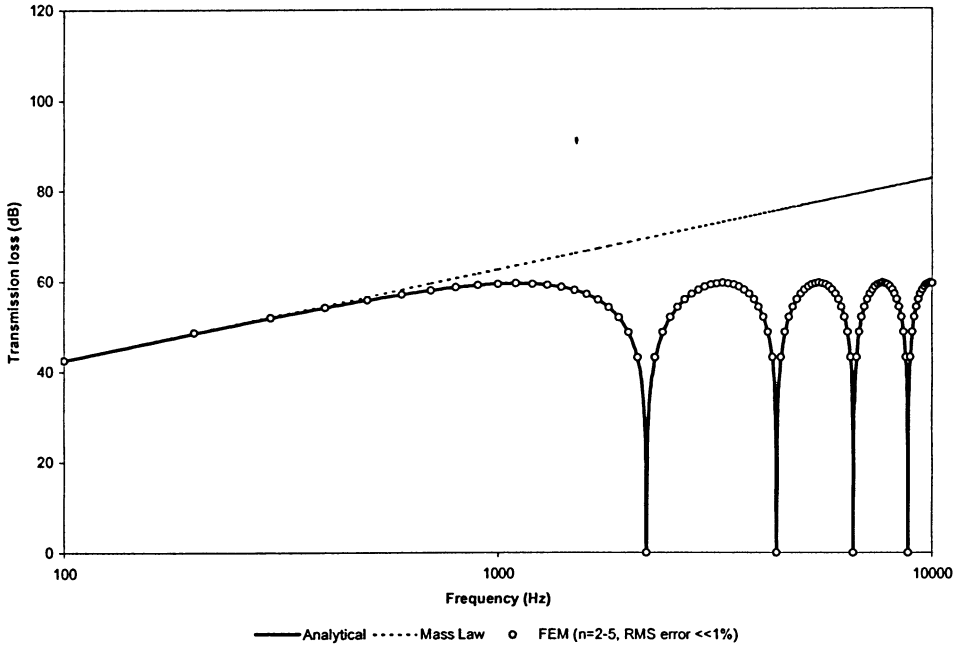

Figure 4-35 - Comparison of analytical and FE transmission loss predictions for drywall (L=0.25m)

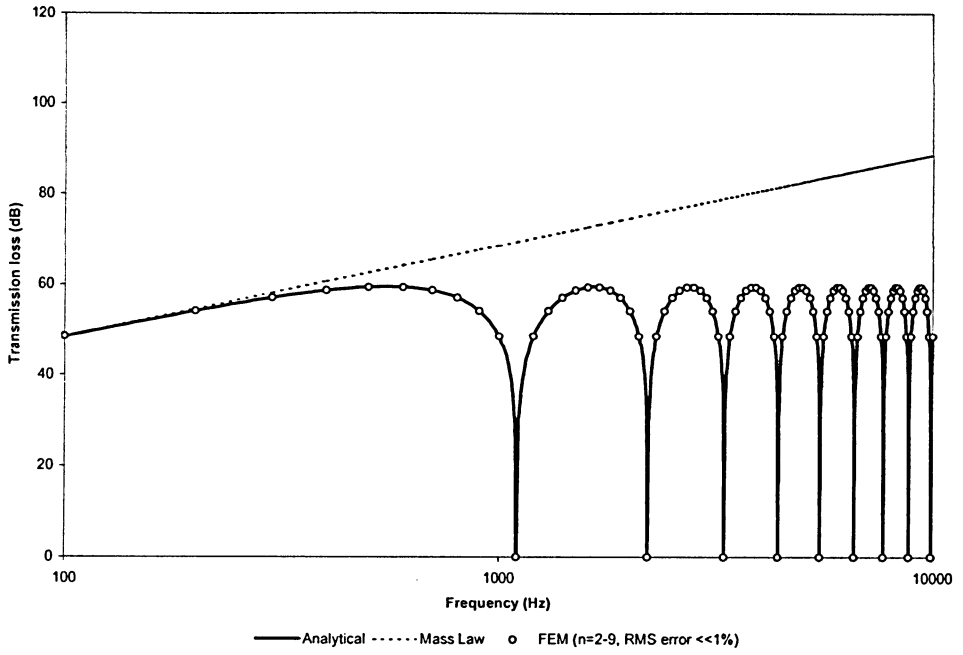

Figure 4-36 Comparison of analytical and FE transmission loss predictions for drywall (L=0.5m)

Pine Wood

The next case involves pine wood (Figure 4-37 to Figure 4-39), which has a very low density and a fairly high speed of sound, a typical characteristic of many woods. Wood is one of the most commonly used resources in construction projects. Examples of its use include the framing of walls in various structures and homes. As such, it is important to understand the transmission characteristics of pine wood.

Excellent agreement is found between the analytical and finite element transmission loss predictions. The RMS percentage error for each length is well below 1%. Only two elements are required to produce an accurate solution regardless of the solid length. This is due to the high speed of sound in the solid, which causes a longer wavelength than in a material with a lower speed of sound, such as drywall.

The high speed of sound also causes the first system resonance to fall outside the 10 kHz range for the 0.1m solid. Predictably, as the solid length increases, the resonances appear lower in the frequency range, showing up for both the 0.25m and 0.5m lengths. For each solid length, the peak transmission loss is approximately 65 dB. Agreement with the mass law is good before approaching a system resonance.

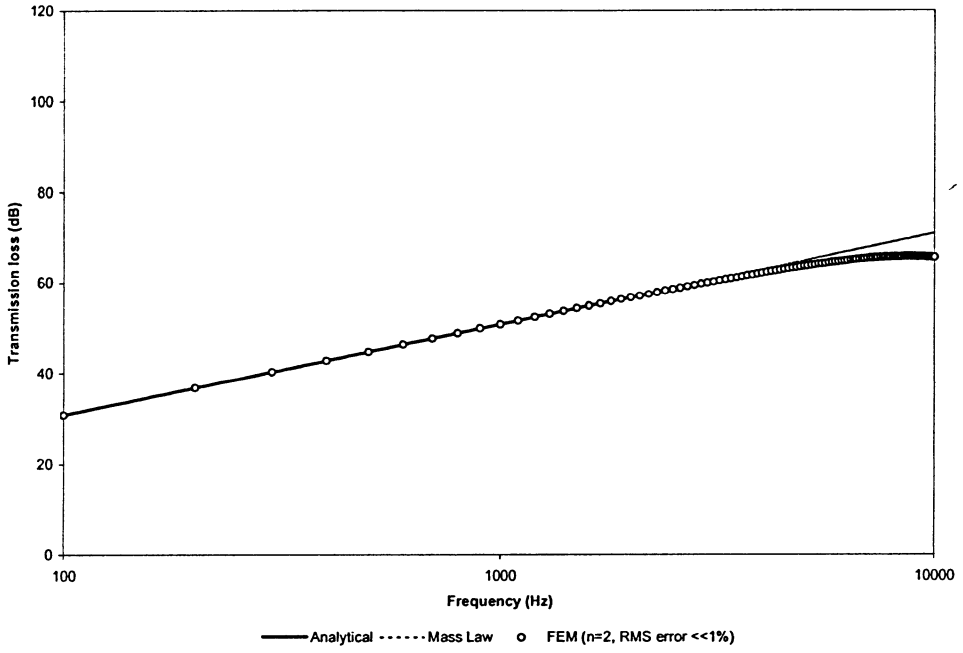

Figure 4-37 - Comparison of analytical and FE transmission loss predictions for pine wood (L=0.1m)

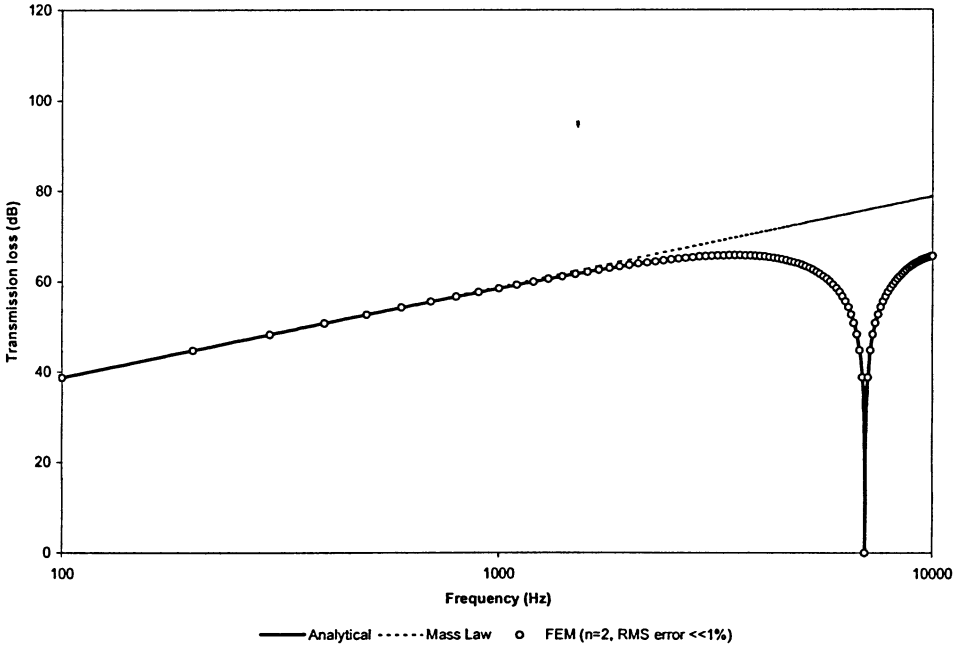

Figure 4-38 - Comparison of analytical and FE transmission loss predictions for pine wood (L=0.25m)

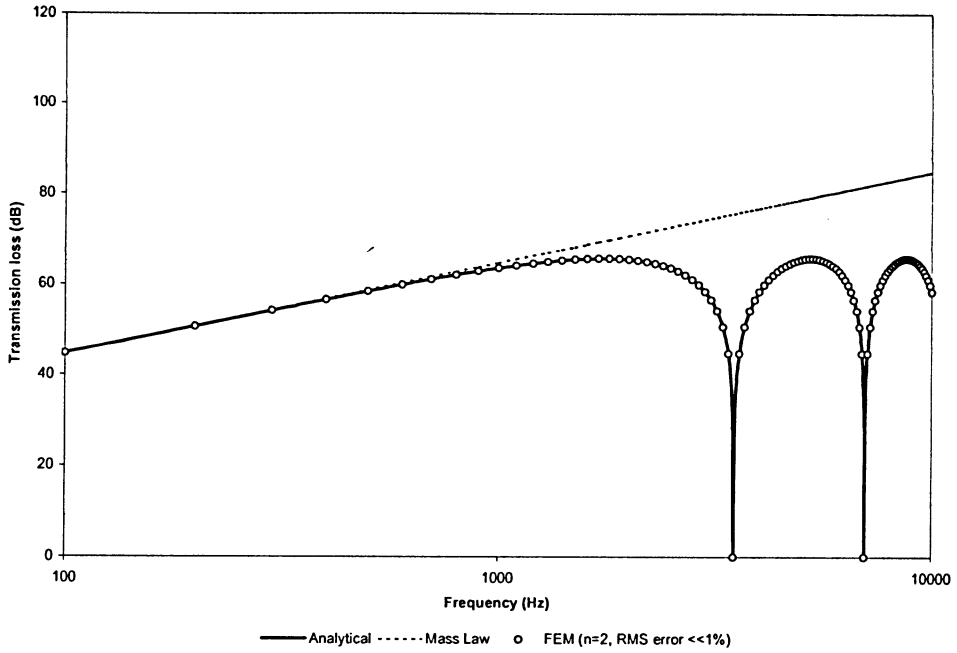

Figure 4-39 - Comparison of analytical and FE transmission loss predictions for pine wood (L=0.5m)

Concrete

The next case involves concrete (Figure 4-40 to Figure 4-42), which has a moderately low density and a fairly high speed of sound. Concrete can be found in just about any building application. Often used to create foundations, walls, and barriers in larger structures, concrete and its transmission characteristics, are of great interest to the field of acoustics.

Excellent agreement is found between the analytical and finite element transmission loss predictions. The RMS percentage error for each length is well below 1%. Due to the high speed of sound, only two elements are required to produce an accurate solution, regardless of the solid length.

The high speed of sound also causes the first system resonance to fall outside the 10 kHz range for the 0.1m solid. However, as the solid length increases, the resonances appear lower in the frequency range, showing up for both the 0.25m and 0.5m lengths. For each solid length, the peak transmission loss is approximately 79 dB. Agreement with the mass law is good before approaching a system resonance.

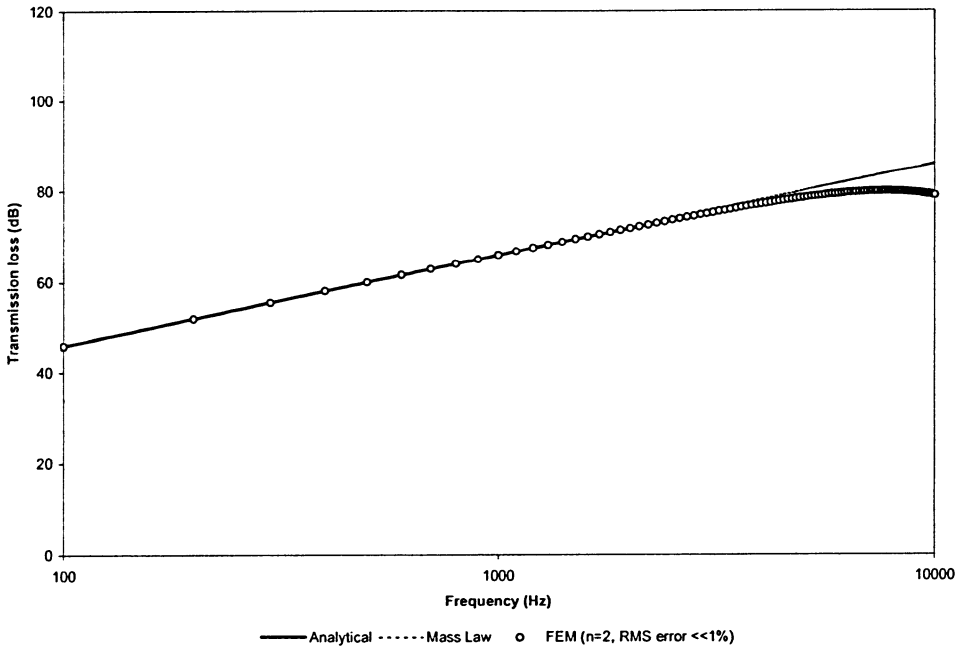

Figure 4-40 - Comparison of analytical and FE transmission loss predictions for concrete (L=0.1m)

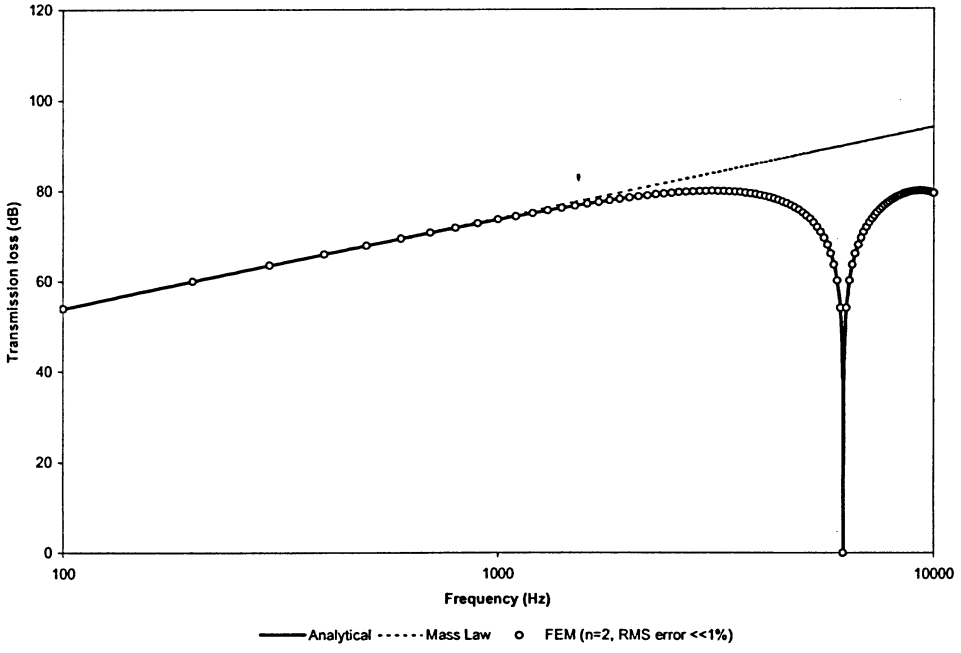

Figure 4-41 - Comparison of analytical and FE transmission loss predictions for concrete (L=0.25m)

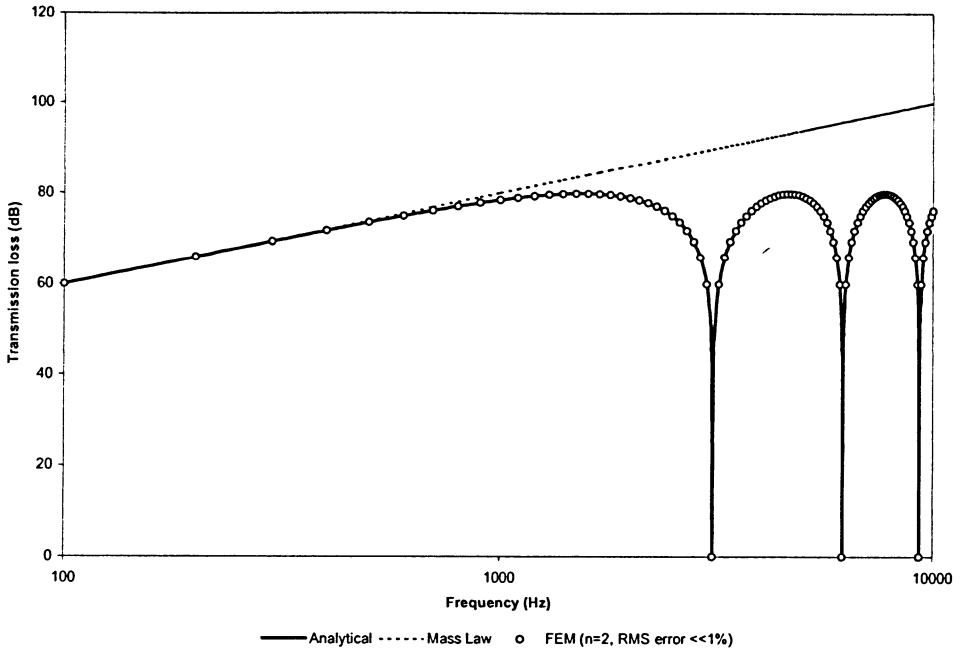

Figure 4-42 - Comparison of analytical and FE transmission loss predictions for concrete (L=0.5m)

Lead

The next case involves the analysis of lead (Figure 4-43to Figure 4-45), which has a very high density and a very low speed of sound. Lead is not a typical practical material in construction, or acoustics problems, but its material properties make it ideal to test the limits of the finite element approach, lending greater confidence to the results.

Again, excellent agreement is found between the analytical and finite element transmission loss predictions. The RMS percentage error for each length is well below 1%. Due to the low speed of sound, only a minimum of two elements and maximum of eight elements are required to produce accurate results for the various frequencies and solid lengths.

The low speed of sound also yields many resonances within the 10 kHz frequency range, especially for increasing length. For each solid length, the peak transmission loss is approximately 85 dB. Agreement with the mass law is good before approaching a system resonance, as expected.

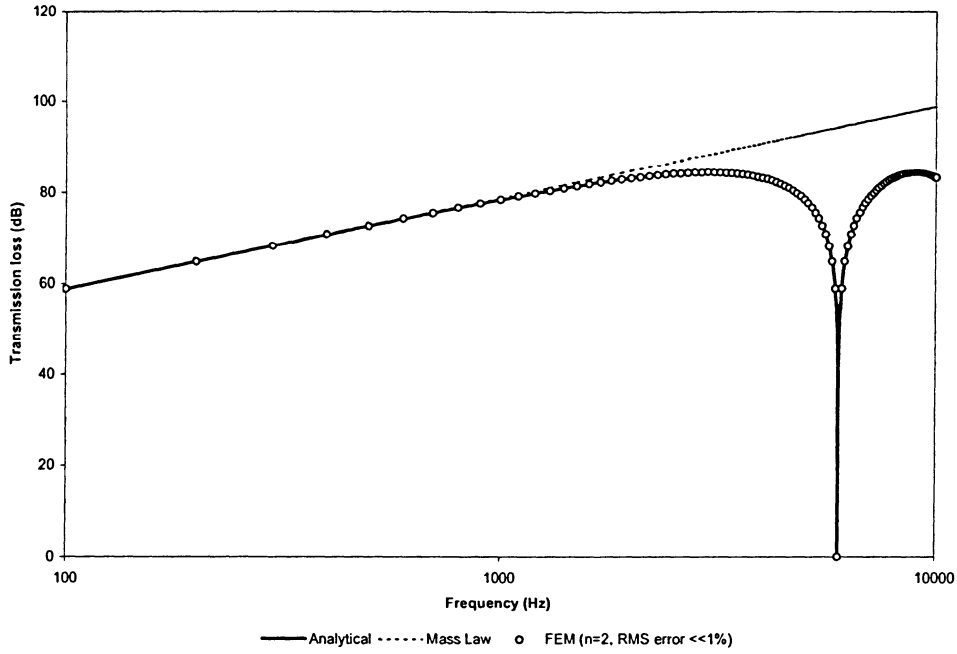

Figure 4-43 - Comparison of analytical and FE transmission loss predictions for lead(L=0.1m)

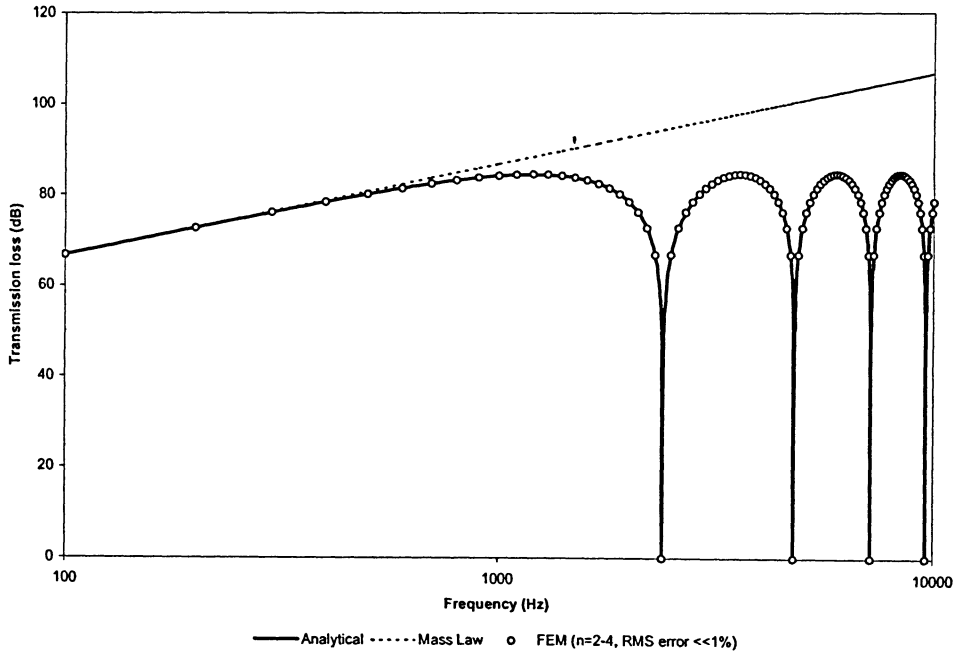

Figure 4-44 - Comparison of analytical and FE transmission loss predictions for lead(L=0.25m)

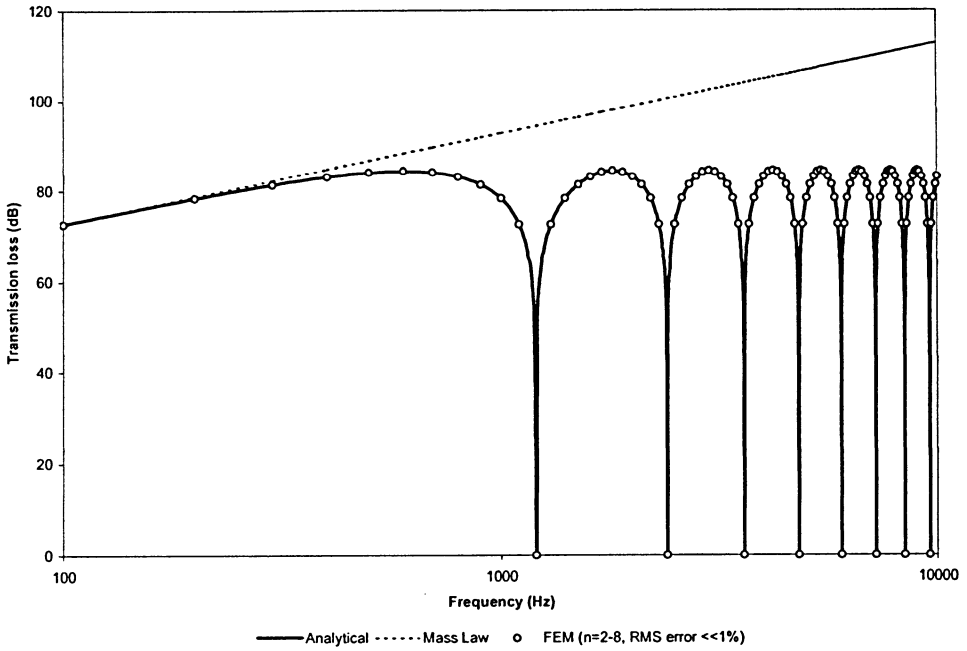

Figure 4-45 - Comparison of analytical and FE transmission loss predictions for lead (L=0.5m)

Aluminium

The next case involves aluminium (Figure 4-46 to Figure 4-48), which has a moderately low density and a high speed of sound. Aluminium is replacing wood in some building applications, and is currently becoming more popular as a framing material for residential homes. As it finds greater application in areas where noise is concerned, its transmission characteristics will become more important.

Excellent agreement is found between the analytical and finite element transmission loss predictions. The RMS percentage error for each length is well below 1%. Due to the high speed of sound, only two elements are required to produce an accurate solution, regardless of length.

The high speed of sound also causes the first system resonance to fall well outside the 10 kHz range for the 0.1m length, and just outside for the 0.25m length. However, for the 0.5m length, a system resonance appears. For each length, the peak transmission loss is approximately 85 dB. Agreement with the mass law is good before approaching a system resonance, as expected.

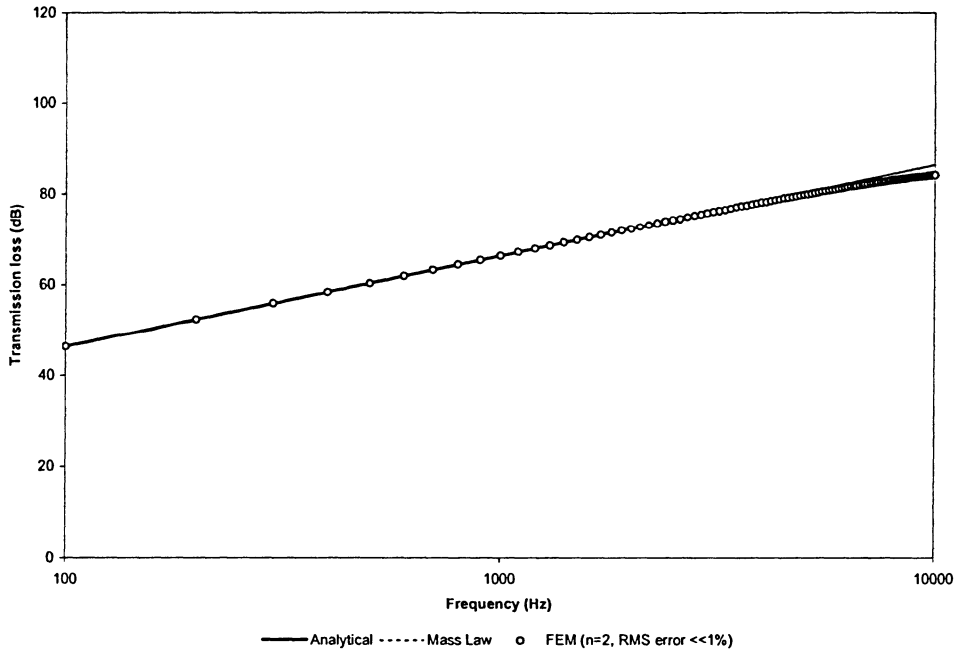

Figure 4-46 - Comparison of analytical and FE transmission loss predictions for aluminium (L=0.1m)

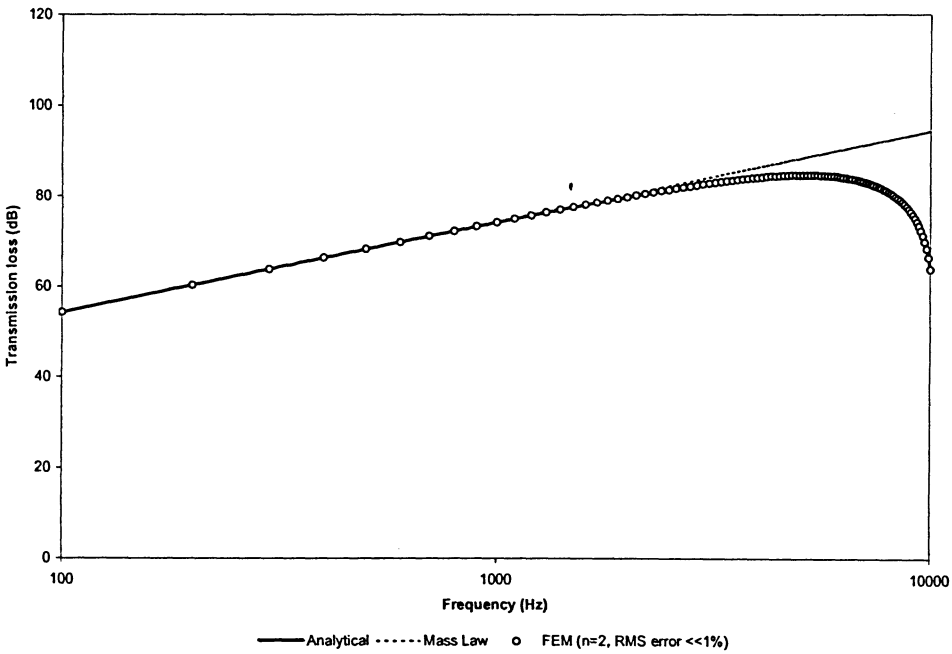

Figure 4-47 - Comparison of analytical and FE transmission loss predictions for aluminium (L=0.25m)

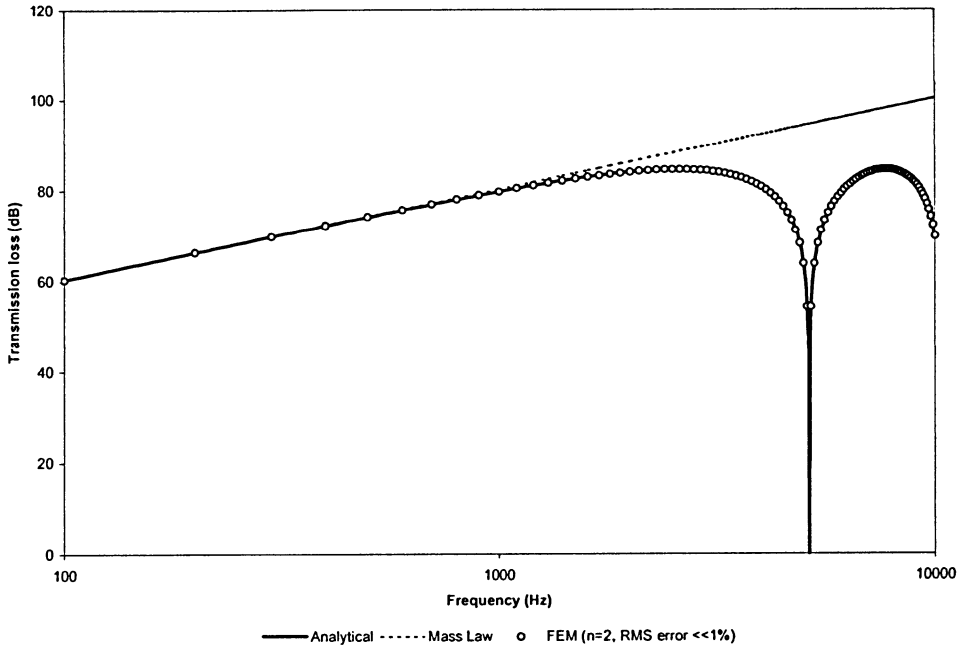

Figure 4-48 - Comparison of analytical and FE transmission loss predictions for aluminium (L=0.5m)

For all tested materials, frequencies and lengths, the finite element prediction of transmission loss shows excellent agreement with the analytical prediction. As expected, agreement is shown with the mass law at low frequencies before system resonances occur. The RMS percentage error between the exact analytical solution and the finite element solution in each case is well below 1%. This agreement further enhances the confidence in the present finite element procedure.

Element requirements vary depending on solid length and the speed of sound in the solid material according to [4-11]. This suggests that a solid material that has a low speed of sound requires more elements as the length of solid material increases. This was shown in the test cases, where drywall and lead required more elements than the materials with higher speeds of sound for an accurate solution.

Every system tested showed signs of resonances at some solid length. At resonance, the transmission loss across the solid approaches zero. Materials with a low speed of sound showed a greater number of resonances. Drywall, which had the lowest speed of sound, showed nine resonances for the system with a 0.5m length. Conversely, aluminium, which has the highest tested speed of sound, showed only one resonance for the 0.5m length.

In each case, the peak transmission loss is reached before the first resonance, and again in between resonances. The peak value for each material does not change with varying length, but rather occurs at different frequencies as a result of the resonance dependency on length. The peak transmission loss value for each material is shown in Table 4-11. It can be seen that the material with the highest characteristic impedances (aluminium) has the highest peak transmission loss, while the material with lowest characteristic impedance (drywall) has the lowest peak transmission loss.

Table 4-11 - Peak transmission loss for tested materials

MATERIAL	PEAK TRANSMISSION LOSS	CHARACTERISTIC IMPEDANCE
	(dB)	(rayls)
Drywall	59.5	77000
Pine Wood	65.7	1575000
Concrete	79.9	8060000
Lead	84.4	13560000
Aluminium	84.6	13905000

This analysis gives insight into some of the critical design aspects that can be used to design a thick, non-bending, solid material barrier to maximize sound transmission loss. A material should be chosen with maximum characteristic impedance and the highest possible speed of sound to ensure that the barrier's resonances fall outside of the intended operating frequencies. The geometric properties of the solid also play a role, as increasing the length decreases the frequencies at which resonance occurs. So, a relatively thin barrier with a high density and speed of sound will produce the most effective barrier to sound transmission.

CHAPTER FIVE – CONCLUSIONS AND FUTURE WORK

Recent years have seen an increased demand for sound insulation and noise control solutions. As a result, there has been a research focus on developing and implementing numerical modeling techniques for acoustic problems. The goal of the present research was to develop an accurate and computationally efficient finite element formulation for one-dimensional sound propagation through solid and porous materials. The finite element procedure developed made use of three-node higher order, non-isoparametric finite elements and quintic polynomials as the interpolation function to increase computational efficiency. The acoustic displacement based procedure was coded using MATLAB to obtain the pressure and velocity fields in various acoustic systems, and this information was used to calculate acoustic parameters such as the absorption coefficient of porous media and the transmission loss in solid media.

The finite element procedure was applied to three acoustic systems. The first of these systems was the impedance tube. Here, the finite element procedure was used to predict the standing pressure field in the air column. Compared with the analytical solution, the finite element procedure showed excellent agreement. This system was also used as the basis of a sensitivity analysis which provided a means of estimating the number of finite elements required for high accuracy.

The second acoustic system studied in this thesis was a coupled air/porous solid system. Agreement between the analytical and finite element predictions of the absorption coefficient in the solid was again excellent. This system validated the development and implementation of interface conditions in multiple component systems.

The final acoustic system investigated was a coupled air/non-porous solid system which was utilized to predict the transmission loss for a variety of acoustic materials and barrier geometries. In each case, excellent agreement was found between the finite

element solution and the corresponding analytical predictions. This analysis showed that barrier resonances are a key factor in limiting the effectiveness of a noise control barrier over a wide range of frequencies.

A preliminary goal of this research was to investigate transmission loss of double panel systems with various panel connectors. By studying the various connections, a means of effectively connecting the panels for maximum transmission loss can be determined. This goal was not pursued here due to time constraints.

In the future, the present one-dimensional formulation can be used to investigate the acoustic properties of multiple component sound systems, i.e., systems with three or more air and solid components. In such an analysis, multiple solid components could be connected via spring and dampers and the effect of this coupling analyzed. This information could produce insight into the effects of various connectors on the transmission of sound through multiple connected media.

The one-dimensional approach is limited in its application as it does not capture bending or shear waves in the system. These waves are present in many acoustic systems including thin panels and absorbing materials. As such, the next step would be to extend the finite element formulation to two and even three dimensions. The two- or three-dimensional finite element procedure could be used to study a variety of practical acoustic structures, including the double panel system. In addition, experimentation would be required to validate the numerical predictions. Adapting the one-dimensional finite element procedure presented in this thesis to two- or three- dimensional problems to handle acoustic systems of increasing complexity will afford a better understanding of, and the ability to control, noise pollution.

References

[1] Fahy, F.J. and Walker, J.F. *Fundamentals of Noise and Vibration.* New York, E & F SPON, ©1998.

[2] Rossing, T., Moore, F.R., and Wheeler, P. *The Science of Sound. Third Edition.* San Francisco, Pearson Education Inc, ©2002.

[3] G.M.L Gladwell. On energy and complementary energy formulations of acoustic and structural vibration problems. *Journal of Sound and Vibration.* **3**(3), 233-241. 1966.

[4] G.M.L Gladwell. A variational formulation of damped acousto-structural vibration problems. *Journal of Sound and Vibration.* **4**(2), 172-186. 1966.

[5] Craggs, A. The transient response of a coupled plate-acoustic system using plate and acoustic finite elements. *Journal of Sound and Vibration.* **15**(4), 509-528. 1971.

[6] Craggs, A. A finite element method for damped acoustic systems: An application to evaluate the performance of reactive mufflers. *Journal of Sound and Vibration.* **48**(3), 377-392. 1976.

[7] Craggs, A. A finite element model for rigid porous absorbing materials. *Journal of Sound and Vibration.* **61**(1), 605-613. 1979.

[8] Craggs, A. Coupling of Finite Element Acoustic Absorption Models. *Journal of Sound and Vibration.* **66**(4), 605-613. 1979.

[9] P.M. Morse and K. U. Ingard. *Theoretical Acoustics.* New York, McGraw-Hill Book Company Inc. ©1968.

[10] Everstine, G.C. Finite element formulations of structural acoustics problems. *Computers and Structures.* **65**(3). 307-321. 1995.

[11] Kinsler, E., Frey, A. *Fundamentals of Acoustics.* New York, John Wiley & Sons, ©1982.

[12] C. Zwikker and C.W. Kosten, *Sound Absorbing Materials.* New York, Elsevier, 1949.

[13] Tabarrok, B., and Rimrott, F. P. J, *Variational Methods and Complementary Formulations in Dynamics.* The Netherlands, Kluwer Academic Publishers, ©1994.

[14] Meirovitch, L., *Principles and Techniques of Vibrations*. New Jersey, Prentice Hall, ©1997.

[15] Yeon June Kang and J. Stuart Bolton. Finite element modeling of isotropic elastic porous materials coupled with acoustical finite elements. *Journal of Acoustic Society of America*. **98**(1), 635-643. 1995.

Bibliography

[1] Bathe, K. J., Nitikitpaiboon, C., and Wang, X. A mixed displacement finite element formulation for acoustic fluid-structure interaction. *Computers and Structures.* **56**(2), 225-237. 1995.

[2] Yeon June Kang and J. Stuart Bolton, Finite element modeling of isotropic elastic porous materials coupled with acoustical finite elements. *Journal of Acoustic Society of America.* **98**(1), 635-643. 1995.

[3] Yeon June Kang., Bolton, J.S. A finite element model for sound transmission through foam lined double-panel structures. *Journal of Acoustic Society of America.* **99**(5), 2755-2765. 1996.

[4] Bolton, J.S., Shiau, N.-M., and Kang, Y.J. Sound transmission through multi-panel structures lined with elastic porous materials. *Journal of Sound and Vibration.* **191**(3), 317-347. 1996.

[5] Yeon June Kang., Bolton, J.S., Sound transmission through elastic porous wedges and foam layers having spatially graded properties. *Journal of Acoustic Society of America.* **102**(6), 3319-3332. 1996.

[6] Yeon June Kang., Bolton, J.S., An axisymmetric poroelastic finite element formulation. *Journal of Acoustic Society of America.* **106**(2), 565-574. 1999.

[7] R. Panneton and N. Atalla. Numerical prediction of sound transmission through finite multilayer systems with poroelastic materials. *Journal of Acoustic Society of America.* **100**(1), 346-354. 1996.

[8] R. Panneton and N. Atalla. An efficient finite element scheme for solving the three-dimensional poroelasticity problem in acoustics. *Journal of Acoustic Society of America.* **101**(6), 3287-3298. 1997.

[9] R. Panneton and N. Atalla. A mixed displacement-pressure formulation for poroelastic materials. *Journal of Acoustic Society of America.* **104**(3), 2383-2390. 1998.

[10] P. Debergue, R. Panneton and N. Atalla. Boundary conditions for the weak formulation of the mixed (u,p) poroelasticity problem. *Journal of Acoustic Society of America.* **106**(5), 2383-2390. 1999.

[11] Easwaran, V., Lauriks, W., and Coyette, J.P. Displacement-based finite element method for guided wave propagation problems: Application to poroelastic media. *Journal of Acoustic Society of America.* **100**(5), 2989-3002. 1996.

[12] Lauriks, W., Mees, P., Allard, J.F. The Acoustic transmission through layered systems. *Journal of Sound and Vibration.* **155**(1), 125-132. 1992.

[13] Lauriks, W., Cops, A., Verhaegen, C., Acoustical properties of elastic porous materials. *Journal of Sound and Vibration.* **131**(1), 143-156. 1989.

[14] Rebillard, P., Allard, J.F., Depollier, C., Guignouard, P., The effect of a porous facing on the impedance and the absorption coefficient of a layer of porous material. *Journal of Sound and Vibration.* **156**(3), 541-555. 1992.

[15] Brouard, B., LaFarge, D., Allard, J.F., A general method of modeling sound propagation in layered media. *Journal of Sound and Vibration.* **183**(1), 129-142. 1995.

[16] Allard, J.F., Depollier, C., Measurement and prediction of surface impedance at oblique incidence of a plastic foam of high flow resistivity. *Journal of Sound and Vibration.* **132**(1), 51-60. 1989.

[17] Fellah, Z. E. A., Wirgin, A., Fellah, M., Sebaa, N., Depollier, C., Lauriks, W., A time-domain model of transient acoustic wave propagation in double-layered porous media. *Journal of Acoustic Society of America.* **118**(2), 661-670. 2005.

[18] Allard, J.F., Lauriks, W., Verhaegen, C., The acoustic sound field above a porous layer and the estimation of the acoustic surface impedance from free-field measurements. *Journal of Acoustic Society of America.* **91**(5), 3057-3060. 1992.

[19] Coyette, J.P., Van den Nieuwenhof, B., Treatment of frequency-dependent admittance boundary conditions in transient acoustic finite/infinite-element models. Journal *of Acoustic Society of America.* **110**(4), 1743-1751. 2001.

[20] Astley, R.J., Gamallo, P., Special short wave elements for flow acoustics. *Computer Methods in Applied Mechanics and Engineering.* **194**(2005), 341-353. 2005.

[21] Dauchez, N., Sahraoui, S,. Atalla, N., Investigation and modeling of damping in a plate with a bonded porous layer. *Journal of Sound and Vibration.* **265**(2003), 437-449. 2003.

[22] Cummings, A., Kirby, R., Low-frequency sound transmission in ducts with permeable walls. *Journal of Sound and* Vibration. **226**(2), 237-251. 1999.

[23] Cummings, A., Finite element computation of attenuation in bar-silencers and comparison with measured data. *Journal of Sound and Vibration.* **196**(3), 351-369. 1996.

[24] Astley, R.J., Infinite elements for wave problems: a review of current formulations and an assessment of accuracy. *Int. J. Numer. Meth. Engng.* **49**, 951-976. 2000.

[25] Cummings, A., The attenuation of sound in unlined ducts with flexible walls. *Journal of Sound and Vibration.* **174**(4), 433-450. 1994.

[26] Astley, R.J., Cummings, A., Wave propagation in catalytic converters: formulation of the problem and finite element solution scheme. *Journal of Sound and Vibration.* **188**(5), 635-657. 1995.

[27] Cummings, A., Sound propagation in narrow tubes of arbitrary cross-section. *Journal of Sound and Vibration.* **162**(1), 27-42. 1993.

[28] Cummings, A., Sound transmission through duct walls. *Journal of Sound and Vibration.* **239**(4), 731-765. 2001.

[29] Cummings, A., Sound transmission from a plate into a porous medium. *Journal of Sound and Vibration.* **247**(3), 389-406. 2001.

[30] Cummings, A., A segmented Raleigh-Ritz method for predicting sound transmission in a dissipative exhaust silencer of arbitrary cross-section. *Journal of Sound and Vibration.* **187**(1), 23-37. 1995.

Appendix A – Impedance Tube

Consider a rigid tube containing air that is excited by a harmonically oscillating rigid piston, as shown in Figure A-1. The oscillation of the piston creates one-dimensional acoustic pressure waves which propagate through the tube and impact an acoustic material with a normalized specific acoustic impedance, z^*. The acoustic material reflects and absorbs a certain amount of the acoustic energy. Under steady state conditions, the combination of an incident and reflected acoustic pressure wave creates a standing pressure wave in the tube. The equations describing this standing pressure wave shall be developed under the assumptions that the fluid in the tube is inviscid and the process is adiabatic.

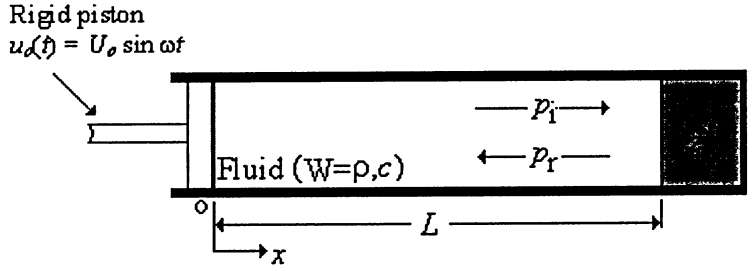

Figure A-1 – Impedance Tube

The piston's displacement at any time, t, is described by:

$$u_0(t) = U_0 \sin \omega t \qquad \text{[A-1]}$$

where, $\omega = 2\pi f$. The piston's velocity is given by:

$$v_0(t) = {}^{du_0}\!/_{dt} = U_0 \omega \cos \omega t = V_0 \cos \omega t \qquad \text{[A-2]}$$

The equation governing the acoustic pressure field in a tube is given by [11]:

$$\frac{\partial^2 p(x,t)}{\partial t^2} = c^2 \left(\frac{\partial^2 p(x,t)}{\partial x^2} \right) \qquad \text{[A-3]}$$

where c is the speed of sound in air, and $p(x,t)$ is the acoustic pressure.

Since the wave generated by the piston is harmonic, the acoustic pressure, $p(x,t)$, can be taken to be of the form:

$$p(x,t) = \mathrm{Re}\left[e^{-i\omega t}\hat{p}(x)\right] \qquad \text{[A-4]}$$

where $e^{-i\omega t}$ represents the time dependence of the pressure field, $i^2 = -1$, and $\hat{p}(x)$ is a complex function of x representing the spatial dependence of the pressure field. $\hat{p}(x)$is given by:

$$\hat{p}(x) = p_R(x) + ip_I(x) \qquad \text{[A-5]}$$

where $p_R(x)$ and $p_I(x)$ are the real and imaginary parts, respectively, of $\hat{p}(x)$. It should be noted that the time dependence of $p(x,t)$ can be based on $e^{+i\omega t}$. In that case, $\hat{p}(x)$ becomes: $\hat{p}(x) = p_R(x) - ip_I(x)$.

From, [A-4] and [A-5], the actual pressure field is given as:

$$p(x,t) = p_R(x)\cos\omega t + p_I(x)\sin\omega t \qquad \text{[A-6]}$$

The corresponding velocity field is given by

$$v(x,t) = \mathrm{Re}\left[e^{-i\omega t}\hat{v}(x)\right] \qquad \text{[A-7]}$$

where $\hat{v}(x)$ is a is a complex function of x representing the spatial dependence of the velocity field. $\hat{v}(x)$ is given by:

$$\hat{v}(x) = v_R(x) + iv_I(x) \qquad \text{[A-8]}$$

where $\hat{v}_R(x)$ and $\hat{v}_I(x)$ are the real and imaginary parts, respectively, of $\hat{v}(x)$. From [A-7] and [A-8], one obtains the actual velocity field as:

$$v(x,t) = v_R(x)\cos\omega t + v_I(x)\sin\omega t \qquad \text{[A-9]}$$

The normalized *specific* acoustic impedance is defined as

$$z(x) = z_R(x) + iz_I(x) = \frac{\hat{p}(x)/W}{\hat{v}(x)} \qquad \text{[A-10]}$$

where z_R and z_I are, respectively, the real and imaginary parts of z, and $W = \rho c$ is the *characteristic* impedance of air with a density ρ and speed of sound c.

For an incident acoustic pressure wave:

$$p_i(x,t) = \mathrm{Re}\left[e^{-i\omega t}\hat{p}_i(x)\right] \qquad \text{[A-11]}$$

The corresponding incident velocity wave is given by:

$$v_i(x,t) = \frac{p_i(x,t)}{W} \qquad \text{[A-12]}$$

with,

$$\hat{v}_i(x) = \frac{\hat{p}_i(x)}{W}$$

Similarly, for a reflected acoustic wave,

$$p_r(x,t) = \mathrm{Re}\left[e^{-i\omega t}\hat{p}_r(x)\right] \qquad \text{[A-13]}$$

and,

$$v_r(x,t) = -\frac{p_r(x,t)}{W} \qquad \text{[A-14]}$$

with,

$$\hat{v}_r(x) = -\frac{\hat{p}_r(x)}{W}$$

From the governing equation for the acoustic pressure field, [A-3], and [A-4], it follows that:

$$c^2 e^{-i\omega t}\frac{\partial^2 \hat{p}}{\partial x^2} - \hat{p}(-i\omega)^2 e^{-i\omega t} = 0 \qquad \text{[A-15]}$$

With $i^2 = -1$, since $e^{-i\omega t} \neq 0$, one obtains

$$\frac{\partial^2 \hat{p}}{\partial x^2} + k^2 \hat{p} = 0 \qquad \text{[A-16]}$$

where $k = \omega/c$.

The acoustic system shown in Figure A-1 is subject to the following boundary conditions: At $x = 0$, the acoustic velocity is equal to the piston velocity, so from [A-2] and [A-9],

$$\begin{aligned} v(0,t) &= v_R(0)\cos\omega t + v_I(0)\sin\omega t \\ &= V_0 \cos\omega t \end{aligned} \qquad \text{[A-17]}$$

The normalized *specific* acoustic impedance at $x = L$ is that of the acoustic material positioned at the end of the tube. So, from [A-10]:

$$z(L) = \frac{\hat{p}(L)/W}{\hat{v}(L)} = z^* = z_R^* + iz_R^* \qquad \text{[A-18]}$$

Note that $Z^* = \hat{p}(L)/\hat{v}(L)$ and $z^* = Z^*/W$.

Under steady state conditions, a standing pressure wave exists in the tube caused by the combination of the incident pressure wave, $p_i(x,t)$, and the reflected pressure wave, $p_r(x,t)$. The complex amplitudes of p_i and p_r are given by:

$$\hat{p}_i(x) = A_C e^{ikx} \qquad \text{[A-19]}$$
$$\hat{p}_r(x) = B_C e^{-ikx}$$

where, in general, A_C and B_C are complex constants dependent on the system's boundary conditions. Note that acoustic energy is absorbed at $x = L$, so $|B_C| < |A_C|$. From [A-19]:

$$\hat{p}(x) = \hat{p}_i(x) + \hat{p}_r(x) = A_C e^{ikx} + B_C e^{-ikx} \qquad \text{[A-20]}$$

and from [A-12] and [A-14],

$$\hat{v}(x) = \hat{v}_i(x) + \hat{v}_r(x) = \left(\frac{1}{\rho c}\right)\left[A_C e^{ikx} - B_C e^{-ikx}\right] \qquad \text{[A-21]}$$

It can be shown that the solution of [A-16], subject to the boundary conditions described by [A-17] and [A-18] is:

$$\hat{p}(x) = (\rho c V_0)\left\{\frac{z^* \cos k(L-x) - i \sin k(L-x)}{\cos kL - iz^* \sin kL}\right\} \qquad \text{[A-22]}$$

where, $\hat{p}(x) = p_R(x) + ip_I(x)$ and $z^* = z_R^* + iz_I^*$.

It can be further shown that:

$$p_R^*(x) = A_0 z_R^* \cos kx \qquad \text{[A-23]}$$

and,

$$p_I^*(x) = \sin kx + B_0 \cos kx \qquad \text{[A-24]}$$

where the constant A_0 is given by:

$$A_0 = \frac{1}{\cos^2 kL + \left(z_R^{*2} + z_I^{*2} - 1\right)\sin 2kL + z_I^* \cos 2kL} \qquad \text{[A-25]}$$

and the constant B_0 is given by:

$$B_0 = A_0\left[\frac{\left(z_R^{*2} + z_I^{*2} - 1\right)\sin 2kL}{2} + z_I^* \cos 2kL\right] \qquad \text{[A-26]}$$

Using equations [A-23] and [A-24], the standing pressure wave resulting from the propagation, reflection and absorption of acoustic energy in the tube can be predicted.

Appendix B – Absorption Coefficient

Consider a rigid tube containing air excited by a harmonically oscillating rigid piston, as shown in Figure B-1. The oscillation of the piston creates one-dimensional acoustic pressure waves which propagate through the tube and impact a porous absorbing material at $x = 0$. The porous material is backed by a perfectly hard wall, such that no sound emerges downstream of the solid. The only mechanism of sound attenuation is absorption by the porous material.

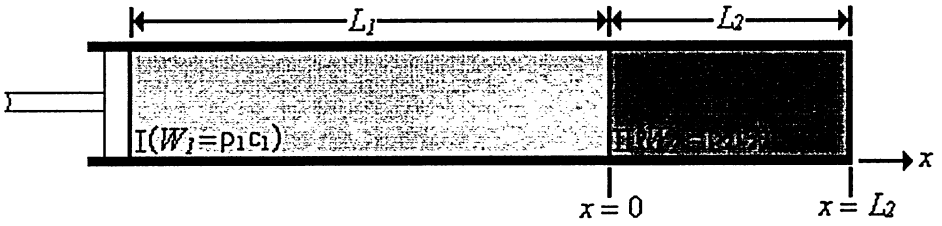

Figure B-1 – Two component air/porous solid system

B-1 Characteristic acoustic impedance of a porous material

The *characteristic* acoustic impedance of a medium, which is denoted by W, is a material property (which may be complex or real) and characterizes the acoustic behavior of the medium *in isolation*. For a non-porous material in which there is no absorption of sound, e.g., air, W is real and is given by [11]:

$$W = \rho c \qquad \text{[B-1]}$$

where ρ is the density of the material, and c is the speed of sound in the material. For a porous material in which sound absorption (i.e., dissipation of acoustic energy) occurs, W is complex, and the expression for W is derived as follows.

For steady state flow of air through the pores or interstices of a porous material, the *viscous* resistance to flow results in a static pressure gradient, $(\partial p/\partial x)_1$, and the flow resistance, R, is defined via the following expression [1]:

$$\left(\frac{\partial p}{\partial x}\right)_I = -Rv' \qquad \text{[B-2]}$$

where p is the fluid pressure and v' is the volume flow per unit cross-sectional are of the material.

The momentum equation for *inviscid* motion of the air in the pores give rise to a pressure gradient, $(\partial p/\partial x)_{II}$, which is given by [1]:

$$\left(\frac{\partial p}{\partial x}\right)_{II} = -\left(\frac{K_s \rho_1}{\Omega}\right)\frac{\partial v'}{\partial t} \qquad \text{[B-3]}$$

where ρ_1 is the density of the free air, and K_s and Ω are, respectively, the structure factor and porosity of the porous material.

Combination of equations [B-2] and [B-3] yields the modified equation of motion of the air within the porous material, which is given by:

$$\begin{aligned}\frac{\partial p}{\partial x} &= \left(\frac{\partial p}{\partial x}\right)_I + \left(\frac{\partial p}{\partial x}\right)_{II} \\ &= -\left(\frac{K_s \rho_1}{\Omega}\right)\frac{\partial v'}{\partial t} - Rv'\end{aligned} \qquad \text{[B-4]}$$

It should be noted that, for simple harmonic motion at an angular frequency ω, $v' \propto e^{i\omega t}$. Hence,

$$\frac{\partial v'}{\partial t} \propto i\omega e^{i\omega t} \propto i\omega v'$$

i.e.,

$$v' = \left(\frac{1}{i\omega}\right)\frac{\partial v'}{\partial t} \qquad \text{[B-5]}$$

where $i = \sqrt{-1}$, and equation [B-4] yields:

$$\frac{\partial p}{\partial x} = -\left[\left(\frac{K_s \rho_1}{\Omega}\right)\frac{\partial v'}{\partial t} + \frac{R}{i\omega}\right]\frac{\partial v'}{\partial t} \qquad \text{[B-6]}$$

Now, for free air, the momentum (Euler) equation is given by:

$$\frac{\partial p}{\partial x} = -\rho_1 \frac{\partial v}{\partial t} \qquad \text{[B-7]}$$

It is evident from a comparison of equation [B-6] and [B-7] that the term in brackets in [B-6] is an effective density, ρ_2, i.e.,

$$\rho_2 = \left(\frac{K_s \rho_1}{\Omega}\right) + \frac{R}{i\omega} \qquad \text{[B-8]}$$

Clearly, ρ_2, is a complex quantity. The parameters K_s, Ω and R serve to alter (reduce) the speed of propagation of sound in the porous material relative to free-air speed of sound, c_1, and to attenuate the acoustic energy in the material.

For free air, the continuity equation is given by:

$$\frac{\partial v}{\partial x} = -\left(\frac{1}{\kappa_1}\right)\frac{\partial p}{\partial t} \qquad \text{[B-9]}$$

Here, κ_1 is the bulk modulus of air given by

$$\kappa_1 = \rho_1 c_1^{\,2} \qquad \text{[B-10]}$$

where c_1 is the speed of sound in free air. For the porous material, the continuity equation is [1]:

$$\frac{\partial v'}{\partial x} = -\left(\frac{1}{\kappa_2}\right)\frac{\partial p}{\partial t} \qquad \text{[B-11]}$$

In this expression, κ_2 is an effective bulk modulus given by:

$$\kappa_2 = \kappa_1/\Omega = \rho_1 c_1^{\,2}/\Omega \qquad \text{[B-12]}$$

The effective speed of sound in the porous material, c_2, is defined via the following expression [1]:

$$c_2^{\,2} = c_1^{\,2}/(k_2\Omega) \qquad \text{[B-13]}$$

From equations [B-10], [B-12] and [B-13] it follows that:

$$\kappa_2 = \rho_1 K_s c_2^{\,2} \qquad \text{[B-14]}$$

Hence, equation [B-11 becomes:

$$\frac{\partial v'}{\partial x} = -\left(\frac{1}{\rho_1 K_s {c_2}^2}\right)\frac{\partial p}{\partial t} \qquad \text{[B-15]}$$

From [B-15],

$$\frac{\partial^2 v'}{\partial x \partial t} = -\left(\frac{1}{\rho_1 K_s {c_2}^2}\right)\frac{\partial^2 p}{\partial t^2} \qquad \text{[B-16]}$$

And from equations [B-4] and [B-15],

$$\frac{\partial^2 p}{\partial x^2} = -\left(\frac{K_s \rho_1}{\Omega}\right)\frac{\partial^2 v'}{\partial t \partial x} + \left(\frac{R}{\rho_1 K_s {c_2}^2}\right)\frac{\partial p}{\partial t} \qquad \text{[B-17]}$$

Combination of [B-16] and [B-17] yields:

$$\left(\frac{1}{\Omega}\right)\frac{\partial^2 p}{\partial t^2} + \left(\frac{R}{\rho_1 K_s}\right)\frac{\partial p}{\partial t} = {c_2}^2 \frac{\partial^2 p}{\partial x^2} \qquad \text{[B-18]}$$

Equation [B-18] is the modified one-dimensional wave equation for a porous material. Note that, in free air, $K_s = 1$, $\Omega = 1$, and $R = 0$, so ${c_2}^2 = {c_1}^2$ and [B-18] becomes:

$$\frac{\partial^2 p}{\partial t^2} = {c_1}^2 \frac{\partial^2 p}{\partial x^2}, \qquad \text{[B-19]}$$

which is the classical one-dimensional plane wave equation for a non-porous material [11].

The solution of equation [B-18] for harmonic motion in a porous material takes the form:

$$p_c(x,t) = A_c e^{i\omega t} e^{-\gamma x} \qquad \text{[B-20]}$$

In this expression, p_c is a complex pressure, A_c is the complex amplitude of the pressure wave, and γ is a complex quantity called the propagation constant. This quantity is defined as:

$$\gamma = \alpha + i\beta \qquad \text{[B-21]}$$

where α is the attenuation constant, and β is the phase constant. Substitution of [B-20] into [B-18] yields the following expression for the propagation constant:

$$\gamma = i\omega\sqrt{\rho_2 / \kappa_2} \qquad \text{[B-22]}$$

From equation [B-6], for harmonic motion,

$$\frac{\partial p}{\partial x} = -\rho_2 \frac{\partial v'}{\partial t} \qquad \text{[B-23]}$$

Hence, from [B-20], the complex velocity, $v_c'(x,t)$, corresponding to the complex pressure, $p_c'(x,t)$, is given by:

$$v_c'(x,t) = \int \left(\frac{\gamma}{\rho_2} \right) A_c e^{i\omega t} e^{-\gamma x} dt$$
$$= \left(\frac{\gamma}{i\omega\rho_2} \right) A_c e^{i\omega t} e^{-\gamma x}$$

i.e.,

$$\gamma p_c = i\omega\rho_2 v_c' \qquad \text{[B-24]}$$

Now, by definition, the *characteristic* acoustic impedance of the porous material is given by [12]:

$$W = \frac{p_c}{v_c'} \qquad \text{[B-25]}$$

Hence, from equation [B-22] and [B-24],

$$W = \frac{i\omega\rho_2}{\gamma} = \sqrt{\rho_2 \kappa_2} \qquad \text{[B-26]}$$

where ρ_2, the complex effective density, is given by equation [B-8], and κ_2 is given by equation [B-12]. Clearly the *characteristic* acoustic impedance of a porous material is a frequency dependent, complex quantity.

B-2 Specific acoustic impedance of a porous material in a coupled system

Consider a one-dimensional plane sound wave propagating through the coupled four-component air/solid system depicted in Figure B-2.

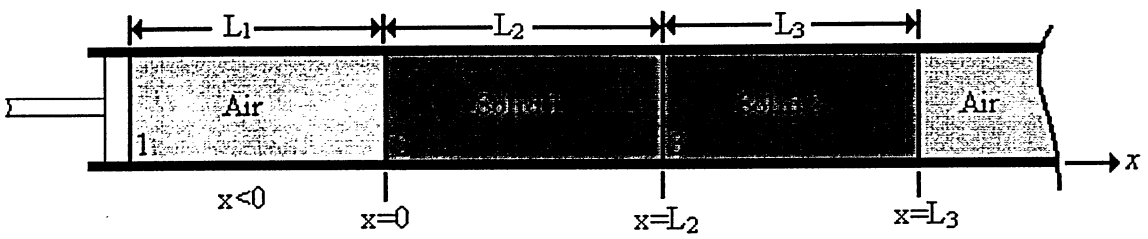

Figure B-2 – Four component air/solid system

Each component can be characterized by a *characteristic* acoustic impedance W, and complex pressure and velocity waves given by, respectively,

$$p_c(x',t) = A_c e^{i\omega t} e^{-\gamma x'} = e^{i\omega t}\,\hat{p}(x') \qquad \text{[B-27]}$$

and,

$$v_c(x',t) = p_c(x,t)/W = e^{i\omega t}\,\hat{p}(x')/W \qquad \text{[B-28]}$$

where,

$$\hat{p}(x') = A_c e^{-\gamma x'}$$

with x' and γ depending on the component and the propagation direction. If absorption occurs in a given component, then W for that component (a porous material), is complex and $\alpha > 0$. (Refer to equation [B-21].) If absorption does not occur in a given component, then W for that component (a non-porous material) is real and is given by $W = \rho c$, where ρ is the density of the component and c is the speed of sound in the component; also, $\alpha = 0$ and $\beta = 2\pi f/c$, i.e., β is the same as the wave number, k.

In the upstream air body (i.e., for $x \le 0$), there is a (complex) incident wave and a (complex) reflected wave, with reflection occurring at the interface located at $x = 0$. In the solid bodies, there are transmitted waves and reflected waves, with reflection occurring at the interfaces located at $x = L_2$ and $x = L_3$. In the downstream air body (i.e., for $x \ge (L_2 + L_3)$), there is only a transmitted wave. For a component with an incident or transmitted wave and a reflected wave, the total complex pressure is given by:

$$\begin{aligned} p_c(x,t) &= p_{ci/t}(x,t) + p_{cr}(-x,t) \\ &= e^{i\omega t}\left[\hat{p}_{i/t}(x) + \hat{p}_r(-x)\right] \end{aligned} \qquad \text{[B-29]}$$

And the corresponding total complex velocity is given by

$$v_c(x,t) = e^{i\omega t}\left[\hat{p}_{i/t}(x) - \hat{p}_r(-x)\right]/W \qquad \text{[B-30]}$$

Note that the propagation direction for a reflected wave is opposite that for an incident or transmitted wave, so x' becomes x for an incident or transmitted wave and $-x$ for a reflected wave. The relevant pressures and velocities for the system are as follows:

Component 1 (Air)

$$p_{c1}(x,t) = e^{i\omega t}\hat{p}_1(x) \qquad \text{[B-31]}$$

and,
$$v_{c1}(x,t) = e^{i\omega t}\hat{v}_1(x) \qquad \text{[B-32]}$$

where,
$$\hat{p}_1(x) = A_{c1}e^{-\gamma_1 x} + B_{c1}e^{+\gamma_1 x} \qquad \text{[B-33]}$$

and,
$$\hat{v}_1(x) = \left(A_{c1}e^{-\gamma_1 x} - B_{c1}e^{+\gamma_1 x}\right)/W_1 \qquad \text{[B-34]}$$

with $W_1 = \rho_1 c_1$ and $\gamma_1 = ik_1 = i2\pi f/c_1$

Also, $x \le 0$.

Component 2 (Solid 1)

$$p_{c2}(x,t) = e^{i\omega t}\hat{p}_2(x) \qquad \text{[B-35]}$$

and,
$$v_{c2}(x,t) = e^{i\omega t}\hat{v}_2(x) \qquad \text{[B-36]}$$

where,
$$\hat{p}_2(x) = A_{c2}e^{-\gamma_2 x} + B_{c2}e^{+\gamma_2 x} \qquad \text{[B-37]}$$

and,
$$\hat{v}_2(x) = \left(A_{c2}e^{-\gamma_2 x} - B_{c2}e^{+\gamma_2 x}\right)/W_2 \qquad \text{[B-38]}$$

If solid 1 is a porous material, then W_2 will be complex, and $\gamma_2 = \alpha_2 + i\beta_2$; if solid 1 is a non-porous material, then W_2 will be real and given by $W_2 = \rho_2 c_2$, and $\gamma_2 = ik_2 = i2\pi f/c_2$. Also, $0 \le x \le L_2$.

Component 3 (Solid 2)

$$p_{c3}(x,t) = e^{i\omega t}\hat{p}_3(x) \qquad \text{[B-39]}$$

and, $$v_{c3}(x,t) = e^{i\omega t}\hat{v}_3(x) \quad \text{[B-40]}$$

where, $$\hat{p}_3(x) = A_{c3}e^{-\gamma_3(x-L_2)} + B_{c3}e^{+\gamma_3(x-L_2)} \quad \text{[B-41]}$$

and, $$\hat{v}_3(x) = \left(A_{c3}e^{-\gamma_3(x-L_2)} - B_{c3}e^{+\gamma_3(x-L_2)}\right)/W_3 \quad \text{[B-42]}$$

If solid 2 is a porous material, then W_3 will be complex, and $\gamma_3 = \alpha_3 + i\beta_3$; if solid 2 is a non-porous material, then W_3 will be real and given by $W_3 = \rho_3 c_3$, and $\gamma_3 = ik_3 = i2\pi f/c_3$. Also, $L_2 \le x \le (L_2 + L_3)$.

Component 4 (Air)

$$p_{c4}(x,t) = e^{i\omega t}\hat{p}_4(x) \quad \text{[B-43]}$$

and, $$v_{c4}(x,t) = e^{i\omega t}\hat{v}_4(x) \quad \text{[B-44]}$$

where, $$\hat{p}_4(x) = A_{c4}e^{-\gamma_4(x-[L_2+L_3])} \quad \text{[B-45]}$$

and, $$\hat{v}_4(x) = \left(A_{c4}e^{-\gamma_4(x-[L_2+L_3])}\right)/W_4 \quad \text{[B-46]}$$

with $W_4 = \rho_1 c_1$, and $\gamma_4 = ik_1 = i2\pi f/c_1$.

Since the pressures and velocities are continuous at the interfaces, the following boundary conditions must be satisfied

At x=0

$$p_{c1}(0,t) = p_{c2}(0,t)$$

Hence, from equations [B-33] and [B-37],

$$A_{c1} + B_{c1} = A_{c2} + B_{c2} \quad \text{[B-47]}$$

Also, $$v_{c1}(0,t) = v_{c2}(0,t)$$

Hence, from [B-34] and [B-38],

$$(A_{c1} - B_{c1})/W_1 = (A_{c2} - B_{c2})/W_2 \quad \text{[B-48]}$$

Similarly, at $x=L_2$

From equations [B-37] and [B-41]

$$A_{c2}e^{-\gamma_2 L_2} + B_{c2}e^{+\gamma_2 L_2} = A_{c3} + B_{c3} \qquad \text{[B-49]}$$

And, from equations [B-38] and [B-42]

$$\left(A_{c2}e^{-\gamma_2 L_2} - B_{c2}e^{+\gamma_2 L_2}\right)/W_2 = \left(A_{c3} - B_{c3}\right)/W_3 \qquad \text{[B-50]}$$

The *specific* acoustic impedance of component 2 (solid 1) is defined at x=0 as follows:

$$Z_2^* = \frac{p_{c2}(0,t)}{v_{c2}(0,t)} = \frac{\hat{p}_{c2}(0)}{\hat{v}_{c2}(0)} \qquad \text{[B-51]}$$

Hence, from equation [B-37] and [B-38]

$$Z_2^* = \frac{W_2\left(A_{c2} + B_{c2}\right)}{A_{c2} - B_{c2}} \qquad \text{[B-52]}$$

Also, from equations [B-47] and [B-48], it follows that

$$Z_2^* = \frac{W_1\left(A_{c1} + B_{c1}\right)}{A_{c1} - B_{c1}} \qquad \text{[B-53]}$$

The complex amplitude ratios associated with Z_2^* are given by:

$$R_{c2} = B_{c2}/A_{c2} \qquad \text{[B-54]}$$

and,

$$R_{c1} = B_{c1}/A_{c1} \qquad \text{[B-55]}$$

Hence, from equations [B-52] and [B-53] it follows that

$$Z_2^* = \frac{W_2\left(1 + R_{c2}\right)}{\left(1 - R_{c2}\right)} \qquad \text{[B-56]}$$

and,

$$Z_2^* = \frac{W_1\left(1 + R_{c1}\right)}{\left(1 - R_{c1}\right)} \qquad \text{[B-57]}$$

The *specific* acoustic impedance of component 3 (solid 2) is defined at x=L_2 as follows:

$$Z_3^* = \frac{p_{c3}(0,t)}{v_{c3}(0,t)} = \frac{\hat{p}_{c3}(0)}{\hat{v}_{c3}(0)} \qquad \text{[B-58]}$$

Hence, from equation [B-41] and [B-42]

$$Z_3^* = \frac{W_3(A_{c3} + B_{c3})}{A_{c3} - B_{c3}} \qquad \text{[B-59]}$$

Also, from equations [B-49] and [B-50], it follows that

$$Z_3^* = \frac{W_2\left(A_{c2}e^{-\gamma_2 L_2} + B_{c2}e^{+\gamma_2 L_2}\right)}{A_{c2}e^{-\gamma_2 L_2} - B_{c2}e^{+\gamma_2 L_2}} \qquad \text{[B-60]}$$

The complex amplitude ratios associated with Z_3^* are R_{c2}, given by [B-54], and R_{c3} which is defined as:

$$R_{c3} = B_{c3}/A_{c3} \qquad \text{[B-61]}$$

From equations [B-59] and [B-61], it follows that,

$$Z_3^* = \frac{W_3(1 + R_{c3})}{(1 - R_{c3})} \qquad \text{[B-62]}$$

And from equations [B-54] and [B-60]

$$Z_3^* = \frac{W_2\left(e^{-\gamma_2 L_2} + R_{c2}e^{+\gamma_2 L_2}\right)}{e^{-\gamma_2 L_2} - R_{c2}e^{+\gamma_2 L_2}} \qquad \text{[B-63]}$$

Equation [B-63] yields

$$R_{c2} = \frac{e^{-\gamma_2 L_2}\left(Z_3^* - W_2\right)}{e^{+\gamma_2 L_2}\left(Z_3^* + W_2\right)} \qquad \text{[B-64]}$$

From equations [B-56] and [B-64], it follows that

$$Z_2^* = W_2 \frac{Z_3^* \cosh \gamma_2 L_2 + W_2 \sinh \gamma_2 L_2}{Z_3^* \sinh \gamma_2 L_2 + W_2 \cosh \gamma_2 L_2} \qquad \text{[B-65]}$$

Now, suppose that component 2 (solid 1) is a porous material and that component 3 (solid 2) is a perfectly hard wall with $L_3 << L_2$, such that it reflects all the sound that impinges on it. In other words, no sound emerges through component 3 into component 4 (air). This means that, in equation [B-61], $A_{c3} = B_{c3}$, i.e., $R_{c3} = 1$. Hence, from equation [B-62]

$$Z_3^* = \frac{W_3(1 + R_{c3})}{(1 - R_{c3})} \to \infty$$

and, from equation [B-65], it follows that

$$Z_2^* = \lim_{Z_3^* \to \infty} \left\{ W_2 \left[\frac{\cosh \gamma_2 L_2 + \left(\frac{W_2 \sinh \gamma_2 L_2}{Z_3^*} \right)}{\sinh \gamma_2 L_2 + \left(\frac{W_2 \cosh \gamma_2 L_2}{Z_3^*} \right)} \right] \right\} \qquad \text{[B-66]}$$

$$= W_2 \left[\frac{\cosh \gamma_2 L_2}{\sinh \gamma_2 L_2} \right]$$

Thus, for a coupled two-component air/solid system involving a porous material with a perfectly hard backing, the specific acoustic impedance of the porous material is given by:

$$Z_2^* = W_2 \coth \gamma_2 L_2 \qquad \text{[B-67]}$$

where the *characteristic* acoustic impedance of the material, W_2, is given by equation [B-26], and the material's propagation constant, γ_2, is given by equation [B-22].

It should be noted that, for this two-component system, at x=L_2, from equation [B-42], with $A_{c3} = B_{c3}$, $\hat{v}_{c3} = 0$, i.e., the complex velocity at the end of the porous material is zero. Hence, with respect to the finite element technique, the boundary condition at x=L_2 is that the displacement is zero.

B-3 Absorption Coefficient

For the above coupled air/solid system involving a porous material with a perfectly hard backing, no sound emerges from the material. Thus, all the acoustic energy in the material is absorbed. This means that the acoustic power absorbed must equal the acoustic power associated with the incident wave (in the air upstream of the material) minus the acoustic power associated with the reflected wave. Now, the acoustic power associated with a complex harmonic pressure wave with an amplitude A_c is directly proportional to $|A_c|^2$ [11]. Hence, the incident acoustic power is directly proportional to $|A_{c1}|^2$ and the reflected acoustic power is directly proportional to $|B_{c1}|^2$. The (sound power) absorption coefficient, α_a, is defined as the fraction of the incident acoustic power that is absorbed; so, it is given by:

$$\alpha_a = \frac{|A_{c1}|^2 - |B_{c1}|^2}{|A_{c1}|^2} = 1 - \left|\frac{B_{c1}}{A_{c1}}\right|^2 \qquad \text{[B-68]}$$

From equation [B-55], it follows that

$$\alpha_a = 1 - |R_{c1}|^2 \qquad \text{[B-69]}$$

From equation [B-57], it follows that

$$R_{c1} = \frac{Z_2^* - W_1}{Z_2^* + W_1}$$

or, since $W_1 = \rho_1 c_1$

$$R_{c1} = \frac{Z_2^* - \rho_1 c_1}{Z_2^* + \rho_1 c_1} \qquad \text{[B-70]}$$

Hence, from equations [B-69] and [B-70],

$$\alpha_a = 1 - \frac{|Z_2^* - \rho_1 c_1|^2}{|Z_2^* + \rho_1 c_1|^2} \qquad \text{[B-71]}$$

where Z_2^* is given by equation [B-67]. With Z_2^* expressed as

$$Z_2^* = Z_{2R}^* + iZ_{2I}^*,$$

equation [B-71] yields

$$\alpha_a = 1 - \frac{\left|\left[Z_{2R}^* - \rho_1 c_1\right] + iZ_{2I}^*\right|^2}{\left|\left[Z_{2R}^* + \rho_1 c_1\right] + iZ_{2I}^*\right|^2} \qquad \text{[B-72]}$$

$$= \frac{4Z_{2R}^*(\rho_1 c_1)}{\left[Z_{2R}^* + \rho_1 c_1\right]^2 + Z_{2I}^{*2}}$$

With

$$z_{2R}^* = Z_{2R}^* / \rho_1 c_1$$

and,

$$z_{2I}^* = Z_{2I}^* / \rho_1 c_1$$

equation [B-72] can be written as

$$\alpha_a = \frac{4z_{2R}^*}{\left[z_{2R}^* + 1\right]^2 + z_{2I}^{*2}} \qquad \text{[B-73]}$$

It should be noted that the absorption coefficient can be expressed in terms of the so-called *input specific* acoustic impedance of the system, Z_1^*. This impedance is defined via the complex acoustic pressure and velocity at the location of the piston, x=-L_1, i.e.,

$$Z_1^* = \frac{p_{c1}(x=-L_1,t)}{v_{c1}(x=-L_1,t)} = \frac{\hat{p}_{c1}(-L_1)}{\hat{v}_{c1}(-L_1)} = \frac{\hat{p}_{c1}(-L_1)}{V_0}$$

since $\hat{v}_{c1}(-L_1)$ is the amplitude of the piston velocity. With Z_1^* expressed as

$$Z_1^* = Z_{1R}^* + iZ_{1I}^*$$

$$z_{1R}^* = Z_{1R}^*/\rho_1 c_1$$

and,

$$z_{1I}^* = Z_{1I}^*/\rho_1 c_1$$

it can be shown that the absorption coefficient is also given by

$$\alpha_a = \frac{4z_{1R}^*}{\left[z_{1R}^* + 1\right]^2 + z_{1I}^{*2}} \qquad \text{[B-74]}$$

From equation [A-22], with $\rho c = \rho_1 c_1$, $\kappa = \kappa_1$, $L = L_1$, and $z^* = z_2^*$, it can be shown that z_{1R}^* and z_{1I}^* for the air are related to z_{2R}^* and z_{2I}^* for the porous material, as follows:

$$z_{1R}^* = \frac{z_{2R}^*}{\left(\cos k_1 L_1 + z_{2I}^* \sin k_1 L_1\right)^2 + z_{2I}^{*2} \sin^2 k_1 L_1} \qquad \text{[B-75]}$$

and,

$$z_{1I}^* = \frac{\left(\sin k_1 L_1 + z_{2I}^* \cos k_1 L_1\right)\left(\cos k_1 L_1 + z_{2I}^* \sin k_1 L_1\right) - z_{2R}^{*2} \cos k_1 L_1 \sin k_1 L_1}{\left(\cos k_1 L_1 + z_{2I}^* \sin k_1 L_1\right)^2 + z_{2I}^{*2} \sin^2 k_1 L_1} \qquad \text{[B-76]}$$

Both equations [B-73] and [B-74] give the same result because, physically, there is no absorption of acoustic energy in the air upstream of the porous material, i.e., the air does not affect the absorption process that occurs in the porous material.

Appendix C - Transmission Coefficient and Transmission Loss

Consider a rigid tube containing air that is excited by a harmonically oscillating rigid piston, as shown in Figure C-3. The oscillation of the piston creates one-dimensional acoustic pressure waves which propagate through the tube and impact solid material at $x = 0$. Air is assumed to be downstream of the solid, such that sound may be transmitted into it from the solid at $x = L$. The only constraint on L is that it is finite.

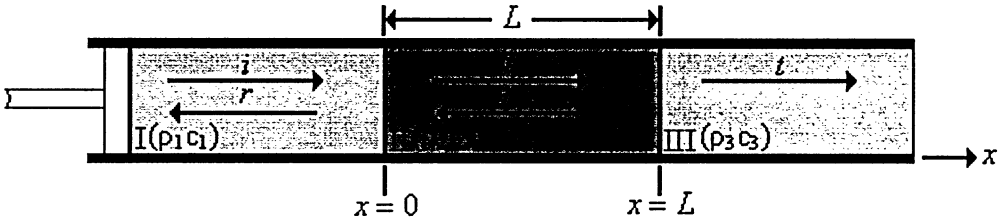

Figure C-3 – Three component system

The incident wave, i, traveling in the positive x-direction, impinges on the boundary between air I and solid II located at $x = 0$. A reflected wave, r, is generated in air I, and a transmitted wave, t, is generated in solid II. The transmitted wave travels through the solid until it impinges on the boundary between solid II and air III located at $x = L$. At this point, a reflected wave is generated in solid II, and a transmitted wave is generated in air III. Since only the sound transmission loss as the sound propagates through the solid is of interest, the sound is assumed to be completely absorbed at some distance downstream from the solid material at the right edge of the of air III.

The complex sinusoidal acoustic pressure waves relevant to the system are as follows:

Component I (Air 1)

Incident pressure wave,

$$p_{ci1} = A_{c1} e^{i(\omega t - k_1 x)} \qquad \text{[C-1]}$$

Reflected pressure wave,

$$p_{cr1} = B_{c1} e^{i(\omega t + k_1 x)} \qquad \text{[C-2]}$$

The total acoustic pressure wave,

$$p_{c1} = p_{ci1} + p_{cr1} \qquad \text{[C-3]}$$

where, $x \leq 0$, A_{c1} and B_{c1} are complex amplitudes, $\omega = 2\pi f$, f being the frequency, k_1 is the wave number given by $k_1 = \omega/c_1$, c_1 being the speed of sound in medium I.

Component II (Solid 1)

Transmitted wave, $$p_{ci2} = A_{c2}e^{i(\omega t - k_2 x)} \quad \text{[C-4]}$$

Reflected wave, $$p_{cr2} = B_{c2}e^{i(\omega t + k_2 x)} \quad \text{[C-5]}$$

The total acoustic pressure wave,

$$p_{c2} = p_{ci2} + p_{cr2} \quad \text{[C-6]}$$

where, $0 \leq x \leq L$, A_{c2} and B_{c2} are complex amplitudes, k_2 is the wave number given by $k_2 = \omega/c_2$, c_2 being the speed of sound in medium II.

Component III (Air 2)

The total and transmitted acoustic pressure wave,

$$p_{c3} = p_{ci3} = A_{c3}e^{i(\omega t - k_3(x-L))} \quad \text{[C-7]}$$

where, $x \geq L$, A_{c3} is a complex amplitude, k_3 is the wave number given by $k_3 = \omega/c_3$, c_3 being the speed of sound in medium III.

The complex acoustic velocity waves relevant to the system are as follows:

Component I (Air 1)

Incident velocity wave, $$v_{ci1} = A_{c1}e^{i(\omega t - k_1)}/(\rho_1 c_1) \quad \text{[C-8]}$$

Reflected velocity wave, $$v_{cr1} = -B_{c1}e^{i(\omega t + k_1)}/(\rho_1 c_1) \quad \text{[C-9]}$$

The total acoustic velocity wave,

$$v_{c1} = v_{ci1} + v_{cr1} \quad \text{[C-10]}$$

where, $x \leq 0$ and ρ_1 is the density of medium I.

Component II (Solid 1)

Transmitted velocity wave,

$$v_{ci2} = A_{c2} e^{i(\omega t - k_2)} / (\rho_2 c_2) \quad \text{[C-11]}$$

Reflected velocity wave,

$$v_{cr2} = -B_{c2} e^{i(\omega t + k_2)} / (\rho_2 c_2) \quad \text{[C-12]}$$

The total acoustic velocity wave,

$$v_{c2} = v_{ci2} + v_{cr2} \quad \text{[C-13]}$$

where, $0 \le x \le L$, and ρ_2 is the density of medium II.

Component III (Air 2)

The total and transmitted acoustic velocity wave,

$$v_{c3} = v_{ct3} = A_{c3} e^{i(\omega t - k_3 (x - L))} \quad \text{[C-14]}$$

where, $x \ge L$, and ρ_3 is the density of medium III.

The boundary conditions of the model are based on the fact that the acoustic pressure and velocity must be continuous across the boundaries at $x = 0$ and $x = L$. The boundary conditions are as follows:

At x = 0

$$p_{c1} = p_{c2} \quad \text{[C-15]}$$

or,

$$p_{ci1} + p_{cr1} = p_{ct2} + p_{cr2} \quad \text{[C-16]}$$

Hence,

$$A_{c1} + B_{c1} = A_{c2} + B_{c2} \quad \text{[C-17]}$$

And,

$$v_{c1} = v_{c2} \quad \text{[C-18]}$$

or,

$$v_{ci1} + v_{cr1} = v_{ct2} + v_{cr2} \quad \text{[C-19]}$$

Hence,

$$(A_{c1} - B_{c1}) = \left(\frac{\rho_1 c_1}{\rho_2 c_2}\right)(A_{c2} + B_{c2}) \qquad \text{[C-20]}$$

<u>At x = L</u>

$$p_{c2} = p_{c3} \qquad \text{[C-21]}$$

or,

$$p_{ct2} + p_{cr2} = p_{ct3} \qquad \text{[C-22]}$$

Hence,

$$A_{c2}e^{-ik_2L} + B_{c2}e^{ik_2L} = A_{c3} \qquad \text{[C-23]}$$

And,

$$v_{c3} = v_{c3} \qquad \text{[C-24]}$$

or,

$$v_{ci2} + v_{cr2} = v_{ct2} \qquad \text{[C-25]}$$

Hence,

$$\left(A_{c2}e^{-ik_2L} - B_{c2}e^{ik_2L}\right) = \left(\frac{\rho_2 c_2}{\rho_1 c_1}\right)A_{c3} \qquad \text{[C-26]}$$

From these boundary conditions, it follows that

$$2A_{c2}e^{-ik_2L} = \left[1 + \left(\frac{\rho_2 c_2}{\rho_3 c_3}\right)\right]A_{c3} \qquad \text{[C-27]}$$

so,

$$A_{c2} = \left[\left(\frac{\rho_3 c_3 + \rho_2 c_2}{2\rho_3 c_3}\right)\right]A_{c3}{}^{ik_2L} \qquad \text{[C-28]}$$

and

$$2B_{c2}e^{ik_2L} = \left[1 - \left(\frac{\rho_2 c_2}{\rho_3 c_3}\right)\right]A_{c3} \qquad \text{[C-29]}$$

so,

$$B_{c2} = \left[\left(\frac{\rho_3 c_3 - \rho_2 c_2}{2\rho_3 c_3}\right)\right]A_{c3}{}^{-ik_2L} \qquad \text{[C-30]}$$

The (complex) *specific* acoustic impedance of the solid is given by

$$Z_s^* = \frac{p_{c1}}{v_{c1}} \qquad \text{[C-31]}$$

where p_{C1} denotes a complex acoustic pressure, and v_{c1} denotes the corresponding acoustic velocity evaluated at the boundary of the medium of interest. This acoustic impedance depends on frequency and material properties, as will be established.

At x=0, it follows that

$$Z_s^* = \frac{(A_{c1} + B_{c1})(\rho_1 c_1)}{A_{c1} - B_{c1}} \qquad \text{[C-32]}$$

From the boundary conditions, [C-32] becomes

$$Z_s^* = \frac{(\rho_2 c_2)(\rho_1 c_1)\cos k_2 L + i(\rho_2 c_2)^2 \sin k_2 L}{(\rho_2 c_2)\cos k_2 L + i(\rho_3 c_3)^2 \sin k_2 L} \qquad \text{[C-33]}$$

Since medium I and medium III are the same, [C-33] becomes

$$Z_s^* = \frac{(\rho_2 c_2)(\rho_1 c_1)\cos k_2 L + i(\rho_2 c_2)^2 \sin k_2 L}{(\rho_2 c_2)\cos k_2 L + i(\rho_1 c_1)^2 \sin k_2 L} \qquad \text{[C-34]}$$

Clearly, Z_s^* depends on frequency (since $k = 2\pi f / c$) and on the density (ρ_2) and the bulk modulus ($\kappa = \rho_2 c_2^2$) of the solid.

By definition, the reflection coefficient for the present system is given by

$$\alpha_r = |R_c|^2 \qquad \text{[C-35]}$$

where $|R_c|^2$ represents the ratio of the acoustic power *reflected* by the solid (component II) to the acoustic power *incident* on the solid. Since the acoustic power associated with a complex pressure wave with an amplitude A_c is directly proportional to $|A_c|^2$ [11], it follows from equations [C-1] and [C-2] that $|R_c|^2$ is given by:

$$|R_c|^2 = \left|\frac{B_{c1}}{A_{c1}}\right|^2 \qquad \text{[C-36]}$$

One can therefore define R_c as follows:

$$R_c = \frac{B_{c1}}{A_{c1}} \qquad \text{[C-37]}$$

which is the complex amplitude ratio associated with Z_s^*. It is evident that, for the present system, the acoustic power transmitted into and through the solid (component II) is the difference between the incident acoustic power and the reflected acoustic power in the upstream air (component I). Accordingly, the transmitted power is directly proportional to $|A_{c1}|^2 - |B_{c1}|^2$, and the so-called (sound power) transmission coefficient, which is the ratio of the transmitted acoustic power to the incident acoustic power is given by:

$$\begin{aligned} \alpha_t &= \frac{|A_{c1}|^2 - |B_{c1}|^2}{|A_{c1}|^2} \\ &= 1 - \alpha_r \\ &= 1 - |R_c|^2 \end{aligned} \qquad \text{[C-38]}$$

Combination of equations [C-32] and [C-37] yields:

$$Z_s^* = \frac{(1+R_c)(\rho_1 c_1)}{1-R_c} \qquad \text{[C-39]}$$

Hence,

$$R_c = \frac{Z_s^* - \rho_1 c_1}{Z_s^* + \rho_1 c_1} \qquad \text{[C-40]}$$

From [C-40], it follows that

$$\alpha_t = 1 - \frac{|Z_s^* - \rho_1 c_1|}{|Z_s^* + \rho_1 c_1|} \qquad \text{[C-41]}$$

From equations [C-34] and [C-41], the transmission coefficient is given by

$$\alpha_t = \frac{4}{4\cos^2 k_2 L + \left(\frac{\rho_2 c_2}{\rho_1 c_1} + \frac{\rho_1 c_1}{\rho_2 c_2}\right)^2 \sin^2 k_2 L} \qquad \text{[C-42]}$$

For typical solids that are used as acoustic barriers,

$$\rho_2 c_2 >> \rho_1 c_1$$

So [C-42] becomes,

$$\alpha_t = \frac{4}{4\cos^2 k_2 L + \left(\frac{\rho_2 c_2}{\rho_1 c_1}\right)^2 \sin^2 k_2 L} \qquad \text{[C-43]}$$

By definition, the transmission loss for the system is given by

$$TL(dB) = 10\log_{10}(1/\alpha_t) \qquad \text{[C-44]}$$

The following condition applies to most materials under certain geometric and frequency constraints. If $\sim 0.05 \le L \le \sim 1$ m, $c_2 \ge \sim 1{,}000$ m/s, $\rho_2 \ge \sim 1{,}000$ kg/m^3, $\sim 10 \le f \le 1{,}000$ Hz, and $k_2 \le \pi$ then

$$\left(\frac{\rho_2 c_2}{\rho_1 c_1}\right)^2 \sin^2 k_2 L >> 4\cos^2 k_2 L \qquad \text{[C-45]}$$

So, [C-43] becomes

$$\alpha_t = \frac{4(\rho_1 c_1)^2}{(\rho_2 c_2)^2 \sin^2 k_2 L} \qquad \text{[C-46]}$$

If $L \le 0.1$ m, $c_2 \ge \sim 1{,}000$ m/s, and $f \le 5{,}00$ Hz, then $\sin k_2 L \cong k_2 L$, so [C-46] becomes

$$\alpha_t = \left(\frac{\rho_1 c_1}{\pi \rho_2 c_2}\right)^2 \left(\frac{1}{f}\right) \qquad \text{[C-47]}$$

The density of the solid is given by

$$\rho_2 = \frac{M_2}{A_2 L} \qquad \text{[C-48]}$$

where M_2 is the mass of the solid, and A_2 is its cross sectional area. The area density of the solid is given by

$$\sigma_2 = \frac{M_2}{A_2} = \rho_2 L \qquad \text{[C-49]}$$

So, from [C-47] and [C-49], the TL is given by

$$TL(dB) = 20\log_{10}\left(\frac{\pi\sigma_2}{\rho_1 c_1}\right) + 20\log_{10} f \qquad \text{[C-50]}$$

This represents the classical mass law for solid acoustic barriers, which has been verified by experimental data for various materials and certain frequency ranges [11].

It should be noted that the *specific* acoustic impedance of the system at x=L is the *characteristic* acoustic impedance of air, since, from equations [C-7] and [C-14],

$$\begin{aligned} Z(x=L) &= p_{c3}(L,t)/v_{c3}(L,t) \\ &= \rho_3 c_3 = \rho_1 c_1 \end{aligned}$$

Moreover, with the respect to the present finite element technique, the boundary condition at x=L is that there is a pressure force acting on the solid due to the pressure in component III (i.e., the air downstream of the solid).

Appendix D – Matlab Programs

D-1 Impedance Tube

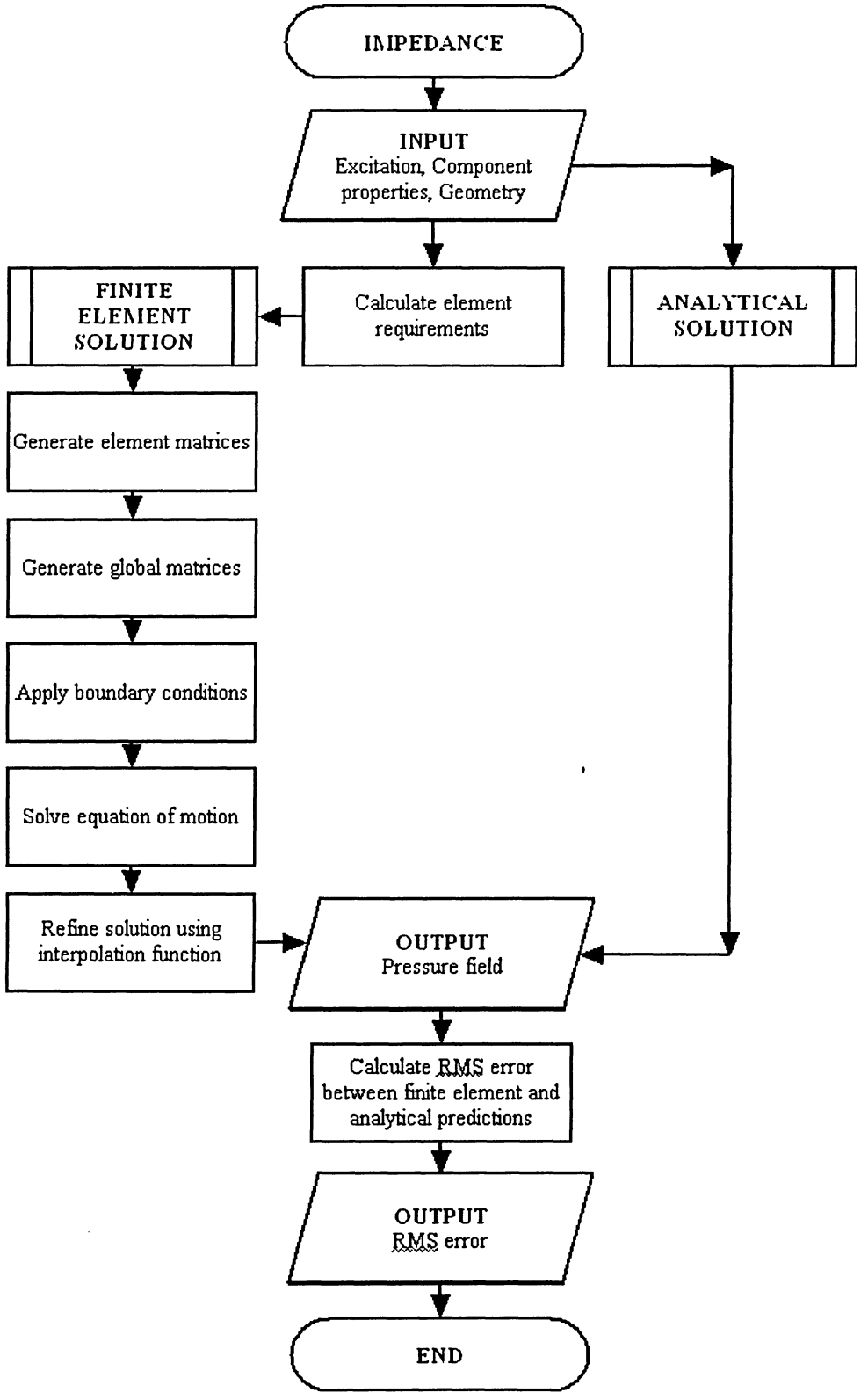

Matlab Code

IMPEDANCE (Impedance.m)

```
%Calculation of finite element and analytical pressure field, with RMS error comparison.
clear;
clc;
format short g;
hold;
%System definition
%=================
%Excitation
f=10000; Vocos=0; Vosin=10^-2; Vo=10^-2; w=2*pi*f; uocos=-Vocos/w; uosin=Vosin/w;
%Geometric
L=1.5; Area=1;
%Medium
row=1.2; c=341; Zrstar=4; Zistar=3; k=Zistar*row*c*w; d=Zrstar*row*c;
%Finite Element Specific
for n=1:1:120
% n=10;
np=20;
le=L/(n);
%Analytical Specific
K=w/c;

%Call Finite Element Solution
ImpedancewallFE
%Call Analytical Solution
DP=n*np-(n-1);
ImpedancewallAnalytical

% Peak pressure error
PrsinANmax=max(PrsinAN);
PrcosANmax=max(PrcosAN);
PrsinFEmax=max(PrsinFE);
PrcosFEmax=max(PrcosFE);

Esin(n,1)=abs((PrsinFEmax-PrsinANmax)/PrsinANmax*100);
Ecos(n,1)=abs((PrcosFEmax-PrcosANmax)/PrcosANmax*100);
if Esin(n,1)<=1 & Ecos(n,1)<=1 & Esin(n-1,1)<=1 & Ecos(n-1,1)<=1
d=n
 break
end
end
 plot(Esin)
 figure;
 plot(Ecos)

%RMS Error
difsin=PrsinFE-PrsinAN;
difcos=PrcosFE-PrcosAN;

for i=i:1:DP
   Pdiffsin(i,1)=((difsin(i,1)/PrsinAN(i,1))*100)^2;
   Pdiffcos(i,1)=((difcos(i,1)/PrcosAN(i,1))*100)^2;
end

AVGsin=sum(Pdiffsin)/DP;
AVGcos=sum(Pdiffcos)/DP;

RMSEsin(n,1)=sqrt(AVGsin);
```

```
RMSEcos(n,1)=sqrt(AVGcos);

if RMSEsin(n,1)<=10.0 & RMSEcos(n,1)<=10.0 & RMSEsin(n-1,1)<=10.0 & RMSEcos(n-1,1)<=10.0

 break
end
end
 plot(RMSEsin)
 figure;
 plot(RMSEcos)

% Pressure Plots FE and AN
plot(x,PrsinFE,'d')
figure;
plot(x,PrsinAN)
xlabel('Axial distance from the piston, x(m)')
ylabel('Imaginary part of acoustic pressure, P(Pa)')
legend('Finite Element','Analytical')
figure;
hold;
plot(x,PrcosFE,'d')
figure;
plot(x,PrcosAN)
xlabel('Axial distance from the piston, x(m)')
ylabel('Real part of acoustic pressure, P(Pa)')
legend('Finite Element','Analytical')
```

FINITE ELEMENT SOLUTION (ImpedancewallFE.m)

```
%Finite element Impedance wall Pressure Calculations

%int(transpose(N)*N,z,0,le)=
intN=[le,1/2*le^2,1/3*le^3,1/4*le^4,1/5*le^5,1/6*le^6;1/2*le^2,1/3*le^3,1/4*le^4,1/5*le^5,1/6*le^6,1/7*le^7;1/3*le^
3,1/4*le^4,1/5*le^5,1/6*le^6,1/7*le^7,1/8*le^8;1/4*le^4,1/5*le^5,1/6*le^6,1/7*le^7,1/8*le^8,1/9*le^9;1/5*le^5,1/6*le
^6,1/7*le^7,1/8*le^8,1/9*le^9,1/10*le^10;1/6*le^6,1/7*le^7,1/8*le^8,1/9*le^9,1/10*le^10,1/11*le^11];
%int(transpose(Nprime)*Nprime,z,0,le)=
intNprime=[0,0,0,0,0,0,0;0,le,le^2,le^3,le^4,le^5;0,le^2,4/3*le^3,3/2*le^4,8/5*le^5,5/3*le^6;0,le^3,3/2*le^4,9/5*le^5,2*
le^6,15/7*le^7;0,le^4,8/5*le^5,2*le^6,16/7*le^7,5/2*le^8;0,le^5,5/3*le^6,15/7*le^7,5/2*le^8,25/9*le^9];

D1=[1,0,0;0,1,0;-23/le^2,-6/le,16/le^2];
D2=[0,0,0;0,0,0;-8/le,7/le^2,-1/le];
D3=[66/le^3,13/le^2,-32/le^3;-68/le^4,-12/le^3,16/le^4;24/le^5,4/le^4,0];
D4=[32/le^2,-34/le^3,5/le^2;-40/le^3,52/le^4,-8/le^3;16/le^4,-24/le^5,4/le^4];

De = [D1,D2;D3,D4];              %element geometric matrix

%Element matrices
%================
me = row*Area*transpose(De)*intN*De;          %element mass matrix
ke = row*c^2*Area*transpose(De)*intNprime*De;  %element stiffness matrix

%Global matrices
%===============
for i=1:1:(6*n)-2*(n-1)
   for j=1:1:(6*n)-2*(n-1)
      totalm(i,j)=0; %zero mass matrix
      totalk(i,j)=0; %zero stiffness matrix
      totald(i,j)=0; %zero damping matrix
   end
end
```

```
%Global Stiffness assembly and Global Mass assembly
for m=1:n
   a=0;
   b=0;
   for i=(4*(m)-3):(4*(m)-3+5)     %Counts for rows
      a = a+1;
      b=0;
      for j=(4*(m)-3):(4*(m)-3+5) %Counts for columns
         b = b+1;
         totalk(i,j) = totalk(i,j)+ke(a,b);
         totalm(i,j) = totalm(i,j)+me(a,b);
      end
   end
end

%Effects of Impedance
%====================

totald((6*n)-2*(n-1),(6*n)-2*(n-1))=0;  %zeroes impedance damping
ndof=(6*n)-2*(n-1)-1;
totalk(ndof,ndof)=totalk(ndof,ndof)+k;
totald(ndof,ndof)=totald(ndof,ndof)+d;
%adds impedance stiffness to total stiffnes matrix
%adds impedance damping to total damping matrix

%Equation of motion
%==================
Qsin=(totalk(1:(6*n)-2*(n-1),1)-totalm(1:(6*n)-2*(n-1),1)*w^2)*uosin;
Qcos=(totalk(1:(6*n)-2*(n-1),1)-totalm(1:(6*n)-2*(n-1),1)*w^2)*uocos;
% Qsin=-totalm(1:(6*n)-2*(n-1),1)*-uosin*w^2+totalk(1:(6*n)-2*(n-1),1)*uo;
% Qcos=totald(1:(6*n)-2*(n-1),1)*uo*w;

%remove first row and first column from matrices
totalk=totalk(2:(6*n)-2*(n-1),2:(6*n)-2*(n-1));
totald=totald(2:(6*n)-2*(n-1),2:(6*n)-2*(n-1));
totalm=totalm(2:(6*n)-2*(n-1),2:(6*n)-2*(n-1));
fcos=Qcos(2:(6*n)-2*(n-1),1);
fsin=Qsin(2:(6*n)-2*(n-1),1);

%Solution
%========
A1=totalk-totalm*w^2;
A2=-totald*w;
A3=-A2;
A4=A1;
A=[A1,A2;A3,A4];

force=[fcos;fsin];

x=inv(A)*force;

%Application of the ahape function
%=================================
j=0;
for i=1:1:((6*n)-2*(n-1)-1)
   j=j+1;
   uc(j,1)=x(i,1);
end
j=0;
for i=((6*n)-2*(n-1)):1:((6*n)-2*(n-1)-1)*2
   j=j+1;
```

```
  us(j,1)=x(i,1);
end

ucos=[uocos;uc];
usin=[-uosin;us];


delta = le/(np-1);

i=1;
for element=1:n
  i=i-1;
  in1=2*element-1; in2=2*element; in3=2*element+1;
  ndof(1)= 2*in1-1; ndof(2)= 2*in1;
  ndof(3)= 2*in2-1; ndof(4)= 2*in2;
  ndof(5)= 2*in3-1; ndof(6)= 2*in3;
  Ucos=[ucos(ndof(1),1);ucos(ndof(2),1);ucos(ndof(3),1);ucos(ndof(4),1);ucos(ndof(5),1);ucos(ndof(6),1)];
  Usin=[usin(ndof(1),1);usin(ndof(2),1);usin(ndof(3),1);usin(ndof(4),1);usin(ndof(5),1);usin(ndof(6),1)];

  for inp=1:np
    i=i+1;
    z1=delta*(inp-1);
    xx(i,1)=le*(element-1)+delta*(inp-1); %records global position
    Nprime=[0,1,2*z1,3*z1^2,4*z1^3,5*z1^4];
    PrcosFE(i,1)=-row*c^2*Nprime*De*Ucos;
    PrsinFE(i,1)=row*c^2*Nprime*De*Usin;
  end

end
```

ANALYTICAL SOLUTION (ImpedancewallAnalytical.m)

```
%ANALYTICAL SOLUTION
%SOUND TRANSMISSION IN A PISTON-CYLINDER ARRANGEMENT
Denom=(cos(K*L))^2+(Zrstar^2+Zistar^2)*(sin(K*L))^2+Zistar*(sin(2*K*L));
Ao=(Zrstar^2+Zistar^2-1)*sin(2*K*L)/2+Zistar*cos(2*K*L);
%-------------------------------------------------------------------------
x = linspace(0,L,DP);
Prstar=Zrstar*cos(K*x)/Denom;
Pistar=sin(K*x)+Ao*cos(K*x)/Denom;
PrcosAN=transpose(Prstar*row*c*Vo);
PrsinAN=transpose(Pistar*row*c*Vo);
```

D-2 Absorption Coefficient

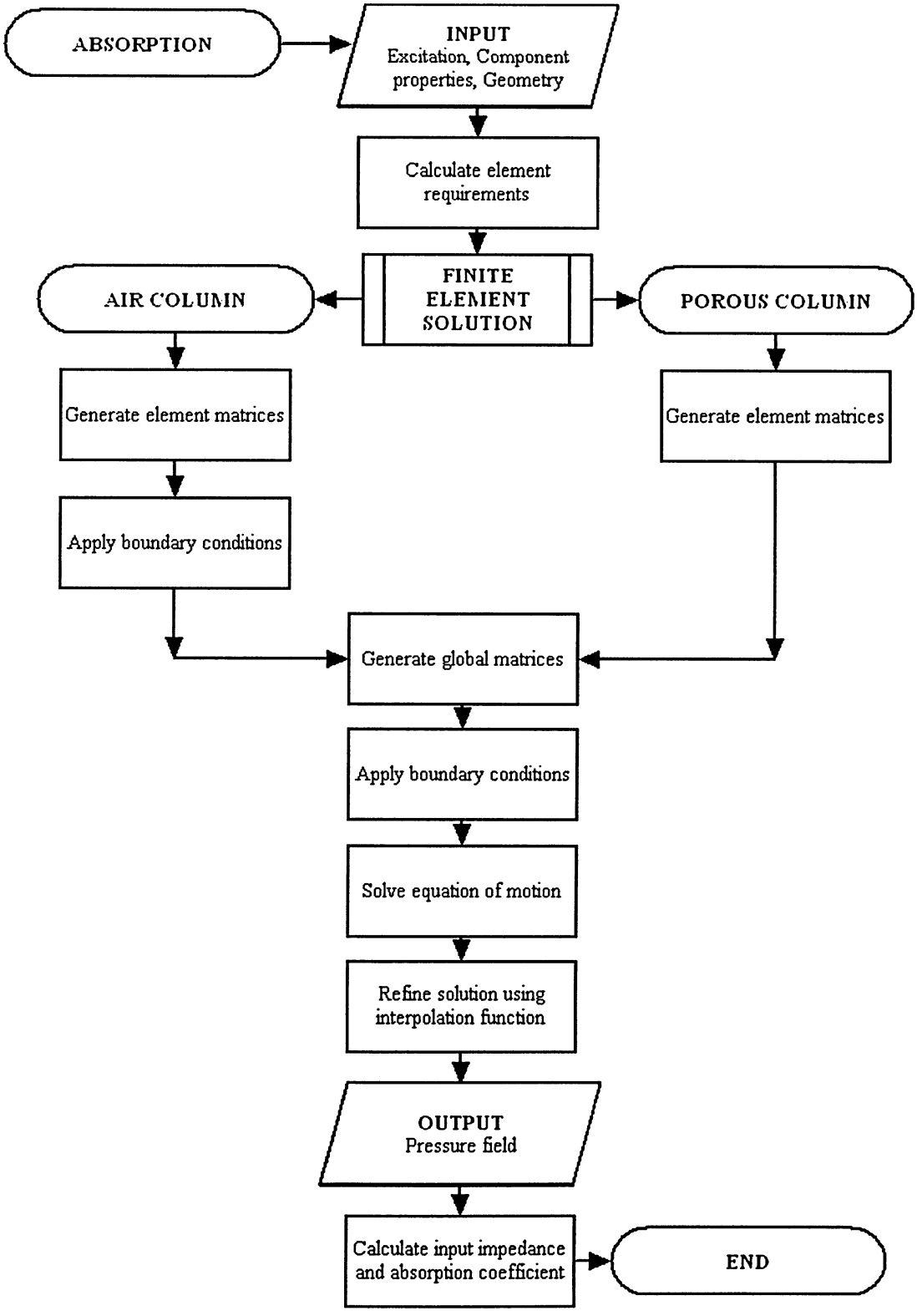

Matlab Code

ABSORPTION (AP1.m)

```
%Sound Propogation in Air and Porous Material
%Coupled FE Analysis

clear;
clc;
format short g;
hold;

%System Definition
%GENERAL
count=0;
for f=1:500:16000
   count=1;
% f=16000;
Vo_cos=10^-2; Vo_sin=0; w=2*pi*f; A=.01; Uo_cos=-Vo_sin/w; Uo_sin=Vo_cos/w;
% w=2*pi*f; A=1; Uo_cos=1; Uo_sin=0;
%AIR
R_air=0; row_air=1.2; c_air=341; L_air=0.05;
% %SOLID
R_solid=2000; row_solid=1.2; L_solid=0.025; c_solid=341 ;dampcoeff_solid=R_solid;
% R_solid=25e3; Omega=1; Ks=5; row_solid=1.2*Ks; L_solid=0.054;
c_solid=341*sqrt(Ks/Omega);dampcoeff_solid=R_solid;
%FINITE ELEMENT
% n_air=10; n_solid=5; ;
np=20;

%FINITE ELEMENT
n_air=(2*L_air*f)/c_air;
n_solid=(2*L_solid*f)/c_solid;

if n_air <=2
   n_air=2;
else
   n_air=round(n_air);
end
if n_solid <=2
   n_solid=2;
   else
   n_solid=round(n_solid);
end
% n_air=15;
% n_solid=30;
n=n_air+n_solid; np=20;
le_air=L_air/n_air; le_solid=L_solid/n_solid;
L=L_air+L_solid;

nn_air=4*n_air+2;
nn_solid=4*n_solid+2;
nn=4*n+2;
n=n_air+n_solid;
le_air=L_air/n_air; le_solid=L_solid/n_solid;
L=L_air+L_solid;

nn_air=4*n_air+2;
nn_solid=4*n_solid+2;
nn=4*n+2;

%Develop Air Element Matrices
```

```
AP2
%Develop Porous Solid Element Matrices
AP3
%Assemble Global Mass, Stiffness, Damping Matrices
AP5

% absorption coeeficient calculation
% at air boundary
% pres0c=PrcosFE_air(1,1);
% pres0s=PrsinFE_air(1,1);
% p0=complex(pres0c,pres0s);
% v0=complex(-usin1(1,1)*w,ucos1(1,1)*w);
%at porous boundary
pres0c=PrcosFE_air(n_air*np-(n_air-1),1);
pres0s=PrsinFE_air(n_air*np-(n_air-1),1);
p0=complex(pres0c,pres0s);
v0=complex(-usin1(nn_air-1,1)*w,ucos1(nn_air-1,1)*w);
%input impedance and absorption coeeficient calcs
z0=p0/v0;
zz0=z0/(row_air*c_air);
zz0r(count,1)=real(zz0);
zz0i(count,1)=imag(zz0);
abscoe(count,1)=(4*zz0r(count,1))/((zz0r(count,1)+1)^2+zz0i(count,1)^2)
freq(count,1)=f;
end
```

FINITE ELEMENT AIR (AP2.m)

```
%Sound Propogation in Air and Porous Material
%Air FE formulation
% global mg_air kg_air
%Air Geometric Matrix
D1_air=[1,0,0;0,1,0;-23/le_air^2,-6/le_air,16/le_air^2];
D2_air=[0,0,0;0,0,0;-8/le_air,7/le_air^2,-1/le_air];
D3_air=[66/le_air^3,13/le_air^2,-32/le_air^3;-68/le_air^4,-12/le_air^3,16/le_air^4;24/le_air^5,4/le_air^4,0];
D4_air=[32/le_air^2,-34/le_air^3,5/le_air^2;-40/le_air^3,52/le_air^4,-8/le_air^3;16/le_air^4,-24/le_air^5,4/le_air^4];

De_air=[D1_air,D2_air;D3_air,D4_air];

%Element Matrices
%int(transpose(N)*N,z,0,le_air)=
intN_air
=[le_air,1/2*le_air^2,1/3*le_air^3,1/4*le_air^4,1/5*le_air^5,1/6*le_air^6;1/2*le_air^2,1/3*le_air^3,1/4*le_air^4,1/5*l
e_air^5,1/6*le_air^6,1/7*le_air^7;1/3*le_air^3,1/4*le_air^4,1/5*le_air^5,1/6*le_air^6,1/7*le_air^7,1/8*le_air^8;1/4*le
_air^4,1/5*le_air^5,1/6*le_air^6,1/7*le_air^7,1/8*le_air^8,1/9*le_air^9;1/5*le_air^5,1/6*le_air^6,1/7*le_air^7,1/8*le_
air^8,1/9*le_air^9,1/10*le_air^10;1/6*le_air^6,1/7*le_air^7,1/8*le_air^8,1/9*le_air^9,1/10*le_air^10,1/11*le_air^11];
%int(transpose(Nprime)*Nprime,z,0,le_air)=
intNprime_air=[0,0,0,0,0,0;0,le_air,le_air^2,le_air^3,le_air^4,le_air^5;0,le_air^2,4/3*le_air^3,3/2*le_air^4,8/5*le_air^
5,5/3*le_air^6;0,le_air^3,3/2*le_air^4,9/5*le_air^5,2*le_air^6,15/7*le_air^7;0,le_air^4,8/5*le_air^5,2*le_air^6,16/7*l
e_air^7,5/2*le_air^8;0,le_air^5,5/3*le_air^6,15/7*le_air^7,5/2*le_air^8,25/9*le_air^9];

me_air=row_air*A*transpose(De_air)*intN_air*De_air;          %element mass matrix
ke_air=row_air*c_air^2*A*transpose(De_air)*intNprime_air*De_air;  %element stiffness matrix

%Global Solid Matrices
mg_air((6*n_air)-2*(n_air-1),(6*n_air)-2*(n_air-1))=0; %zero mass matrix
kg_air((6*n_air)-2*(n_air-1),(6*n_air)-2*(n_air-1))=0; %zero stiffness matrix

%Global Stiffness assembly and Global Mass assembly
for m=1:n_air
   a=0;
```

```
  b=0;
  for i=(4*(m)-3):(4*(m)-3+5)    %Counts for rows
    a = a+1;
    b=0;
    for j=(4*(m)-3):(4*(m)-3+5) %Counts for columns
      b = b+1;
      mg_air(i,j)=mg_air(i,j)+me_air(a,b);
      kg_air(i,j)=kg_air(i,j)+ke_air(a,b);
    end
  end
end
```

FINITE ELEMENT POROUS (AP3.m)

```
%Sound Propogation in Air and Porous Material
%Porus Solid FE formulation

%Solid Geometric Matrix
D1_solid=[1,0,0;0,1,0;-23/le_solid^2,-6/le_solid,16/le_solid^2];
D2_solid=[0,0,0;0,0,0;-8/le_solid,7/le_solid^2,-1/le_solid];
D3_solid=[66/le_solid^3,13/le_solid^2,-32/le_solid^3;-68/le_solid^4,-
12/le_solid^3,16/le_solid^4;24/le_solid^5,4/le_solid^4,0];
D4_solid=[32/le_solid^2,-34/le_solid^3,5/le_solid^2;-40/le_solid^3,52/le_solid^4,-8/le_solid^3;16/le_solid^4,-
24/le_solid^5,4/le_solid^4];

De_solid=[D1_solid,D2_solid;D3_solid,D4_solid];

%Element Matrices
%int(transpose(N)*N,z,0,le_solid)=
intN_solid=[le_solid,1/2*le_solid^2,1/3*le_solid^3,1/4*le_solid^4,1/5*le_solid^5,1/6*le_solid^6;1/2*le_solid^2,1/3*l
e_solid^3,1/4*le_solid^4,1/5*le_solid^5,1/6*le_solid^6,1/7*le_solid^7;1/3*le_solid^3,1/4*le_solid^4,1/5*le_solid^5,1
/6*le_solid^6,1/7*le_solid^7,1/8*le_solid^8;1/4*le_solid^4,1/5*le_solid^5,1/6*le_solid^6,1/7*le_solid^7,1/8*le_solid
^8,1/9*le_solid^9;1/5*le_solid^5,1/6*le_solid^6,1/7*le_solid^7,1/8*le_solid^8,1/9*le_solid^9,1/10*le_solid^10;1/6*le
_solid^6,1/7*le_solid^7,1/8*le_solid^8,1/9*le_solid^9,1/10*le_solid^10,1/11*le_solid^11];
%int(transpose(Nprime)*Nprime,z,0,le_solid)=
intNprime_solid=[0,0,0,0,0,0;0,le_solid,le_solid^2,le_solid^3,le_solid^4,le_solid^5;0,le_solid^2,4/3*le_solid^3,3/2*le
_solid^4,8/5*le_solid^5,5/3*le_solid^6;0,le_solid^3,3/2*le_solid^4,9/5*le_solid^5,2*le_solid^6,15/7*le_solid^7;0,le_s
olid^4,8/5*le_solid^5,2*le_solid^6,16/7*le_solid^7,5/2*le_solid^8;0,le_solid^5,5/3*le_solid^6,15/7*le_solid^7,5/2*le
_solid^8,25/9*le_solid^9];

me_solid=row_solid*A*transpose(De_solid)*intN_solid*De_solid;          %element mass matrix
ke_solid=row_solid*c_solid^2*A*transpose(De_solid)*intNprime_solid*De_solid;  %element stiffness matrix
de_solid=dampcoeff_solid*A*transpose(De_solid)*intN_solid*De_solid;      %element damping matrix

%Global Solid Matrices
mg_solid((6*n_solid)-2*(n_solid-1),(6*n_solid)-2*(n_solid-1))=0; %zero mass matrix
kg_solid((6*n_solid)-2*(n_solid-1),(6*n_solid)-2*(n_solid-1))=0; %zero stiffness matrix
dg_solid((6*n_solid)-2*(n_solid-1),(6*n_solid)-2*(n_solid-1))=0; %zero damping matrix

%Global Stiffness assembly and Global Mass assembly
for m=1:n_solid
  a=0;
  b=0;
  for i=(4*(m)-3):(4*(m)-3+5)    %Counts for rows
    a = a+1;
    b=0;
    for j=(4*(m)-3):(4*(m)-3+5) %Counts for columns
      b = b+1;
      mg_solid(i,j)=mg_solid(i,j)+me_solid(a,b);
      kg_solid(i,j)=kg_solid(i,j)+ke_solid(a,b);
      dg_solid(i,j)=dg_solid(i,j)+de_solid(a,b);
    end
```

```
    end
  end

  %Application of the R matrix
  alpha=(row_air*c_air^2*A)/(row_solid*c_solid^2*A);
  R=[1,0;0,alpha];

  temp_mg1=transpose(R)*mg_solid(1:2,1:2)*R;
  temp_mg2=transpose(R)*mg_solid(1:2,3:6);
  temp_mg3=mg_solid(3:6,1:2)*R;
  mg_solid(1:2,1:2)=temp_mg1;
  mg_solid(1:2,3:6)=temp_mg2;
  mg_solid(3:6,1:2)=temp_mg3;

  temp_kg1=transpose(R)*kg_solid(1:2,1:2)*R;
  temp_kg2=transpose(R)*kg_solid(1:2,3:6);
  temp_kg3=kg_solid(3:6,1:2)*R;
  kg_solid(1:2,1:2)=temp_kg1;
  kg_solid(1:2,3:6)=temp_kg2;
  kg_solid(3:6,1:2)=temp_kg3;

  temp_dg1=transpose(R)*dg_solid(1:2,1:2)*R;
  temp_dg2=transpose(R)*dg_solid(1:2,3:6);
  temp_dg3=dg_solid(3:6,1:2)*R;
  dg_solid(1:2,1:2)=temp_dg1;
  dg_solid(1:2,3:6)=temp_dg2;
  dg_solid(3:6,1:2)=temp_dg3;
```

ASSEMBLY AND SOLUTION (AP5.m)

```
%Assemble total global Mass, Stiffness, and Damping Matrices and Solve acoustic displacement vector

%Assemble Total Global Matrices
%Zero matrices
totalm(nn_air+nn_solid-2,nn_air+nn_solid-2)=0;
totalk(nn_air+nn_solid-2,nn_air+nn_solid-2)=0;
totald(nn_air+nn_solid-2,nn_air+nn_solid-2)=0;

for i=1:nn_air
   for j=1:nn_air
      totalm(i,j)=totalm(i,j)+mg_air(i,j);
      totalk(i,j)=totalk(i,j)+kg_air(i,j);
   end
end
a=0;
b=0;
for i=(nn_air-1):(nn_air+nn_solid-2)
   a=a+1;
   b=0;
   for j=(nn_air-1):(nn_air+nn_solid-2)
      b=b+1;
      totalm(i,j)=totalm(i,j)+mg_solid(a,b);
      totalk(i,j)=totalk(i,j)+kg_solid(a,b);
      totald(i,j)=totald(i,j)+dg_solid(a,b);
   end
end

%Equation of motion
%==================
Qcos=(totalk(1:nn,1)-totalm(1:nn,1)*w^2)*Uo_cos;
Qsin=(totalk(1:nn,1)-totalm(1:nn,1)*w^2)*Uo_sin;
```

```
fcos=Qcos;
fsin=Qsin;

%Boundary Condition
%Apply Boundary condition at right end
totalk(nn-1,:)=[];
totalk(:,nn-1)=[];

totalm(nn-1,:)=[];
totalm(:,nn-1)=[];

totald(nn-1,:)=[];
totald(:,nn-1)=[];

fcos(nn-1,:)=[];
fsin(nn-1,:)=[];

%remove first row and first column from matrices
totalk=totalk(2:nn-1,2:nn-1);
totald=totald(2:nn-1,2:nn-1);
totalm=totalm(2:nn-1,2:nn-1);
fcos=Qcos(2:nn-1,1);
fsin=Qsin(2:nn-1,1);

%Solution
A1=totalk-totalm*w^2;
A2=-totald*w;
A3=-A2;
A4=A1;
AA=[A1,A2;A3,A4];

force=[fcos;fsin];

x=inv(AA)*force;

%Seperates Cos and Sin entries from the global displacement vector
j=0;
for i=1:1:(nn-3)
   j=j+1;
   uc(j,1)=x(i,1);
end
j=0;
for i=(nn-1):1:(nn-2)*2-1
   j=j+1;
   us(j,1)=x(i,1);
end
epsilonc=x(nn-2);
epsilons=x((nn-2)*2);

ucos1=[Uo_cos;uc;0;epsilonc];
usin1=[-Uo_sin;us;0;epsilons];

%Seperate ucos1 and usin1 into two media components
ucos_air=ucos1(1:nn_air,1);
ucos_solid=ucos1(nn_air-1:nn,1);
usin_air=usin1(1:nn_air,1);
usin_solid=usin1(nn_air-1:nn,1);

Alpha_cos=ucos_solid(2,1)*alpha;
Alpha_sin=usin_solid(2,1)*alpha;
ucos_solid(2,1)=Alpha_cos;
usin_solid(2,1)=Alpha_sin;
```

```
% Calculate Pressure
delta_air=le_air/(np-1);
delta_solid=le_solid/(np-1);

i=1;
for element=1:n_air
   i=i-1;
   in1=2*element-1; in2=2*element; in3=2*element+1;
   ndof(1)= 2*in1-1; ndof(2)= 2*in1;
   ndof(3)= 2*in2-1; ndof(4)= 2*in2;
   ndof(5)= 2*in3-1; ndof(6)= 2*in3;

Ucos=[ucos_air(ndof(1),1);ucos_air(ndof(2),1);ucos_air(ndof(3),1);ucos_air(ndof(4),1);ucos_air(ndof(5),1);ucos_air(n
dof(6),1)];

Usin=[usin_air(ndof(1),1);usin_air(ndof(2),1);usin_air(ndof(3),1);usin_air(ndof(4),1);usin_air(ndof(5),1);usin_air(ndof
(6),1)];

   %Calcluates pressure for the air component
   for inp=1:np
      i=i+1;
      z1=delta_air*(inp-1);
      xx_air(i,1)=le_air*(element-1)+delta_air*(inp-1); %records global position
      Nprime=[0,1,2*z1,3*z1^2,4*z1^3,5*z1^4];
      PrcosFE_air(i,1)=-row_air*c_air^2*Nprime*De_air*Ucos;
      PrsinFE_air(i,1)=-row_air*c_air^2*Nprime*De_air*Usin;
   end
end

i=1;
for element=1:n_solid
   i=i-1;
   in1=2*element-1; in2=2*element; in3=2*element+1;
   ndof(1)= 2*in1-1; ndof(2)= 2*in1;
   ndof(3)= 2*in2-1; ndof(4)= 2*in2;
   ndof(5)= 2*in3-1; ndof(6)= 2*in3;

Ucos=[ucos_solid(ndof(1),1);ucos_solid(ndof(2),1);ucos_solid(ndof(3),1);ucos_solid(ndof(4),1);ucos_solid(ndof(5),1);
ucos_solid(ndof(6),1)];

Usin=[usin_solid(ndof(1),1);usin_solid(ndof(2),1);usin_solid(ndof(3),1);usin_solid(ndof(4),1);usin_solid(ndof(5),1);usi
n_solid(ndof(6),1)];

   %Calcluates pressure for the air component
   for inp=1:np
      i=i+1;
      z1=delta_solid*(inp-1);
      if element==1 & inp==1
         xx_solid(i,1)=xx_air(19*n_air+1,1);
      else
         xx_solid(i,1)=xx_solid(i-1,1)+delta_solid;
      end
      Nprime=[0,1,2*z1,3*z1^2,4*z1^3,5*z1^4];
      PrcosFE_solid(i,1)=-row_solid*c_solid^2*Nprime*De_solid*Ucos;
      PrsinFE_solid(i,1)=-row_solid*c_solid^2*Nprime*De_solid*Usin;
   end
end

xx=[xx_air;xx_solid];
PrcosFE=[PrcosFE_air;PrcosFE_solid];
PrsinFE=[PrsinFE_air;PrsinFE_solid];
```

D-3 Transmission Coefficient and Transmission Loss

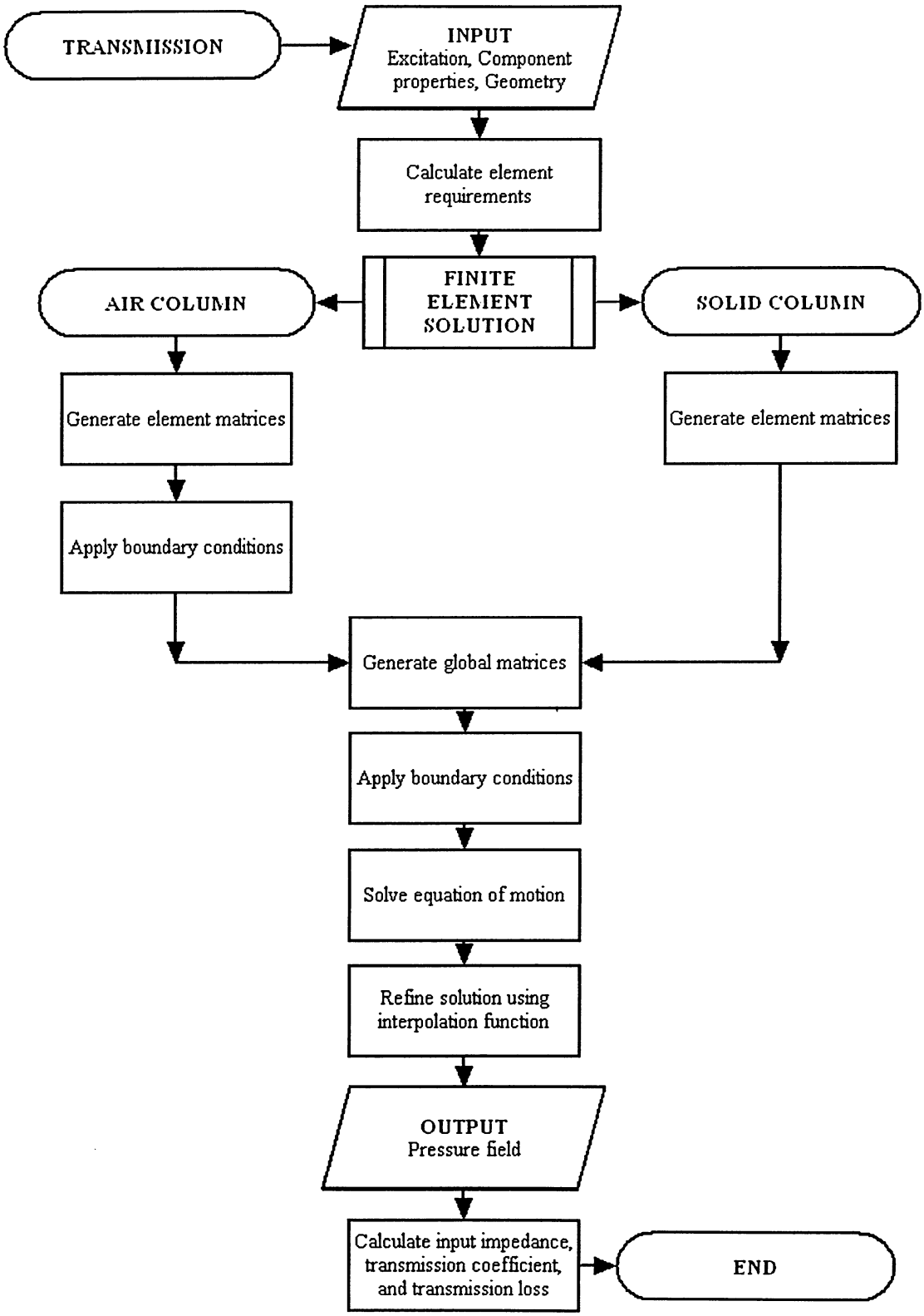

Matlab Code

TRANSMISSION (TR1.m)

```
%Sound Propogation in Air and Porous Material
%Coupled FE Analysis

clear;
clc;
format short g;
% hold;

%System Definition
%GENERAL
count=0;
for f=100:100:10000
   count=1;
Vo_cos=1; Vo_sin=0; w=2*pi*f; A=0.01; Uo_cos=-Vo_sin/w; Uo_sin=Vo_cos/w;
%AIR
R_air=0; row_air=1.2; c_air=341; L_air=0.01; pc_air=row_air*c_air;
% %SOLID
R_solid=0; row_solid=700; L_solid=0.5; c_solid=1100; dampcoeff_solid=R_solid; pc_solid=row_solid*c_solid;
% R_solid=0; Omega=2; Ks=3; row_solid=1.2*Ks; L_solid=0.025;
c_solid=341*sqrt(Ks/Omega);dampcoeff_solid=R_solid;
%AIR 2
row_2=1.2;
c_2=341;
Zrstar=0; Zistar=1; k=Zistar*row_2*c_2*w; d=Zrstar*row_2*c_2;

%FINITE ELEMENT
n_air=(2*L_air*f)/c_air;
n_solid=(2*L_solid*f)/c_solid;

if n_air <=2
   n_air=2;
else
   n_air=round(n_air);
end
if n_solid <=2
   n_solid=2
   else
   n_solid=round(n_solid)
end
% n_air=15;
% n_solid=30;
n=n_air+n_solid; np=20;
le_air=L_air/n_air; le_solid=L_solid/n_solid;
L=L_air+L_solid;

nn_air=4*n_air+2;
nn_solid=4*n_solid+2;
nn=4*n+2;

%Develop Air Element Matrices
TR2
%Develop Porous Solid Element Matrices
TR3
%Assemble Global Mass, Stiffness, Damping Matrices
TR5

%Left face
PrLc=PrcosFE_solid(1,1);
```

```
PrLs=PrsinFE_solid(1,1);
%PrLc=PrcosFE_air(1,1);
%PrLs=PrsinFE_air(1,1);
% PrLc=PrcosFE_air((n_air*np-(n_air-1)),1);
% PrLs=PrsinFE_air((n_air*np-(n_air-1)),1);
PrL=complex(PrLc,PrLs);
vL=complex(-usin1(nn_air-1,1)*w,ucos1(nn_air-1,1)*w);
%vL=complex(-usin1(1,1)*w,ucos1(1,1)*w);
%Right face
% PrRc=PrcosFE_solid(n_solid*np-(n_solid-1),1);
% PrRs=PrsinFE_solid(n_solid*np-(n_solid-1),1);
% PrR=complex(PrRc,PrRs);

%Transmission loss
Z=(PrL)/vL;
% X=abs(Z/(2*row_air*c_air));
alphat=4*real(Z)*(row_air*c_air)/((real(Z)+row_air*c_air)^2+imag(Z)^2);
TL=10*log10(1/alphat);
TLM=sqrt(real(TL)^2+imag(TL)^2);
end

% plot(TL)

%Plots pressure values for a single frequency
% figure;
% plot(xx,PrcosFE)
% title('Cos Harmonic Pressure values')
% figure;
% plot(xx,PrsinFE)
% title('Sin Harmonic Pressure values')
```

FINITE ELEMENT AIR (TR2,m)

```
%Sound Propogation in Air and Porous Material
%Air FE formulation
% global mg_air kg_air
%Air Geometric Matrix
D1_air=[1,0,0;0,1,0;-23/le_air^2,-6/le_air,16/le_air^2];
D2_air=[0,0,0;0,0,0;-8/le_air,7/le_air^2,-1/le_air];
D3_air=[66/le_air^3,13/le_air^2,-32/le_air^3;-68/le_air^4,-12/le_air^3,16/le_air^4;24/le_air^5,4/le_air^4,0];
D4_air=[32/le_air^2,-34/le_air^3,5/le_air^2;-40/le_air^3,52/le_air^4,-8/le_air^3;16/le_air^4,-24/le_air^5,4/le_air^4];

De_air=[D1_air,D2_air;D3_air,D4_air];

%Element Matrices
%int(transpose(N)*N,z,0,le_air)=
intN_air
=[le_air,1/2*le_air^2,1/3*le_air^3,1/4*le_air^4,1/5*le_air^5,1/6*le_air^6;1/2*le_air^2,1/3*le_air^3,1/4*le_air^4,1/5*le_air^5,1/6*le_air^6,1/7*le_air^7;1/3*le_air^3,1/4*le_air^4,1/5*le_air^5,1/6*le_air^6,1/7*le_air^7,1/8*le_air^8;1/4*le_air^4,1/5*le_air^5,1/6*le_air^6,1/7*le_air^7,1/8*le_air^8,1/9*le_air^9;1/5*le_air^5,1/6*le_air^6,1/7*le_air^7,1/8*le_air^8,1/9*le_air^9,1/10*le_air^10;1/6*le_air^6,1/7*le_air^7,1/8*le_air^8,1/9*le_air^9,1/10*le_air^10,1/11*le_air^11];
%int(transpose(Nprime)*Nprime,z,0,le_air)=
intNprime_air=[0,0,0,0,0,0;0,le_air,le_air^2,le_air^3,le_air^4,le_air^5;0,le_air^2,4/3*le_air^3,3/2*le_air^4,8/5*le_air^5,5/3*le_air^6;0,le_air^3,3/2*le_air^4,9/5*le_air^5,2*le_air^6,15/7*le_air^7;0,le_air^4,8/5*le_air^5,2*le_air^6,16/7*le_air^7,5/2*le_air^8;0,le_air^5,5/3*le_air^6,15/7*le_air^7,5/2*le_air^8,25/9*le_air^9];

me_air=row_air*A*transpose(De_air)*intN_air*De_air;          %element mass matrix
ke_air=row_air*c_air^2*A*transpose(De_air)*intNprime_air*De_air;  %element stiffness matrix

%Global Solid Matrices
mg_air((6*n_air)-2*(n_air-1),(6*n_air)-2*(n_air-1))=0; %zero mass matrix
```

```
kg_air((6*n_air)-2*(n_air-1),(6*n_air)-2*(n_air-1))=0; %zero stiffness matrix

%Global Stiffness assembly and Global Mass assembly
for m=1:n_air
   a=0;
   b=0;
   for i=(4*(m)-3):(4*(m)-3+5)    %Counts for rows
      a = a+1;
      b=0;
      for j=(4*(m)-3):(4*(m)-3+5) %Counts for columns
         b = b+1;
         mg_air(i,j)=mg_air(i,j)+me_air(a,b);
         kg_air(i,j)=kg_air(i,j)+ke_air(a,b);
      end
   end
end
```

FINITE ELEMENT SOLID (TR3.m)

```
%Sound Propogation in Air and Porous Material
%Porus Solid FE formulation

%Solid Geometric Matrix
D1_solid=[1,0,0;0,1,0;-23/le_solid^2,-6/le_solid,16/le_solid^2];
D2_solid=[0,0,0;0,0,0;-8/le_solid,7/le_solid^2,-1/le_solid];
D3_solid=[66/le_solid^3,13/le_solid^2,-32/le_solid^3;-68/le_solid^4,-
12/le_solid^3,16/le_solid^4;24/le_solid^5,4/le_solid^4,0];
D4_solid=[32/le_solid^2,-34/le_solid^3,5/le_solid^2;-40/le_solid^3,52/le_solid^4,-8/le_solid^3;16/le_solid^4,-
24/le_solid^5,4/le_solid^4];

De_solid=[D1_solid,D2_solid;D3_solid,D4_solid];

%Element Matrices
%int(transpose(N)*N,z,0,le_solid)=
intN_solid=[le_solid,1/2*le_solid^2,1/3*le_solid^3,1/4*le_solid^4,1/5*le_solid^5,1/6*le_solid^6;1/2*le_solid^2,1/3*l
e_solid^3,1/4*le_solid^4,1/5*le_solid^5,1/6*le_solid^6,1/7*le_solid^7;1/3*le_solid^3,1/4*le_solid^4,1/5*le_solid^5,1
/6*le_solid^6,1/7*le_solid^7,1/8*le_solid^8;1/4*le_solid^4,1/5*le_solid^5,1/6*le_solid^6,1/7*le_solid^7,1/8*le_solid
^8,1/9*le_solid^9;1/5*le_solid^5,1/6*le_solid^6,1/7*le_solid^7,1/8*le_solid^8,1/9*le_solid^9,1/10*le_solid^10;1/6*le
_solid^6,1/7*le_solid^7,1/8*le_solid^8,1/9*le_solid^9,1/10*le_solid^10,1/11*le_solid^11];
%int(transpose(Nprime)*Nprime,z,0,le_solid)=
intNprime_solid=[0,0,0,0,0,0;0,le_solid,le_solid^2,le_solid^3,le_solid^4,le_solid^5;0,le_solid^2,4/3*le_solid^3,3/2*le
_solid^4,8/5*le_solid^5,5/3*le_solid^6;0,le_solid^3,3/2*le_solid^4,9/5*le_solid^5,2*le_solid^6,15/7*le_solid^7;0,le_s
olid^4,8/5*le_solid^5,2*le_solid^6,16/7*le_solid^7,5/2*le_solid^8;0,le_solid^5,5/3*le_solid^6,15/7*le_solid^7,5/2*le
_solid^8,25/9*le_solid^9];

me_solid=row_solid*A*transpose(De_solid)*intN_solid*De_solid;              %element mass matrix
ke_solid=row_solid*c_solid^2*A*transpose(De_solid)*intNprime_solid*De_solid;  %element stiffness matrix
de_solid=dampcoeff_solid*A*transpose(De_solid)*intN_solid*De_solid;        %element damping matrix

%Global Solid Matrices
mg_solid((6*n_solid)-2*(n_solid-1),(6*n_solid)-2*(n_solid-1))=0; %zero mass matrix
kg_solid((6*n_solid)-2*(n_solid-1),(6*n_solid)-2*(n_solid-1))=0; %zero stiffness matrix
dg_solid((6*n_solid)-2*(n_solid-1),(6*n_solid)-2*(n_solid-1))=0; %zero damping matrix

%Global Stiffness assembly and Global Mass assembly
for m=1:n_solid
   a=0;
   b=0;
   for i=(4*(m)-3):(4*(m)-3+5)    %Counts for rows
      a = a+1;
      b=0;
```

```
      for j=(4*(m)-3):(4*(m)-3+5) %Counts for columns
        b = b+1;
        mg_solid(i,j)=mg_solid(i,j)+me_solid(a,b);
        kg_solid(i,j)=kg_solid(i,j)+ke_solid(a,b);
        dg_solid(i,j)=dg_solid(i,j)+de_solid(a,b);
      end
    end
  end

  %Application of the R matrix
  alpha=(row_air*c_air^2*A)/(row_solid*c_solid^2*A);
  R=[1,0;0,alpha];

  temp_mg1=transpose(R)*mg_solid(1:2,1:2)*R;
  temp_mg2=transpose(R)*mg_solid(1:2,3:6);
  temp_mg3=mg_solid(3:6,1:2)*R;
  mg_solid(1:2,1:2)=temp_mg1;
  mg_solid(1:2,3:6)=temp_mg2;
  mg_solid(3:6,1:2)=temp_mg3;

  temp_kg1=transpose(R)*kg_solid(1:2,1:2)*R;
  temp_kg2=transpose(R)*kg_solid(1:2,3:6);
  temp_kg3=kg_solid(3:6,1:2)*R;
  kg_solid(1:2,1:2)=temp_kg1;
  kg_solid(1:2,3:6)=temp_kg2;
  kg_solid(3:6,1:2)=temp_kg3;

  temp_dg1=transpose(R)*dg_solid(1:2,1:2)*R;
  temp_dg2=transpose(R)*dg_solid(1:2,3:6);
  temp_dg3=dg_solid(3:6,1:2)*R;
  dg_solid(1:2,1:2)=temp_dg1;
  dg_solid(1:2,3:6)=temp_dg2;
  dg_solid(3:6,1:2)=temp_dg3;
```

ASSEMBLY AND SOLUTION (TR5.m)

```
%Assemble total global Mass, Stiffness, and Damping Matrices and Solve acoustic displacement vector

%Assemble Total Global Matrices
%Zero matrices
totalm(nn_air+nn_solid-2,nn_air+nn_solid-2)=0;
totalk(nn_air+nn_solid-2,nn_air+nn_solid-2)=0;
totald(nn_air+nn_solid-2,nn_air+nn_solid-2)=0;

for i=1:nn_air
  for j=1:nn_air
    totalm(i,j)=totalm(i,j)+mg_air(i,j);
    totalk(i,j)=totalk(i,j)+kg_air(i,j);
  end
end
a=0;
b=0;
for i=(nn_air-1):(nn_air+nn_solid-2)
  a=a+1;
  b=0;
  for j=(nn_air-1):(nn_air+nn_solid-2)
    b=b+1;
    totalm(i,j)=totalm(i,j)+mg_solid(a,b);
    totalk(i,j)=totalk(i,j)+kg_solid(a,b);
    totald(i,j)=totald(i,j)+dg_solid(a,b);
  end
```

```
end

%Effects of Impedance
%====================

ndof=nn-1;
totalk(ndof,ndof)=totalk(ndof,ndof)+k;
totald(ndof,ndof)=totald(ndof,ndof)+d;

%Equation of motion
%==================
Qcos=(totalk(1:nn,1)-totalm(1:nn,1)*w^2)*Uo_cos;
Qsin=(totalk(1:nn,1)-totalm(1:nn,1)*w^2)*Uo_sin;
fcos=Qcos;
fsin=Qsin;

 %remove first row and first column from matrices
totalk=totalk(2:nn,2:nn);
totald=totald(2:nn,2:nn);
totalm=totalm(2:nn,2:nn);
fcos=Qcos(2:nn,1);
fsin=Qsin(2:nn,1);

%Solution
A1=totalk-totalm*w^2;
A2=-totald*w;
A3=-A2;
A4=A1;
AA=[A1,A2;A3,A4];

force=[fcos;fsin];

x=inv(AA)*force;

%Seperates Cos and Sin entries from the global displacement vector
j=0;
for i=1:1:(nn-1)
   j=j+1;
   uc(j,1)=x(i,1);
end
j=0;
for i=(nn):1:(nn)*2-2
   j=j+1;
   us(j,1)=x(i,1);
end

ucos1=[Uo_cos;uc];
usin1=[-Uo_sin;us];

%Seperate ucos1 and usin1 into two media components
ucos_air=ucos1(1:nn_air,1);
ucos_solid=ucos1(nn_air-1:nn,1);
usin_air=usin1(1:nn_air,1);
usin_solid=usin1(nn_air-1:nn,1);

Alpha_cos=ucos_solid(2,1)*alpha;
Alpha_sin=usin_solid(2,1)*alpha;
ucos_solid(2,1)=Alpha_cos;
usin_solid(2,1)=Alpha_sin;

% Calculate Pressure
delta_air=le_air/(np-1);
```

```
delta_solid=le_solid/(np-1);

i=1;
for element=1:n_air
   i=i-1;
   in1=2*element-1; in2=2*element; in3=2*element+1;
   ndof(1)= 2*in1-1; ndof(2)= 2*in1;
   ndof(3)= 2*in2-1; ndof(4)= 2*in2;
   ndof(5)= 2*in3-1; ndof(6)= 2*in3;

Ucos=[ucos_air(ndof(1),1);ucos_air(ndof(2),1);ucos_air(ndof(3),1);ucos_air(ndof(4),1);ucos_air(ndof(5),1);ucos_air(n
dof(6),1)];

Usin=[usin_air(ndof(1),1);usin_air(ndof(2),1);usin_air(ndof(3),1);usin_air(ndof(4),1);usin_air(ndof(5),1);usin_air(ndof
(6),1)];

   %Calcluates pressure for the air component
   for inp=1:np
      i=i+1;
      z1=delta_air*(inp-1);
      xx_air(i,1)=le_air*(element-1)+delta_air*(inp-1); %records global position
      Nprime=[0,1,2*z1,3*z1^2,4*z1^3,5*z1^4];
      PrcosFE_air(i,1)=-row_air*c_air^2*Nprime*De_air*Ucos;
      PrsinFE_air(i,1)=-row_air*c_air^2*Nprime*De_air*Usin;
   end
end

i=1;
for element=1:n_solid
   i=i-1;
   in1=2*element-1; in2=2*element; in3=2*element+1;
   ndof(1)= 2*in1-1; ndof(2)= 2*in1;
   ndof(3)= 2*in2-1; ndof(4)= 2*in2;
   ndof(5)= 2*in3-1; ndof(6)= 2*in3;

Ucos=[ucos_solid(ndof(1),1);ucos_solid(ndof(2),1);ucos_solid(ndof(3),1);ucos_solid(ndof(4),1);ucos_solid(ndof(5),1);
ucos_solid(ndof(6),1)];

Usin=[usin_solid(ndof(1),1);usin_solid(ndof(2),1);usin_solid(ndof(3),1);usin_solid(ndof(4),1);usin_solid(ndof(5),1);usi
n_solid(ndof(6),1)];

   %Calcluates pressure for the air component
   for inp=1:np
      i=i+1;
      z1=delta_solid*(inp-1);
      if element==1 & inp==1
         xx_solid(i,1)=xx_air(19*n_air+1,1);
      else
         xx_solid(i,1)=xx_solid(i-1,1)+delta_solid;
      end
      Nprime=[0,1,2*z1,3*z1^2,4*z1^3,5*z1^4];
      PrcosFE_solid(i,1)=-row_solid*c_solid^2*Nprime*De_solid*Ucos;
      PrsinFE_solid(i,1)=-row_solid*c_solid^2*Nprime*De_solid*Usin;
   end
end

xx=[xx_air;xx_solid];
PrcosFE=[PrcosFE_air;PrcosFE_solid];
PrsinFE=[PrsinFE_air;PrsinFE_solid];
```